

CO-EXISTENCE OF APOPTOTIC AND NECROTIC
FEATURES DURING CHRONIC ALCOHOL INDUCED
CELL DEATH IN RAT BRAIN

Thesis submitted for the Degree of

DOCTOR OF PHILOSOPHY

By

B. S. SOLOMON RAJU
Enrolment No. 01LAPH04



Department of Animal Sciences
School of Life Sciences
University of Hyderabad
Hyderabad-500 046
Andhra Pradesh, India
DECEMBER-2006



University of Hyderabad

(A central university established in 1974 by an act of parliament)
HYDERABAD- 500 046, INDIA

DECLARATION

I hereby state that the work embodied in this thesis entitled "**Co-existence of apoptotic and necrotic features during chronic alcohol induced cell death in rat brain**" has been carried out by me under the supervision of Prof. P. Prakash Babu and that this has not been submitted for any degree or diploma of any other University earlier.

A handwritten signature in black ink, appearing to be "P. Prakash Babu", with a date "2018" written next to it.

Prof. P. Prakash Babu
Research Supervisor

A handwritten signature in black ink, appearing to be "B.S. Solomon Raju".

B.S. Solomon Raju
Research Student

Prof. P. PRAKASH BABU
DEPARTMENT OF LIFE SCIENCES
CENTRE FOR CELL BIOLOGY
UNIVERSITY OF HYDERABAD
HYDERABAD-500 046, INDIA



University of Hyderabad

(A central university established in 1974 by an act of parliament)

HYDERABAD- 500 046, INDIA

This is to certify that Mr. B.S. Solomon Raju has carried out the research work embodied in the present thesis under my supervision and guidance for the full period prescribed under the Ph.D. ordinance of this University. We recommend his thesis entitled "**Co-existence of apoptotic and necrotic features during chronic alcohol induced cell death in rat brain**" for submission for the award of the degree of **Doctor of Philosophy**/of this University.

A handwritten signature in black ink, appearing to read "P. Prakash Babu".

Prof. P. Prakash Babu
Supervisor

A faint, circular stamp, likely an official seal or registration mark, located to the right of the supervisor's signature.

A handwritten signature in black ink, appearing to read "A. D. ...".

Head
Department of Animal Sciences

H E A D
DEPT. OF ANIMAL SCIENCES
SCHOOL OF LIFE SCIENCES
UNIVERSITY OF HYDERABAD
HYDERABAD - 500 046.

Dean
School of Life Sciences

A handwritten signature in black ink, appearing to read "A. S. ...".

Dean, School of Life Science,
University of Hyderabad
Hyderabad - 500 046. (India)

8/1/08

Acknowledgements

At the outset, I would like to express my sincere gratitude to my research supervisor, Prof. P. Prakash Babufor his guidance, support and encouragement.

I am thankful to Prof. Aparna Dutta Gupta, Head, Department of Animal Sciences and former heads Prof. P. Reddanna, Late Prof. CH. R. K. Murthy, Dean Prof. A. S. Raghavendra and former Dean Prof. T. Suryanarayana, School of Life Sciences for providing the necessary facilities.

My sincere thanks to doctoral committee members Prof. Ramanadham and Dr. Manjula Sritharanfor their invaluable suggestions throughout my work tenure.

I thank Prof. K. Subba Rao for allowing me to use his lab facilities for a part of the research work carried out in this thesis and for the generous gift of Actin and DNA polymerase antibodies. I also thank him for his critical suggestions.

I thank all the faculty and non teaching staff of School of Life Sciences. I am also thankful to the Animal house staff of the university. I thank Lallan and Khan for their co-operation during my stay at department. I thank Ankeneedu for his assistance in matters pertaining to administration. A special note of thanks to David Raju for his extraordinary helpful nature in academic and non academic matters is worth mentioning.

I thank for the senior research fellowship provided to me by ILS-MoU SRF Scheme, University of Hyderabad, Hyderabad, India. I am thankful to all the funding agencies, CSIR, UGC, SAP, DST, FIST and ILS.

I would like to extend my sincere thanks to Dr. Manas Panigrahi, Neurosurgeon, NIMS, Hyderabad for helping me in teaching the dissection procedures. I thank Dr. Balakrishna, NINfor helping me with statistical methods.

A bunch of thanks to my senior labmates Dr. Arun, Dr. Rukhsanafor encouragement during my initial days of PhD. My biggest thanks to Dr. Kranthi, Dr. Meena, Dr. Padmini, Vasanth, Vijay Chaitanya, Ashwin, Anand, Gangadhar, Dr. Sridevi, Srilaxmifor exuberant friendship. Also my due thanks to Kantha Rao and Narasimha for their prompt service in the Lab. I am thankful to the project students Atheesh Antony, and Kumar for their help. I am thankful to all the research scholars of School of Life Sciences.

I thank my friends Srikanth, Sundaram, Subhajit, Madhusudhan for their loving companionship. My heartfelt thanks to my off campus friends Shiva, Ramesh, Gokul and Praveenfor being with me in bliss and blues of life.

Words become short to express my sincere gratitude to my parents for their constant encouragement, unconditional love and invaluable support. I owe all my success to them. I take this opportunity to thank my younger sister, Brother-in-law and brother who made life easy with their ever smiling faces. I thank the recreating company ofJinu, the little one who made life simple and enjoyable. I thank my wife Rachel for her encouraging words.

I thank almighty for giving me patience to wade through the ebbs and tides of my research.

B.S. Solomon Raju

INDEX

General Introduction	Page No.
Abbreviations	1
List of figures	4
Tables	6
Publications	7
Abstract	8
Ethanol and central nervous system	11
Ethanol neurotoxicity in the developing nervous system	11
Ethanol neurotoxicity in the mature nervous system	13
Ethanol related neurodegeneration in animal models	15
Ethanol related brain damage-mechanisms	18
Apoptotic pathways in neuronal apoptosis	19
Structural organization and activation of caspases	20
Chapter 1: Differential modulation of cell death associated proteins in rat hippocampus and frontal cortex after chronic ethanol consumption.	
Introduction	23
Caspase activation	23
Release of apoptosis inducing factor	23
Release of cytochrome c	24
Bcl-2 family	25
Bad	25
NMDA receptor	26
Calpains	27
Scope of the present study	29
Chemicals and General methods	30
Results	34
Discussion	59
Chapter 2 <i>In situ</i> detection of cell death in hippocampus and frontal cortex of rats treated with ethanol chronically	
Introduction	63
Materials and methods	70
Results	75
Discussion	84
Chapter 3 Oxidative stress and Base excision repair in hippocampus and frontal cortex of rats treated with ethanol chronically	
Introduction	88
Ethanol and oxidative stress	88
Catalase	89
Glutathione, DNA damage and repair	89,90
DNA damage, Base modifications in DNA after exposures	91
Consequences of DNA damage	92
Repair of damage to DNA	93
Materials and methods	95

Results	102
Discussion	116
Summary and Conclusions	119
References	122

Abbreviations

APAF-1 Apoptosis protease activating factor-1

AIF - Apoptosis inducing factor

ATP- Adenosine triphosphate

Bcl-2 B-cell leukemia/lymphoma-2

Bax- bcl-2-Associated X Protein

Bad bcl-Associated Death Protein

BER - Base excision repair

BSA - Bovine Serum Albumin

BSO - Buthionine Sulfoximine

CARD- caspase recruitment domain

CBA-Control cerebellum astrocytes

CBN-Control cerebellum neurons

CCA-Control cortex astrocytes

CCN-Control cortex neurons

CNS- Central nervous system

CT- Computed Tomography

⁰C- Degree centigrade

DEM- Di ethyl maleate

dH₂O- Double distilled water

DN- Dark neuron

DTT- Dithio threitol

EBA-Ethanol treated cerebellum astrocytes

EBN-Ethanol treated cerebellum neurons

ECA-Ethanol treated cortex astrocytes

ECN-Ethanol treated cortex neurons

FADD- Fas associated death domain

FAS- Fetal alcohol syndrome

FC-control frontal cortex

FE- ethanol treated frontal cortex.

g- gram
GABA- γ -Amino- Butyric Acid
GFAP- glial fibrillary acidic protein
GPX- Glutathione Peroxidase
GSH- reduced glutathione
GSSG- Oxidized glutathione
GST - glutathione –S- transferase
h- hour
H&E - Hematoxylin and Eosin
H₂O₂ Hydrogen Peroxide
HC-control hippocampus,
HCl- Hydrochloric acid
HE- ethanol treated hippocampus
HIV- Human Immuno Virus
HRP- Horse radish peroxidase
i.p -intra peritoneal
IEG- Immediate early genes
IL1 β - Interleukin 1 beta
kDa- Kilo Dalton
KO- Knock out
M- Molar
MAPK- Mitogen associated protein kinase
 μ l – Microliter
 μ m- Micrometer
Min- minutes
ml –milliliter
mm³ Millimeter cube
MRI- magnetic resonance imaging
N- Normal
NaCl- Sodium Chloride
NaOH- Sodium Hydroxide

NER Nucleotide excision repair

nm- Nanometer

NMDAR1- N-methyl D-aspartate Receptor Subunit 1

NMDAR2B - N-methyl D-aspartate Receptor Subunit 2B

NMDAR2C- N-methyl D-aspartate Receptor Subunit 2C

O₂ - Molecular Oxygen

OH⁻ Hydroxyl Radical

PBS- Phosphate buffered saline

pol β - DNA polymerase Beta

PD- Parkinson's disease

PI- Propidium iodide

PKA- Protein Kinase A

PKC- Protein Kinase c delta

Pol β- DNA Polymerase beta

PARP-1 - poly (ADP-ribose) polymerase-1

PUFA- Poly unsaturated fatty acids

ROS- Reactive oxygen species

RT- Room Temperature

SDS-PAGE - Sodium dodecyl sulphate- poly acylamide gel electrophoresis

s-seconds

TUNEL - terminal deoxynucleotidyl transferase (TdT) - mediated dUTP-biotin nick end labeling.

TNF α - Tumour necrosis factor alpha

UV- Ultra violet

w/v - weight/volume

WHO- World Health organization

XIAP- X-Linked inhibitor of apoptosis protein

List of Figures

Fig 1 Areas of the brain vulnerable to damage by alcohol

Fig 2. Pathways of apoptosis,

Fig 3. Mechanism of caspase activation

Fig 4 Caspase dependent and independent cell death

Fig 5 Rat brain showing hippocampus and frontal cortex

Fig 6 Fluid consumption profile

Fig 7 Food consumption profile

Fig 8 Rat weight

Fig 9 SDS page profiles and ponceau staining of subcellular fractions

Fig 10 Immunoblots of Active caspase 3, Active caspase 7, Active caspase 9, Calpain and Actin

Fig 11. Immunoblots of PARP fragment, AIF

Fig 12. Immunoblots of cytochrome c

Fig 13. Immunoblots of Bax

Fig 14. Immunoblots of Bad

Fig 15. Immunoblots of Bcl-2

Fig 16. Immunoblots of NMDAR1, NMDAR2A, NMDAR2B, NMDAR2C

Fig 17 Scanning densitometry of Active caspase 3, Active caspase 7, Active caspase 9 and calpain

Fig 18 Scanning densitometry of PARP fragment, AIF

Fig 19 Scanning densitometry of cytochrome c and Bax

Fig 20 Scanning densitometry of Bad and Bcl2

Fig 21 Scanning densitometry of NMDAR1, NMDAR2A, NMDAR2B, NMDAR2C

Fig 22 Perfusion technique

Fig 23 Method of preparation of brain sections

Fig 24 Hematoxylin-eosin (HE) stain

Fig 25 Toluidine blue stain

Fig 26 Immunostaining for GFAP in sections

Fig 27. Immunostaining for active caspase-3 in sections

Fig 28 DNA nick end labeling of apoptotic cells (TUNEL)

Fig 29. Transmission electron microscope studies

Fig 30 Main critical steps in the signal transduction cascade leading to apoptosis

Fig 31 Involvement of reduced glutathione (GSH) in protective cellular reactions

Fig 32 GSH and GSSG

Fig 33 Glutathione Peroxidase activity, Glutathione S Transferase activity, Catalase activity

Fig 34 DNA Polymerase beta activity

Fig 35 DNA Polymerase beta Immunoblot

Tables

Table 1 Quantitative neuropathological data in different groups of alcoholic patients

Table 2 Caspases and their target (PARP) functions

Table 3 Mean and standard error values of scanning densitometries of cell death associated protein Immunoblots, Test of Homogeneity of Variances, Oneway Anova, Post Hoc Tests and Multiple Comparisons table

Table 4 Morphological comparison of necrosis and apoptosis in chronological sequence

Table 5 Major types of DNA damage repair

Table 6 Mean and standard error values of GSH, GSSG, Glutathione Peroxidase activity, Glutathione S Transferase activity, Catalase activity and Test of Homogeneity of Variances, One-way Anova, Post Hoc Tests and Multiple Comparisons table

Table 7 Mean and standard error values of DNA polymerase beta activity, scanning densitometric values of DNA polymerase beta Immunoblot and Test of Homogeneity of Variances, One-way Anova and Post Hoc Tests.

Table 8 Summary and conclusions of Cell death associated proteins (Data are derived from cell sub-fractionation and western blot analysis)

Table 9 Summary and conclusions of *In-situ* detection of cell death

Table 10 Summary and conclusions of Oxidative stress and DNA repair

Publications:

- **Bhupanapadu Sunkesula Solomon Raju**, Umakanta Swain, Phanithi Prakash Babu (2007) Cell death is associated with reduced base excision repair during chronic alcohol administration in adult rat brain. *Neurochemical Research*, Accepted 2007.

Posters Presented at Conferences :

- **Solomon Raju B S**, Ashwini Kumar K M, Prakash Babu P (2005), Apoptosis-Necrosis morphological continuum as a mode of cell death during chronic alcohol induced toxicity in rat brain, Symposium on emerging trends in Neurosciences and XXIII Annual meeting of Indian academy of Neurosciences organized by Department of Biophysics, National Institute of Mental Health and Neurosciences 11th- 14th December, 2005 at Bangalore, India
- **Solomon Raju B S**, Prakash Babu P (2004), Altered NMDA receptor activation during alcohol consumption in male *Wistar* rats, International Neuroscience conference, jointly organized by Indian Academy of Neurosciences (IAN) and Society for NeuroChemistry India (SNCI), India at University of Hyderabad, Hyderabad, India from 6th- 8th May, 2004
- **Solomon Raju B S**, Vasanth kumar, Prakash Babu P (2002), Chronic Ethanol treatment up regulates NMDA receptor subunits in rat brain, Symposium on Brain Genomics jointly organized by society for Neurochemistry India (SNCI) and ICMR center for research on aging and brain, University of Hyderabad, India from 9th- 10th December, 2002 at University of Hyderabad, Hyderabad, India.

Abstract

The cell death cascades in different brain regions namely hippocampus and frontal cortex of rats fed with 10% (v/v) ethanol for 12 weeks, was examined. After western blotting, different cell death associated proteins displayed differential activation in the two regions observed. In hippocampus, activated caspase 3, activated caspase 7 and activated caspase 9 mediated cell death. Cytochrome c release to cytosol and Apoptosis inducing factor (AIF) translocation to nucleus was marginal. B-cell leukemia/lymphoma-2 (Bcl-2) translocation to cytosol was significant whereas bcl-2-Associated X Protein (Bax) and bcl-Associated Death Protein (Bad), were largely located in cytosol. Further, upregulation of N-methyl D-aspartate Receptor Subunit 1 (NMDAR1), N-methyl D-aspartate Receptor Subunit 2B (NMDAR2B), N-methyl D-aspartate Receptor Subunit 2C (NMDAR2C) was associated with activation of calpains. In frontal cortex, caspase 3, caspase 7, caspase 9, calpain, Bax and Bad independent cell death was observed along with cleavage of PARP-1. Nuclear translocation of AIF was more pronounced. Moreover, cytochrome c release to cytosol and Bcl-2 translocation to cytosol was evident. NMDAR1 and NMDAR2A subunits were unaffected. NMDAR2B showed enhanced immunoreactivity compared to controls and was also more intense than the intensity in ethanol treated hippocampal region. NMDAR2C showed decreased immunoreactivity. All the intensities were compared to controls in the same region. Apoptosis was further substantiated by *In situ* staining for terminal deoxynucleotidyl transferase (TdT) - mediated dUTP-biotin nick end labeling (TUNEL). Results of the current study revealed that frontal cortex cell death during chronic alcohol consumption is independent of caspases and calpains and AIF mediated cell death is predominant in

this region. However hippocampal region cell death is mediated by Bcl-2, caspases and calpains. Ultra structural studies using transmission electron microscope (TEM) identified necrosis and apoptosis in hippocampal region, and necrotic features in frontal cortex of ethanol treated rat. Also DNA damage resulting from oxidative stress in both the regions in this study could further enhance the action of cell death machinery in the cell. DNA polymerase Beta assay and Immunoblot analysis of neuronal and astrocyte extracts of control and alcohol treated rat cerebral cortex (which included Hippocampus and frontal cortex) and cerebellum showed significant loss in DNA repair in alcohol treated group.

In conclusion, the present study clearly documents that chronic ethanol treatment can trigger the key biochemical events necessary for cell death in the adult rat brain and the mechanism involves combination of both apoptosis and necrosis, associated with reduced base excision repair.

INTRODUCTION

Ethanol and central nervous system

The World Health Organization (WHO) estimates that there are about 2 billion people worldwide who consume alcoholic beverages and 76.3 million with diagnosable alcohol use disorders (WHO Global Status Report on Alcohol 2004). Excessive drinking can lead to impairment of cognitive function and structural brain changes—some are permanent and some are reversible. Patterns of damage appear to relate to lifetime alcohol consumption but also equally importantly to associated medical complications. The most important of these is Wernicke-Korsakoff syndrome—a nutritional vitamin deficiency state that is caused by thiamin deficiency but which is seen most commonly in alcoholics. (Harper *et al.* 2005). Impairments of neurological function commonly seen in alcohol dependency include deficits in abstract problem solving, visuo-spatial and verbal learning, memory function, perceptual motor skills and even motor function (Oscar-Berman and Hutner 1993). Using transcranial magnetic stimulation, Ravaglia *et al.* (2002) showed that chronic alcoholics had a significant prolongation of central motor conduction time compared with controls, however there was no correlation between intensity and duration of abuse. Moreover, the pattern of cognitive deficits has been considered to be ‘frontal’ in nature but, more recently, findings indicate the possibility that compromised pontocerebellar and cerebellothalamocortical systems might contribute to cognitive and motor impairment. Sullivan (2003) studied each major node of frontocerebellar circuitry using quantitative neuroimaging, demonstrating volume deficits in alcoholics; furthermore, each node could be independently compromised. Disruption of these circuits might underlie alcohol related neuropsychological deficits, either through abnormalities in individual nodes or by disconnection and interruption of selective circuitry. Moreover, alcohol-related neuronal loss has been documented in specific regions of the cerebral cortex (superior frontal association cortex), hypothalamus and cerebellum (Harper *et al.* 1987; Harding *et al.* 1996; Baker *et al.* 1999).

Ethanol neurotoxicity in the developing nervous system

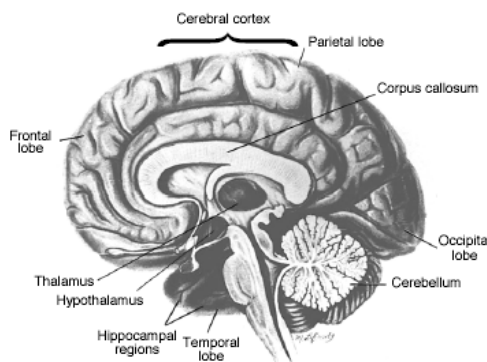
Ethanol is a well-documented developmental toxicant causing a spectrum of physical and mental dysfunctions in children after prenatal exposure. This range of structural and functional abnormalities characterize a syndrome known as fetal alcohol syndrome (FAS) and include pre- and postnatal growth retardation; craniofacial dysmorphologies; and, in particular, CNS dysfunctions, such as microencephaly, brain malformations, mental retardation, and other behavioral abnormalities (Streissguth *et al.* 1980; Nulman *et al.* 1998). The CNS effects of prenatal alcohol exposure are of most concern because they persist into adulthood and are irreversible (Streissguth *et al.* 1991; Spohr *et al.* 1993). A great deal of information exists from human and animal investigations on the neuropathological effects of perinatal alcohol exposure. Autopsies of children with FAS have revealed widespread severe damage, including malformations of brain tissue, failure of certain brain regions to develop, and failure of certain cells to migrate to their appropriate locations during development (Clarren *et al.* 1986; Mattson and Riley 1996). Certain brain regions appear to be particularly affected by ethanol: These include the corpus callosum, which is reduced in size and sometimes missing altogether (Riley *et al.* 1995); the cerebellum, whose size is significantly reduced (Harris-Collazo *et al.* 1998), possibly owing to the loss of specific neuronal cell populations; and the basal ganglia, in particular, the caudate nucleus, whose size is also significantly reduced (Harris-Collazo *et al.* 1998). Other brain areas, such as the cerebral cortex and the limbic system, including the hippocampus, show a much lesser degree of alterations following in utero ethanol exposure in humans. Detailed information on the neuropathological effects caused by developmental ethanol exposure has been provided by animal studies. Studies in rodents have shown that exposure to alcohol, particularly during the third-trimester equivalent (the first two postnatal weeks in the rat) has a profound effect on brain weight. When given during this period, ethanol causes selective microencephaly, which is independent of general growth retardation (Samson 1986) and is irreversible (Balduini and Costa 1989). Further, studies have shown that the effect exhibits temporal and regional selectivity. For example, early gestational exposure to ethanol (first trimester

equivalent) causes a reduction in brainstem growth, whereas postnatal exposure in the rat affects forebrain and cerebellum weight (Maier *et al.* 1997). A large number of studies have documented that developmental ethanol exposure causes loss of specific neuronal populations. Neuronal cell populations that are reduced by developmental ethanol exposure include neurons in the CA1 region of the hippocampus and granule and Purkinje cells in the cerebellum (Bonthius *et al.* 1990; Miller 1995; Pauli *et al.* 1995; Bonthius *et al.* 2001). In addition to affecting neurons, developmental exposure to ethanol has also been shown to affect glial cells (Phillips *et al.* 1992). Reduction in glial cell number has been reported in rat models of FAS (Miller and Potempa 1990; Perez-Torrero *et al.* 1997). Ethanol has also been shown to cause apoptotic cell death of hippocampal, cerebellar, and cortical neurons *in vitro* and *in vivo* (Oberdoerster and Rabin 1999; Ikonomidou *et al.* 2000; Climent *et al.* 2002). It is suggested that mechanisms operative after alcohol consumption in the adult brain are different from those operative in the developing brain (Olney 2002) and the ensuing molecular mechanisms during acute and chronic alcohol treatment are entirely different.

Ethanol neurotoxicity in the mature nervous system

Neurotoxic effect of ethanol may contribute to chronic cognitive dysfunction in alcoholics has been obtained from imaging studies, neuropathological observations,

Fig 1 Areas of the brain vulnerable to damage by alcohol
Adapted from Oscar-Berman and Marinkovic 2003.



and animal experiments.
CT and MRI show

enlargement of the cerebral ventricles and sulci in most alcoholics (Charness and Diamond 1984). Quantitative morphometry suggests that alcoholics lose a disproportionate amount of subcortical white matter as compared with cortical gray matter (Harper *et al.* 1985). Cholinergic neurons in the

nucleus basalis of the basal forebrain, which innervate much of the cerebral cortex and are preferentially depleted in dementia due to Alzheimer's disease, have also been reported lost in three patients with Korsakoff's syndrome (Arendt *et al.* 1983). Neuronal density in the superior frontal cortex was reduced by 22% in alcoholics (Harper *et al.* 1987). Neuronal loss was accompanied by selective glial proliferation in the superior frontal cortex, also a decrease in neuronal area was observed in the superior frontal, cingulate and motor cortices (Harper *et al.* 1987; Kril and Harper 1989). The complexity of basal dendritic arborization of layer III pyramidal neurons in both superior frontal and motor cortices was significantly reduced in a group of 15 alcoholics (Harper and Corbett 1990). A group of five alcoholics without lesions of nutritional deficiency showed a decrease in the density of synaptic spines in layer 5 cortical pyramidal cells (Ferrer *et al.* 1986). Neurodegeneration has been demonstrated during ethanol intoxication (*in vivo* and *in vitro*) and it is suggested that degeneration pattern involves different mechanisms (Crews *et al.* 2004). These data demonstrate a selective neuronal loss, dendritic simplification, and reduction of synaptic complexity in different brain regions of alcoholics. It is known that 50–75% of long-term alcoholics may show permanent cognitive impairment, making chronic alcoholism the second leading cause of dementia behind Alzheimer's disease (Eckardt *et al.* 1986). Chronic alcohol abuse is associated with progressive ataxia, degeneration of cerebellar purkinje neurons, cerebral atrophy, and mild to severe dementia (Olney 2002) and damages frontal lobes (Spencer and Hutchison 1999). Chronic alcohol abuse damages frontal lobes which contain the regions of the cortex devoted to the control of movement, language production, problem-solving ability, ability to formulate and execute plans, and control of appropriate social behavior (Spencer and Hutchison 1999). Region wise effect of alcohol consumption induced neuropathology in humans is shown in Table 1. As evident from this table, it is noteworthy to observe selective vulnerability of different brain regions to alcohol induced neuropathology.

Table 1

Quantitative neuropathological data in different groups of alcoholic patients.^a

Region and effect	Uncomplicated alcoholic	Chronic WE	Korsakoff psychosis	
Brain shrinkage (↑ pericerebral space)	36%	77%	77%	1
↓ Frontal cortical neurones	77%	80%	84%	2
↓ Cortical neuronal dendrites	81%	NA	NA	3
↓ White matter volume	98%	79%	83%	4
Hippocampus	100%	100%	100%	5
↓ Mammillary body neuronal number	98%	53%	32%	6
↓ Thalamic neurones (mediodorsal)	100%	52%	36%	7
↓ Thalamic neurones (ant. principal)	100%	86%	47%	8
↓ Basal forebrain neurones	100%	76%	79%	9
↓ Median raphe neurones	95%	30%	NA	10
↓ Dorsal raphe neurones	98%	36%	NA	11
↓ Cerebellar vermis Purkinje cells	95%	57%	NA	12

^a The groups include those with non-amnesic Wernicke-Korsakoff syndrome (chronic Wernicke's encephalopathy [WE]), those with amnesic Wernicke-Korsakoff syndrome (Korsakoff's psychosis) and those who have no liver disease or Wernicke-Korsakoff syndrome (uncomplicated alcoholics). Figures indicate the percentage of control data. ↑ indicates an increase, ↓ indicates a decrease. NA, not applicable.

1. Harper C, Kril J: Brain atrophy in chronic alcoholics patients: a quantitative pathological study. *J Neurol Neurosurg Psychiatry* 1985, 48:211-217.
2. Harper CG, Kril JJ, Daly J: Are we drinking our neurones away? *Br Med J* 1987, 294:534-536.
3. Harper C, Corbett D: Changes in the basal dendrites of cortical pyramidal cells from alcoholic patients—a quantitative Golgi study. *J Neurol Neurosurg Psychiatry* 1990, 53:856-861.
4. Harper CG, Kril JJ, Holloway RL: Brain shrinkage in chronic alcoholics: a pathological study. *Br Med J* 1985, 290:501-504.
5. Kril JJ, Halliday GM, Svoboda MD, Cartwright H: The cerebral cortex is damaged in chronic alcoholics. *Neuroscience* 1997, 79:983-998.
- 6,7,8. Harding A, Halliday G, Caine D, Kril J: Degeneration of anterior thalamic nuclei differentiates alcoholics with amnesia. *Brain* 2000, 123:141-154.
9. Cullen KM, Halliday GM, Caine D, Kril JJ: The nucleus basalis (Ch4) in the alcoholic Wernicke-Korsakoff syndrome: reduced cell number in both amnesic and non-amnesic patients. *J Neurol Neurosurg Psychiatry* 1997, 63:315-320.
10. Baker K, Halliday GM, Kril JJ, Harper CG: Chronic alcoholism in the absence of Wernicke-Korsakoff syndrome and cirrhosis does not result in the loss of serotonergic neurons in the median raphe nucleus. *Metabolic Brain Disease* 1996, 11:217-227.
11. Baker KG, Halliday GM, Kril JJ, Harper CG: Chronic alcoholics without Wernicke-Korsakoff syndrome or cirrhosis do not lose serotonergic neurons in the dorsal raphe nucleus. *Alcohol Clin Exp Res* 1996, 20:61-66.
12. Baker K, Harding A, Halliday G, Kril JJ, Harper C: Neuronal loss in functional zones of the cerebellum of chronic alcoholics with and without Wernicke's encephalopathy. *Neuroscience* 1999, 91:429-438.

Adapted from Harper and Matsumoto (2005)

Ethanol-related neurodegeneration in animal models.

It has been known that chronic ethanol is associated with neurodegenerative processes in specific regions of the brain (Freund 1973; Walker and Freund 1971, 1973; Walker *et al.* 1980a, b). The neuropathological alterations have been considered the cause of the memory and learning impairments and of the modifications of monoaminergic neurotransmission (McEntee and Mair 1990). The structural and functional changes induced by chronic ethanol administration in the hippocampus have been extensively documented because of the important role of this brain structure in memory function. The hippocampal formation or its afferent innervation from the basal forebrain, or both, are particularly vulnerable to the effect of chronic ethanol consumption resulting in a decreased number of CA1 and CA3 pyramidal neurons, of mossy fiber-CA3 synapses, dentate gyrus granule cells and local circuit interneurons. (Riley and Walker 1978; Walker *et al.* 1980a, b; Lescaudron *et al.* 1986; Beracochea *et al.* 1987; Cadete-Leite *et al.* 1989a, b; Bengoechea and Gonzalo 1991). The extent of neuronal loss ranges from 10 to 40 % of the neurons. Hippocampal neurons appear to be differentially susceptible to the toxic effects of ethanol both within and between cell types. Granular cells in the dentate gyrus are more affected than pyramidal neurons, but the reason for this selectivity is unknown. The time course of the development of the structural changes in the hippocampus parallels that of cognitive deficits and depends on the duration and quantity of ethanol consumed (Walker *et al.* 1980b). However, neuropathological alteration in cortical and hippocampal regions have been also reported in rats after subchronic treatment (3 days) with high, intoxicating doses of ethanol (Zou *et al.* 1996). Human hippocampus is less affected by alcohol; however frontal cortical neurons are significantly affected (Harper and Matsumoto 2005). Many of the executionary pathways of cell death share common molecular mechanisms in different regions of the brain. Our aim in this study was to look at a host of different molecules making a cascade and since rodent hippocampus and cortex has been well studied, we could correlate this study with previous studies.

Chronic ethanol administration in rats produces a loss of cholinergic neurons in the basal forebrain. The loss of neurons in this region is more pronounced in the

medial septum and diagonal band nuclei than in the nucleus basalis (Arendt *et al.* 1988b). The nucleus basalis innervates the neocortex, whereas the cholinergic septohippocampal pathways terminate in the vicinity of the pyramidal (or granular) layers and in various dendritic segments of the hippocampus and modulate its activity (Mesulam *et al.* 1983). Neurodegeneration of these cholinergic pathways is therefore expected to alter the function of the innervated structures.

The alterations in hippocampal morphology after chronic ethanol exposure are associated with functional changes as revealed by electrophysiological methods. These functional changes include reduction in inhibitory processes (Abraham *et al.* 1981; Durand and Carlen 1984a; Rogers and Hunter 1992), alteration in synaptic plasticity and impairment of long-term potentiation in the dentate gyrus (Abraham *et al.* 1984; Durand and Carlen 1984b). The reduction of inhibitory processes (recurrent inhibition in CA1 cells) was observed in hippocampal slices of rats treated for 28 weeks with nutritionally adequate ethanol liquid diet (Rogers and Hunter 1992). The reduction of inhibition has been attributed to damage to GABAergic interneurons (Lescaudron *et al.* 1986) or to a reduction of the inhibitory modulation by cholinergic interneurons (Rothberg *et al.* 1993).

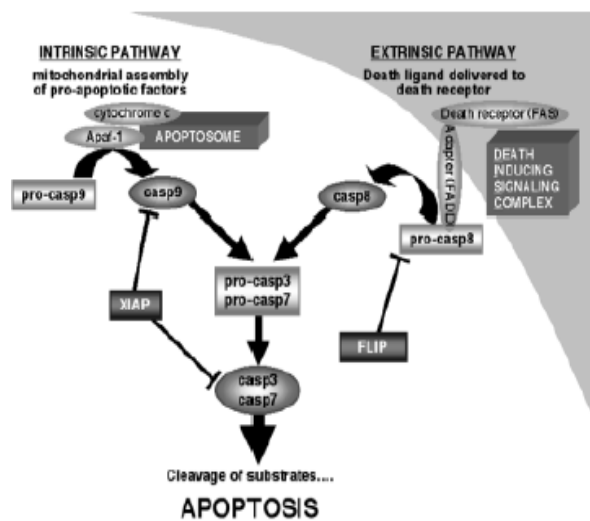
The development of the ethanol-induced neuronal damage is associated with an impairment of memory performance (Arendt *et al.* 1987, 1988b). Ethanol induced cognitive deficits can occur after 3-6 months of treatment (Walker and Freund 1973; Walker *et al.* 1980a; Walker and Hunter 1987). Further, damage to neurons of the cholinergic septohippocampal pathway destruction of postsynaptic neurons in the hippocampus or disruption of the output projections to the fimbria fornix produce impairment in memory, indicating that the integrity of this circuit is necessary for memory formation (Olton *et al.* 1979; Will and Heifti 1985; Hagan *et al.* 1988). Since the impairment of memory in lesioned rats is comparable to that elicited by chronic ethanol treatment, damage to these cholinergic nuclei contributes to the memory deficits associated with chronic ethanol intoxication. In rodent hippocampal neurons, chronic ethanol treatment reduces (Walker *et al.* 1980a) or does not change (McMullen *et al.* 1984) or increases (Durand *et al.* 1989) dendritic complexity, and reversibly decreases or increases the density of synaptic spines

(Durand *et al.* 1989) depending on the cell type. Long term administration of ethanol to rats causes memory deficits associated with 17% loss of neurons in the nucleus basalis (Arendt *et al.* 1988 a, b). Transplantation of cholinergic neurons into the hippocampus and neocortex corrects the memory abnormalities which suggest that in rats' ethanol directly damages cholinergic projection neurons (Arendt *et al.* 1988a; 1983). Animal models indicate that chronic alcohol treatment is associated with neuronal loss in hippocampal formation and basal forebrain (Fadda *et al.* 1998). The mechanisms underlying these deficits are far from known and possible explanation suggested is neurodegeneration.

Ethanol-related brain damage — mechanisms

There are several mechanisms that have been proposed to explain ethanol-related brain damage — these are not mutually exclusive. It is well known that ethanol, when administered acutely in a pharmacologically relevant dose, selectively and potently inhibits the function of N-methyl-D-aspartate (NMDA) receptors. The precise site of action has not yet been demonstrated. Chronic exposure to ethanol causes adaptive upregulation in sensitivity of NMDA receptors both *in vivo* and *in vitro*, which can result in an increased vulnerability for glutamate-induced cytotoxic response (excitotoxicity) (Dodd *et al.* 2000). This 'sensitization' of neuronal cells to excitotoxic insults is one of the most important factors in the mechanism underlying ethanol-induced brain damage. Increased calcium influx through NMDA receptors is tightly coupled to uptake into mitochondria and causes the production of reactive oxygen species that interfere with the function of mitochondria and plasma membranes. Primary inhibition of the mitochondrial respiratory chain can also indirectly induce further NMDA receptor stimulation. When the inhibitory action of ethanol on NMDA receptors is removed during withdrawal, the potential of neuronal injury is markedly increased through this receptor system, more so when withdrawal kindling (increased and/or prolonged withdrawal signs after repeated withdrawal) occurs (Matsumoto *et al.* 2001). Neurotrophic factors, particularly neurotrophins, play a vital role in neuronal survival and maturation, and are important in regulating

naturally occurring cell death through apoptotic mechanisms. Reduced levels of these trophic factors or deprivation of trophic-like effects from glial cells can induce alterations in the pattern of neuronal synaptic connections or cause cell death. Recent studies suggest that chronic exposure to ethanol can reduce the availability of brain-derived neurotrophic factor and alter its receptor (TrKB) function (Climent *et al.* 2002); receptors for nerve growth factor (TrKA) were also reduced (Miller *et al.* 2002). These changes could lead to impairment of the intracellular signaling pathways that control cell survival and death. It is reasonable to postulate that alteration of these chemical cascades could underlie the pathophysiology of neuronal cell death, as well as changes of neuronal circuits that might interfere with normal brain function and increase susceptibility to ethanol-induced cell damage.



Apoptotic pathways in neuronal apoptosis

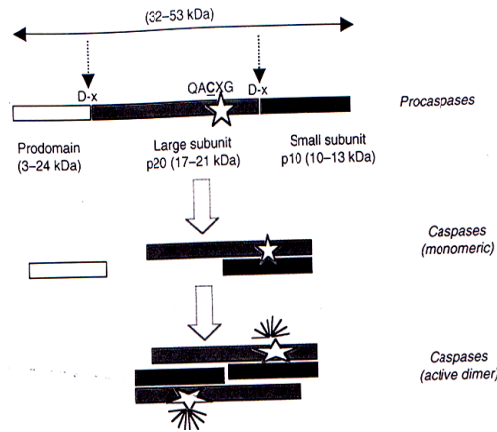
Fig 2. Pathways of apoptosis, adapted from Troy and Salvesen. Apoptotic pathways have been reviewed by Troy and Salvesen (2002). The intrinsic and extrinsic apoptosis pathways (Fig 2) converge on a common execution phase. The intrinsic pathway

responds primarily to cellular stress (ionizing radiation, cytotoxic drugs, etc.) as well as some neurodevelopmental cues, with the mitochondrion acting as an important integrator. Activation of the apical protease caspase 9 occurs when it is driven into a catalytic conformation by its cofactor Apaf-1, which itself requires prior binding to cytochrome c. The extrinsic apoptosis pathway is triggered through the extracellular ligation of death receptors (exemplified here by Fas) by their cognate ligands, resulting in receptor clustering, adapter recruitment (exemplified here by FADD), and activation of the apical protease caspase 8 (active forms of caspases in ovals). Thus, death receptors act as a conduit for the transmission of extracellular death

signals into the cell's interior. Both pathways activate the common executioner proteases caspases 3 and 7. Natural inhibitors (exemplified by FLIP and XIAP) affect different points on the pathways

Structural organization and activation of caspases.

Fig 3. Mechanism of caspase activation



The caspases are produced as pro-enzymes (32-53 k Da), including a prodomain (3-24 k Da), the large subunit (17-21 k Da) containing the active site, and the small subunit (10-13 k Da). To become enzymatically active, these three components must be proteolytically cleaved (D-x site), a phenomenon that is regulated by the prodomain itself; this allows the assembly of the large

and small subunits, with the dimerization into a functional enzyme (Nicholson *et al.* 2004). Functions of active caspase 3, 7, 9 and PARP are shown in Table 2.

Table 2 Caspases and their target (PARP) functions:

Caspase 3	Apoptosis-cleaves PARP (Casciola-Rosen <i>et al.</i> 1996; Duan <i>et al.</i> 1996; Fernandes-Alnemri <i>et al.</i> 1996)
Caspase 7	Apoptosis- cleaves PARP (Casciola-Rosen <i>et al.</i> 1996; Duan <i>et al.</i> 1996)
Caspase 9	Apoptosis- cleaves PARP (Casciola-Rosen <i>et al.</i> 1996; Duan <i>et al.</i> 1996), regulated by Akt and p21-Ras via direct phosphorylation (Cardone <i>et al.</i> 1998)
PARP(Poly	Nuclear enzyme (116 kDa) activated by DNA strand breaks,

{ADP-ribose} indirect role in DNA repair (Lindahl *et al.* 1995; Sallmann *et al.*
polymerase) 1997; Pieper *et al.* 1999; Saraste and Pulkki 2000). Cleaved by
caspases (caspase-3). Signature fragment is 85 kDa (Kaufmann *et al.* 1993; Lazebnik *et al.* 1994; Duriez and Shah 1997)

CHAPTER 1

Differential modulation of cell death associated proteins in rat hippocampus and frontal cortex after chronic ethanol consumption.

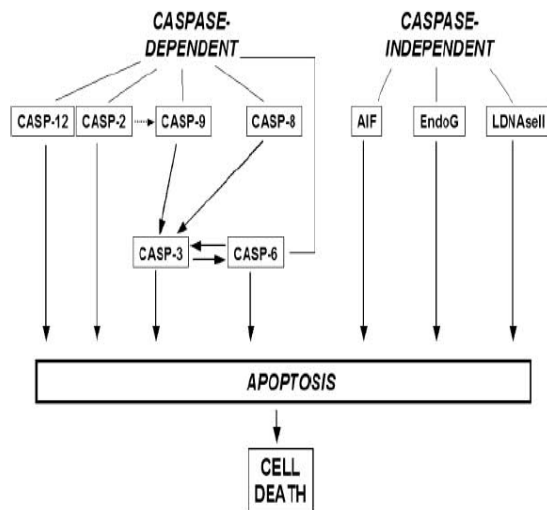
Caspase activation

Recently two studies have revealed cytochrome c release, enhanced processing of procaspase-3 (Rajgopal *et al.* 2003; Valles *et al.* 2004) and procaspase-9 to their respective active forms, increased cleavage of PARP-1 and PKC- δ leading to DNA fragmentation to a higher extent in cerebellum than cortex after *in vivo* chronic ethanol treatment (Rajgopal *et al.* 2003).

Release of apoptosis-inducing factor

Apoptosis inducing factor (AIF) is a 57 k Da flavoprotein that resembles bacterial oxidoreductase and resides in the mitochondrial intermembrane space (Susin *et al.* 1999). Upon induction of apoptosis, AIF

Fig.4 Caspase dependent and independent cell death cascade



translocates from the mitochondria to the nucleus and causes chromatin condensation

and large-scale DNA fragmentation (Susin *et al.* 1999). These effects are

independent of caspases and the

oxidoreductase activity of AIF

(Miramar *et al.* 2001). Deficiency

of AIF has profound effects in

animal development. Disruption

of AIF in mice prevents the

normal apoptosis necessary for

the cavitation of embryoid bodies

in the embryo (Joza *et al.* 2001).

This very early apoptotic event is

essential for mouse morphogenesis. Moreover, embryonic stem cells lacking AIF are

resistant to cell death after vitamin K3 treatment and serum starvation (Joza *et al.*

2001). Because AIF is also an oxidoreductase that may play an important role in normal mitochondrial physiology, it is not clear whether the observed phenotype in the AIF KO mouse embryos is caused entirely by the elimination of the apoptotic activity of AIF or because of the loss of oxidoreductase function of AIF as well. What remains to be worked out is the biochemical mechanism by which AIF induces large-scale DNA fragmentation and chromatin condensation. AIF itself has no measurable Dnase activity (Susin *et al.* 1999), It is possible that AIF may work with another protein to cause such an effect.

Release of cytochrome C

Cytochrome c, a component of the mitochondrial electron transfer chain, initiates caspase activation when released from mitochondria during apoptosis (Liu *et al.* 1996). Cytosolic cytochrome c binds to APAF-1, a cytosolic protein containing a caspase-recruitment domain (CARD), a nucleotide-binding domain, and multiple WD-40 repeats (Zou *et al.* 1999). Apaf-1 alone binds the nucleotide dATP or ATP poorly, despite the presence of Walker's consensus nucleotide binding sequences, however, the binding of cytochrome c, which is not dependent on the presence of nucleotide, increases APAF-1 affinity for dATP/ATP by about 10 fold, perhaps by opening up the nucleotide binding site or stabilizing the bound nucleotide to Apaf-1 (Jiang and Wang 2000). The binding of nucleotide to the Apaf-1/cytochrome c complex triggers its oligomerization to form the apoptosome, a multimeric Apaf-1 and cytochrome c complex (Zou *et al.* 1999). The CARD domains of Apaf-1 become exposed in the apoptosome, which subsequently recruit multiple procaspase-9 molecules to the complex and facilitate their autoactivation. Only the caspase-9 bound to the apoptosome is able to efficiently cleave and activate downstream executioner caspases such as caspase-3 (Rodriguez and Lazebnik 1999). These executioner caspases subsequently cleave many important intracellular substrates, leading to characteristic morphological changes in apoptosis such as chromatin condensation, nucleosomal DNA fragmentation, nuclear membrane breakdown, externalization of phosphatidyl-serine, and formation of apoptotic

bodies (Hengartner 2000).

Bcl-2 Family

Under normal conditions, the anti-apoptotic Bcl-2-like family members (Bcl-2, Bcl-XL, Bcl-W) directly interact and dimerize with the pro-apoptotic Bcl-2 members like Bax and Bak, sequestering them in the cytosol so that they are unable to translocate to mitochondria and trigger apoptogenic factor release (Cheng *et al.* 2001). The neonatal rodent brain, which is roughly developmentally equivalent to the perinatal human brain, shows a marked sensitivity to a variety of insults. Olney and co workers have reported extensive caspase-3 activation and apoptotic neuronal degeneration throughout the central nervous system of neonatal rats and/or mice exposed to antiepileptic drugs, anesthetic agents, or ethanol (Ikonomidou *et al.* 2000; Bittigau *et al.* 2002; Olney *et al.* 2002; Jevtovic-Todorovic *et al.* 2003). Prenatal or early postnatal ethanol exposure results in relative increases of Bax and Bcl-XS mRNA and protein levels as compared to Bcl-2 in the cerebellum and cortex (Heaton *et al.* 1999; Mooney *et al.* 2001; Heaton *et al.* 2003). Additionally, transgenic neonatal mice overexpressing Bcl-2 are protected against ethanol-induced neuronal cell death (Heaton *et al.* 1999). The role of pro-apoptotic Bcl-2 family members in ethanol-induced neuronal apoptosis has been examined in Bax-deficient neonatal mice (Young *et al.* 2003). Unlike wild-type mice, ethanol-exposed Bax-deficient animals show no increase in caspase-3 activity, TUNEL staining, or apoptotic neurons. Quantitative determination of neuron density in ethanol-exposed wild-type and Bax-deficient neonatal mice showed a marked loss of neurons in wild-type mice, but no loss of neurons either 24 or 72 h after ethanol exposure in Bax-deficient mice, indicating that Bax deficiency provides prolonged protection from ethanol-induced neuronal degeneration. These studies suggest that Bax, and likely other Bcl-2 family members, play an important function during the perinatal period of human nervous system development.

Bad

Bad, another BH3 only protein is regulated primarily by phosphorylation and dephosphorylation (Zha *et al.* 1996). In the absence of survival signals, Bad is dephosphorylated. The BH3 domain of Bad binds to and inactivates the antiapoptotic members of Bcl-2 family at the outer mitochondrial membrane, thereby promoting cell death. Conversely, in the presence of trophic factors, Akt and mitochondria anchored PKA phosphorylate Bad, allowing it to bind 14-3-3 protein and to remain in the cytosol (Datta *et al.* 1997; Harada *et al.* 1999). Phosphorylation of Bad also dissociates its interaction with antiapoptotic Bcl-2 family of proteins, allowing these proteins to promote survival. The critical site of phosphorylation induced by survival factors occurs at Ser 155 within the BH3 domain of Bad (Datta *et al.* 2000; Virdee *et al.* 2000; Zhou *et al.* 2000). This phosphorylation requires prior phosphorylation of ser 112 and ser 136, which recruits 14-3-3 proteins to the Bad/Bcl-xL complex (Datta *et al.* 1997; Zha *et al.* 1996; Harada *et al.* 1999). 14-3-3 proteins effectively increase the accessibility of Bad to ser-155 kinases, which then phosphorylate Bad within its BH3 domain. Phosphorylation of this domain permanently blocks the ability of Bad to bind Bcl-xL because of electrostatic and steric constraints and consequently inhibits Bad-mediated death (Datta *et al.* 2000). Several phosphatases, including calcineurin, protein phosphatase 1 alpha, and protein phosphatase 2A, have been shown to dephosphorylate Bad *in vitro* (Wang *et al.* 1999; Ayllon *et al.* 2000; Chiang *et al.* 2001). How these phosphatases are regulated *in vivo* by apoptotic signals remains to be investigated.

NMDA receptor

Chronic consumption of ethanol also leads to enhanced NMDAR –mediated neurotransmission (Nagy 2004). NR1 subunit in combination with one or more NR2 subunits (A-D) will compose an NMDA receptor (Mc Bain and Mayer 1994). NMDA receptor subunits were not altered in hippocampal homogenates by chronic consumption of alcohol (Ferreira *et al.* 2001). Some authors reported no changes in subunit expression due to long term ethanol exposure; others observed changes

solely in the expression of NR2A subunit. Levels of NR2B as well as NR2A and NR1 subunit proteins were reported to be increased in the cortex and hippocampus of rats or mice (Nagy 2004). Our Lab has shown previously an increased immunoreactivity of NR2A subunit in cerebral cortex and no immunoreactivity in cerebellum of alcohol-treated rats (Sultana *et al.* 2003). It is well known that activation of NMDA receptors will lead to influx of calcium. Calcium flux measurements by indicators are neither specific nor sensitive for apoptosis, as apoptosis without Ca⁺² rise has been observed (Whyte *et al.* 1993; McConkey 1996; Berridge *et al.* 1999). Further, calpains are activated due to a rise in intracellular calcium. Calpains are implicated in disease and injury models where intracellular calcium is known to be elevated, including Parkinson's disease (PD), Alzheimers disease, multiple sclerosis, muscular dystrophy and traumatic spinal cord injury (Harwood *et al.* 2005). Calpains have also been implicated in ethanol-mediated cell injury and alcoholic neurodegeneration. (Rajgopal and Vemuri 2002).

Calpains

Calpains are a family of calcium-dependent cysteine proteases that perform limited proteolytic cleavage of a variety of cellular substrates (Goll *et al.* 2003). There are two ubiquitous isoforms of calpains, μ -calpain (calpain I) and m-calpain (calpain II) that are activated by micro- and milli-molar concentrations of Ca²⁺ *in vitro*, respectively. The ubiquitous isoforms are heterodimers composed of a distinct 80 kDa catalytic subunit and an identical 30 kDa regulatory subunit. Both, the large and the small subunit contain multiple calcium-binding sites (Hosfeld *et al.* 1999; Strobl *et al.* 2000). Additional functions have been ascribed to calpains in cell motility and growth cone motility and guidance in neurons (Robles *et al.* 2003). The role of calpains in neuronal cell death has been examined in a number of neuropathological conditions (Lee *et al.* 2000; Kim *et al.* 2001; Ray *et al.* 2003). Inhibition of calpains prevents neuronal and behavioural defects in a mouse model of PD and calpain activation was evident in post-mortem midbrain tissues from cases of PD (Crocker *et al.* 2003). Calpains are also activated in Huntingtons Disease (Gafni and Ellerby

2002) and htt is degraded to small fragments by calpain after ischemic injury in rat brains (Kim *et al.* 2003). Calpain activation has also been reported in a number of *in vivo* and cell culture models of apoptosis. Members of the Bcl- 2 protein family of cell death regulators can be processed by calpains (Gil-Parrado *et al.* 2002). Further, it has been observed calpain-mediated cleavage of caspases can result in its activation (Blomgren *et al.* 2001). Inhibition of calpain by either association with its intrinsic inhibitor calpastatin or by pharmacological inhibitors results in reduced p53 activation and cytochrome c release, preventing death of embryonic cortical neurons. There is also evidence of caspase-independent contribution of calpains to apoptotic events that accompany excitotoxicity (Chen *et al.* 2001; Chen *et al.* 2002). Recent *in vitro* experiments show that, in isolated liver and brain mitochondria, release of cytochrome c does not require active calpain. (Polster *et al.*2004).

Scope of the present study

Although the neuropathology of alcohol consumption has been extensively investigated, the cellular and molecular basis of pathology remains still unclear, particularly the intricacy of the different factors described as being involved in its pathogenesis. Since every cell has the programme for death under the appropriate stimulus (Trump *et al.* 1997), the present study was carried out to look for cell death cascades upon chronic alcohol administration. Very few studies on alcohol induced cell death in mature nervous system are reported. Recently, activation of mitochondrial pathway of apoptosis in rat cerebral cortex and cerebellum of adult rat following *in vivo* chronic ethanol treatment was confirmed by observation of release of cytochrome c from mitochondria with activation of caspase-3, leading to cleavage of PARP. It was also associated with activation of m-calpain (Rajgopal and Vemuri 2002; Rajgopal *et al.* 2003; Valles *et al.* 2004). Further it has been reported that binge drinking induces neurodegeneration that is necrotic (Obernier *et al.* 2002) whereas chronic administration leads to induction of apoptosis (Rajgopal *et al.* 2003) associated with activation of calpains (Rajgopal and Vemuri 2002), which are largely involved in necrotic cell death. Hence we studied the role of cysteine proteases (caspases, calpains) which are involved in the initiation and progression of cell death in brain, by employing a combination of biochemical and morphological techniques. The aim of the present study is to understand the cell death cascade activated in the brain upon chronic alcohol administration in rat. A better understanding of the contribution of the apoptotic and necrotic cascades to the pathology might represent important pharmacological implications for alcohol therapy. In brief, the present study examines the involvement of caspase dependent and caspase independent pathways of apoptosis, in hippocampus and frontal cortex following chronic ethanol administration. For this purpose western immunoblot of active caspase-3 and AIF has been carried out following administration of ethanol. These data have been compared with subfractionation studies analyzing cytochrome-c, Bcl-2, Bax, and Bad translocations. Our aim was to increase understanding on the differential subcellular expression of proteins involved in cell death in hippocampus

and frontal cortex after chronic ethanol administration. To further show the involvement of excitotoxicity, immunoblots of NMDA receptor subunits, and the downstream targets, calpains, were done.

Chemicals

Dithiothreitol (DTT), nitroblue tetrazolium (NBT), 5-bromo-4-chloro-3-indoxyl phosphate (BCIP), Tween 20, phenylmethylsulfonyl fluoride (PMSF), bovine serum albumin (BSA), Ethylenediaminetetraacetic acid (EDTA), magnesium chloride (MgCl₂), sodium chloride (NaCl), potassium chloride (KCl), were purchased from Sisco Research Laboratories Pvt. Ltd. (Mumbai, India). Nitrocellulose sheet was from Millipore (Billerica, MA, USA) and secondary antibodies were purchased from Bangalore Genei Pvt. Ltd. (Bangalore, India). All other chemicals were of analytical grade and Purchased locally.

General Methods

Animals and treatment

Male *Wistar* strain rats (100 ± 10 g) were maintained in the animal house facility at a temperature (25-28°C) and light/dark cycle (12/12 h). Studies in rodents have shown that exposure to ethanol, particularly, the first two postnatal weeks in the rat, causes microencephaly, which is irreversible. Most of the studies concentrate on developmental exposure to ethanol and are usually carried out during this period, however the present studies were not carried out in such age group, hence we considered them to be adult animals, just to differentiate from developmental exposure. Experimental protocols for the use of animals were followed according to Committee for the purpose of control and supervision on experiments on animals (CPCSEA) guidelines for laboratory animal facility [Committee for the purpose of control and supervision on experiments on animals (2003)] and approved by the Institutional Animal Ethics Committee (IAEC), University of Hyderabad,

Hyderabad, India. The animals were assigned to control, and ethanol treated groups. Each group (n = 5 animals) of animals had free access to standard commercial rat chow purchased from National Institute of Nutrition (Hyderabad, India). The control group received basal diet and water, whereas the ethanol treated group received basal diet and 10% (vol/vol) ethanol in water. Every alternate day rat weight, food consumption and fluid consumption profiles were recorded and plotted as graphs. The caloric percentage of ingredients of the final regimen (basal diet + alcohol) consumed by ethanol treated group was 13.8% ethanol, 61.2% carbohydrates, 7.0% fat, and 18.0% protein. On the last day of the experiment (after 12 weeks of ethanol treatment), each animal was killed by cervical dislocation [Committee for the purpose of control and supervision on experiments on animals (2003)]. The brain of each animal was subsequently removed; hippocampus and frontal cortex was dissected and processed for biochemical analysis or stored at -70°C until further use.

Isolation of hippocampus and frontal cortex

Fig 5 Rat brain showing hippocampus and frontal cortex

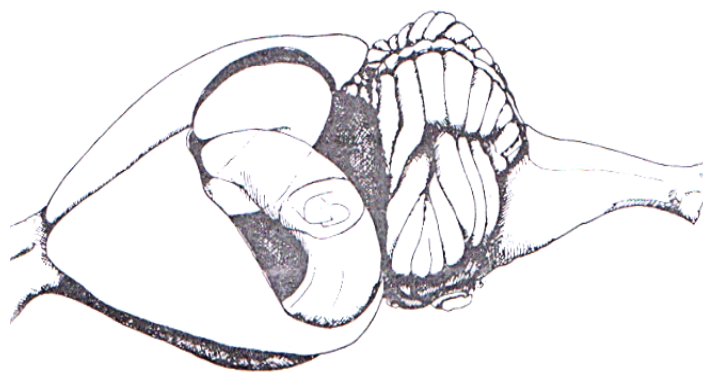


Figure 5 shows the phantom drawing of the hippocampus and frontal cortex of rat brain. Neocortex has been removed to expose underlying hippocampus. The anterior region of the cerebral cortex was considered frontal

cortex. Both the regions were dissected and processed for biochemical studies. (Adapted from Paul *et al.* 1997)

Sub fractionation

The nuclear, cytosolic and mitochondrial fractions were prepared as described by Douglas and Douglas (2002). Briefly, hippocampus and frontal cortex from control and ethanol fed rats were homogenized in 7 vol of ice-cold “Homogenization buffer” containing 250 mM sucrose, 20 mM HEPES-NaOH buffer (pH 7.4), 10 mM KCl, 1 mM MgCl₂, 2 mM EDTA, 1 mM DTT, 1 mM Phenylmethylsulfonyl fluoride, Leupeptin (2 µg/ml) and aprotinin (2 µg/ml) by douncing 30 times in a glass tissue homogenizer (Wheaton, Millville, USA). The homogenates were first centrifuged at 800 x g for 10 min at 4⁰C and the pellet was used as crude nuclei fraction after solubilization in Homogenization buffer. This fraction was used for Poly (ADP-ribose) Polymerase -1 immunoblot analysis. The post nuclear supernatant was further centrifuged at 22,000 x g for 15 min at 4⁰C and the resulting supernatant corresponding to crude cytosolic fraction was used for immunoblot analysis of active caspase 3, active caspase 7, active caspase 9, Bcl-2 family proteins, cytochrome c and calpain. The pellet representing the membrane and mitochondria rich fraction was used for detecting Bcl-2 family proteins, cytochrome c and NMDA receptor subunits after solubilization in Homogenization buffer. Protein content in different subcellular fractions was quantified by the method of Lowry *et al.* (1951).

Gel electrophoresis and Western blotting

Fifty micrograms of cytosolic/mitochondrial protein was separated by reducing sodium dodecyl sulphate polyacrylamide gel electrophoresis (SDS-PAGE). Protein transfer was performed according to the method of Towbin *et al.* (1979). Briefly, proteins were transferred onto nitrocellulose membrane overnight at 30 V in Towbin buffer (25 mM Tris-HCl (pH 8.3), 192 mM glycine, 20% methanol). The non-specific binding sites were blocked with 5% (w/v) non-fat milk for 2 h. The blots were probed with primary antibodies. The primary antibodies were 1: 1000 dilution of Rabbit polyclonal antibody against active caspase 3, active caspase-7, active caspase 9 and PARP (Cell Signaling technology, MA, USA), 1: 500 dilution of

mouse polyclonal antibody against Bad, 1:250 dilution of mouse polyclonal antibody against Bax, 1:500 dilution of mouse polyclonal antibody against Bcl-2 (BD Biosciences, CA, USA), 1:1000 dilution of Rabbit polyclonal antibody against AIF (Oncogene Research Products, CA, USA). 1:1000 dilution of Rabbit polyclonal antibody against NMDAR1, 1: 200 dilution of Rabbit polyclonal antibody against NMDAR2A, 1: 250 dilution of Rabbit polyclonal antibody against NMDAR2B, 1: 200 dilution of Rabbit polyclonal antibody against NMDAR2C (Chemicon international inc, Temecula, CA, USA), 1: 50 dilution of mouse monoclonal antibody against Calpain (Novocastra Laboratories Ltd, UK)-This antibody detects calpain 3 as well as μ -calpain (Calpain 1) and m-calpain (Calpain 2), 1: 1000 dilution of mouse monoclonal antibody against beta-Actin (42 k Da)(Novus biologicals, Inc, CO, USA). The blots were further processed with either Alkaline Phosphatase-conjugated anti-rabbit or anti-mouse secondary antibody. (Bangalore Genei, India). After developing, the membrane was dried, and densitometry analysis was performed using a color scanner (HP Scanjet 3200C) and the NIH Image software, ImageJ 1.34s (available for Windows through NIH: <http://rsb.info.nih.gov/ij/download.html>). As an example active caspase 3 data in cytosolic fraction has been shown in FC and FE region. The data has been analyzed as follows

	Area	Mean	Min	Max	IntDen
FC	1068	103.260	49	131	110282
FE	1068	115.432	35	153	123281
Blank	1068	0	0	0	0

The means were plotted as graphs after dividing with corresponding actin values.

Stripping

The same membrane was reprobed for actin to confirm consistent loading of samples. The membrane (sealed in a freezer bag) was incubated with 10 ml of stripping buffer and immersed in a 55° C water bath for 5 min. The membrane was removed and rinsed for 2 h in dH₂O, with constant changes of water. Recipe for

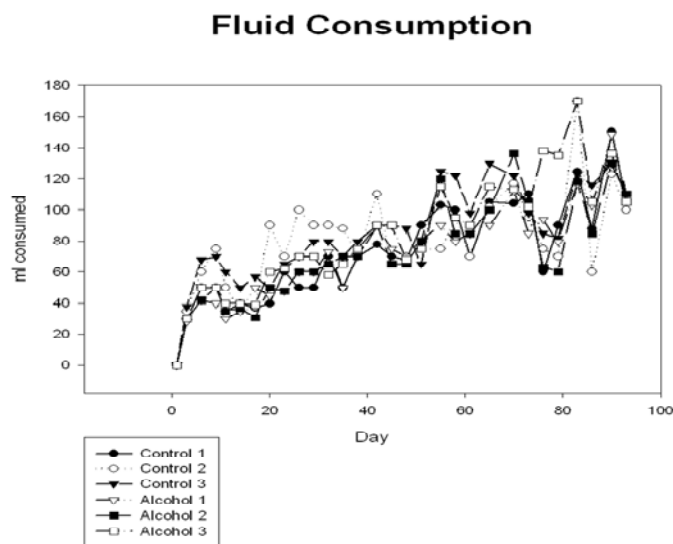
stripping buffer [Douglas and Douglas (2002)]: 50 ml of dH₂O was placed in a 100 ml flask (with stir bar). 7 ml of 1M Tris-HCl (pH 6.8), 2 g SDS, 1 ml of 2-mercaptoethanol were added and the final volume was made to 100 ml with dH₂O. This was stored at room temperature until used.

Data analysis

Data were analysed by one-way analysis of variance (ANOVA). When a significant F value was found, Fisher's least difference (LSD) multiple comparison was performed to test the differences between the means. Data are reported as mean \pm S.E.M. of n experiments. A level of P < 0.05 was considered statistically significant and was determined using SPSS for windows version.

Results

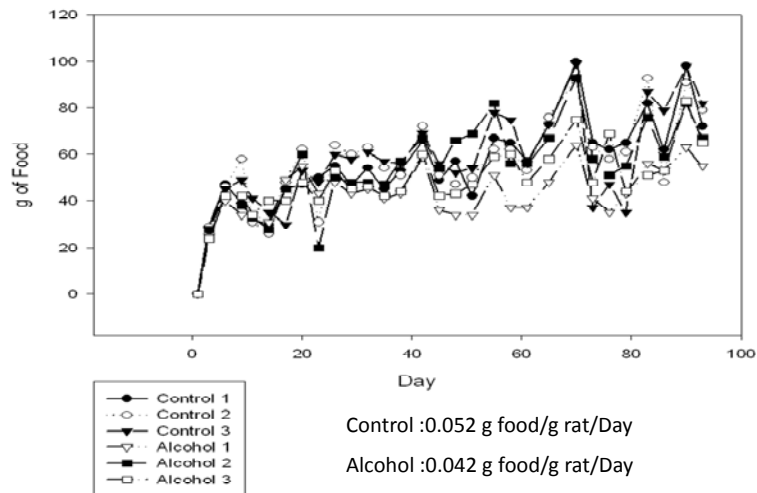
Fluid consumption (Fig 6), food consumption (Fig 7), and Rat weight (Fig 8) profiles:



Control :0.073 ml water/gm rat/Day

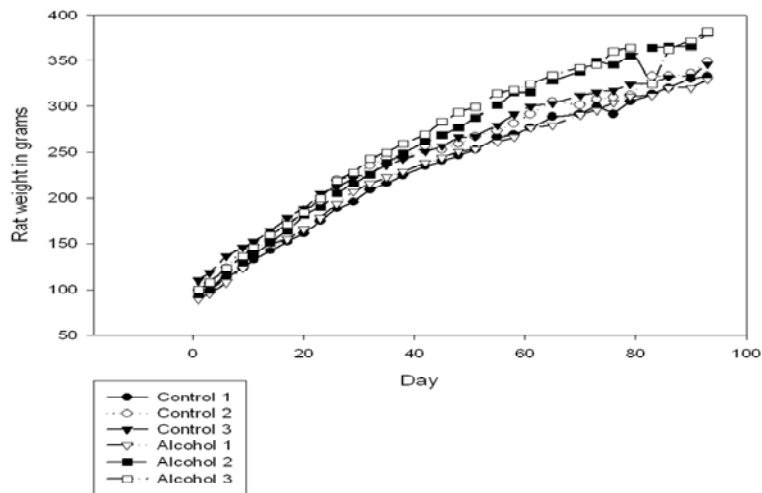
Alcohol :0.066 ml Alcohol/gm rat/Day (i.e 5.28 g/Kg/Day)

Food Consumption



(Laboratory instructions in biochemistry by Louis B.Dotti, chapter 16. Nutrition experiments)

Rat weight



Control group consumed 0.073 ml water/gm rat/Day and Alcohol treated group consumed 0.066 ml Alcohol/gm rat/Day (i.e 5.28 g/Kg/Day) (Fig 6). Control group consumed 0.052 g food/g rat/Day, whereas Alcohol group consumed 0.042 g food/g rat/Day (Fig 7). The body weight at the end of the treatment was slightly higher in alcohol treated group (Fig 8).

Effect on apoptosis associated proteins

SDS PAGE and ponceau staining is shown for equal protein loading in Fig 9. Immunoblot analysis of active caspase-3 (17 k Da), active caspase-7 (20 k Da) and active caspase-9 (17 k Da) showed significant increase in HE compared to control, HC, however no activation was observed in FE compared to control FC. in the cytosolic fractions. Calpain was activated in HE and no change was seen in FE compared to controls (Fig. 10 & 17). PARP-1 signature cleavage fragment (89 k Da) was not altered in HE, whereas significant increase was found in FE, compared to controls. AIF decreased in nuclear and cytosolic fractions of HE and also in cytosolic fraction of FE, however it increased in nuclear fraction of FE compared to control. AIF (57 k Da) translocation from cytosol to nucleus was not observed in HE, whereas significant translocation was observed in FE (Fig.11 & 18).

Mitochondrial cytochrome c, detected as a single band of molecular mass (14 k Da) was decreased in cytosolic fraction of HE and no significant alterations were found in mitochondria fraction of HE, However increased immunoreactivity was found in cytosolic fraction of FE and decreased immunoreactivity was found in mitochondria fraction of FE, compared to controls (Fig. 12 & 19). Clearly release of cytochrome c from the mitochondria to cytosol is observed in FE region. Bax (21 k Da) (Fig. 13 & 19) was not altered in cytosolic fractions in both the regions, however it decreased in mitochondrial fraction of HE and no change in immunoreactivity was found in FE, compared to controls. Bad (23 k Da) (Fig. 14 & 20) was found to be decreased in cytosolic and mitochondrial fractions of HE compared to controls and no significant changes were found in cytosolic and mitochondrial fractions of FE region compared to controls. However Bcl-2 (26 k Da) (Fig.15 & 20) was found to be increased in cytosolic fraction of HE compared to controls and no significant change was observed in FE region. Mitochondrial fraction for Bcl-2 showed a decrease in both the regions compared to controls.

Effect on NMDA receptor subunits and Calpains

Immunoblot analysis of NMDA receptor subunits (Fig.16 & 21) showed alteration of proteins. NMDAR1 (180 k Da) was increased in HE and no change was observed in FE when compared to controls. NMDAR2A (180 k Da) was not altered in both the regions compared to controls. NMDAR2B (180 k Da) was found to be increased in both the regions in this study and further the increase was more in FE than HE. NMDAR2C (140 k Da) revealed single band corresponding to its respective mass and was intensely increased in HE and significantly decreased in FE.

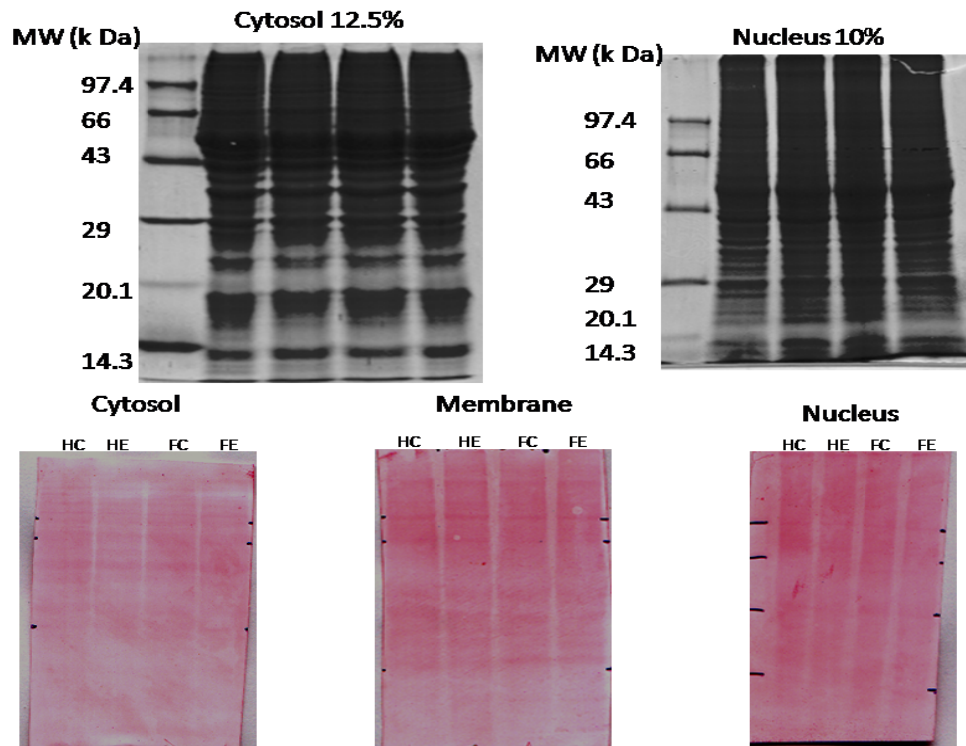


Fig 9 SDS page profiles and ponceau staining of subcellular fractions

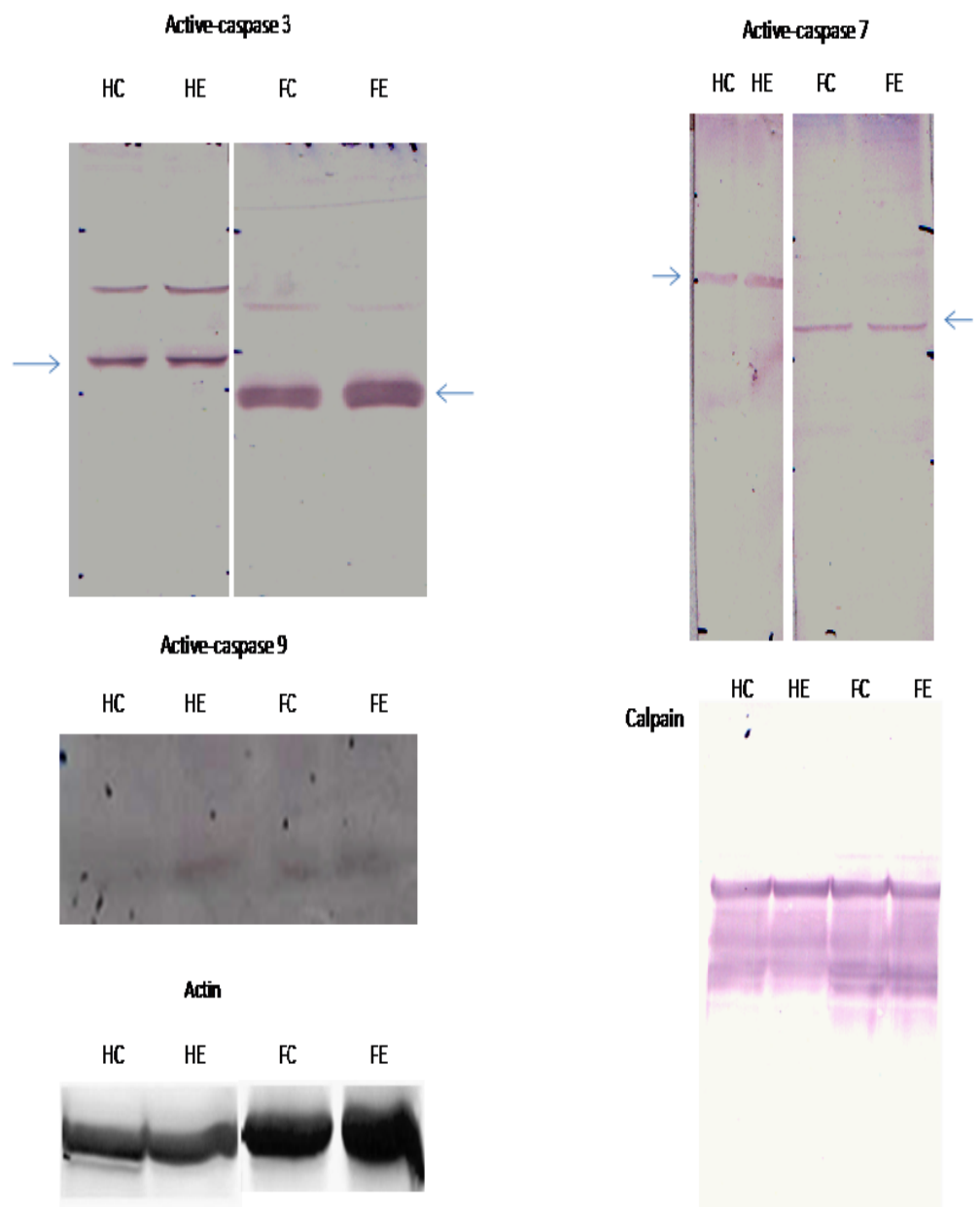


Fig 10. Immunoblot analysis of active caspase 3 (17 k Da), active caspase 7 (20 k Da), active caspase 9 (17 k Da) and calpain (80 k Da), from cytosolic fractions of control (HC-control hippocampus, FC-control frontal cortex) and ethanol-treated rat (HE- ethanol treated hippocampus, FE- ethanol treated frontal cortex). Actin (42 k Da) is shown to illustrate cytosolic equal protein loading.

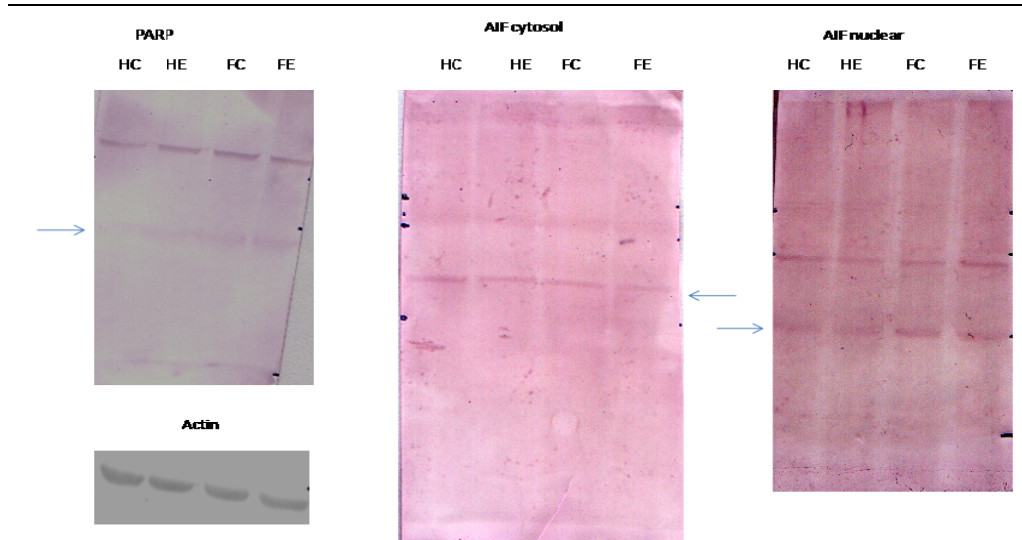


Fig 11. Western blot analysis of control (HC-control hippocampus, FC-control frontal cortex) and ethanol-treated rat (HE- ethanol treated hippocampus, FE- ethanol treated frontal cortex) showing PARP-1 signature cleavage fragment (89 k Da) and AIF (57 k Da). Actin is shown for loading control.

Cytochrome c

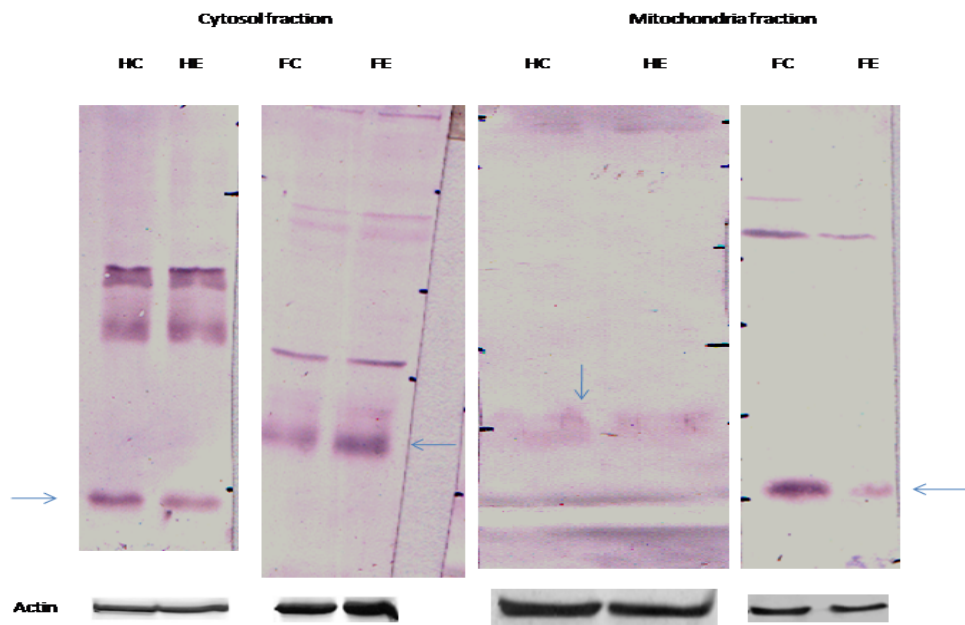


Fig 12. Western blot analysis of control (HC-control hippocampus, FC-control frontal cortex) and ethanol-treated rat (HE- ethanol treated hippocampus, FE- ethanol treated frontal cortex) showing Cytochrome c (14 k Da). Actin is shown for loading control.

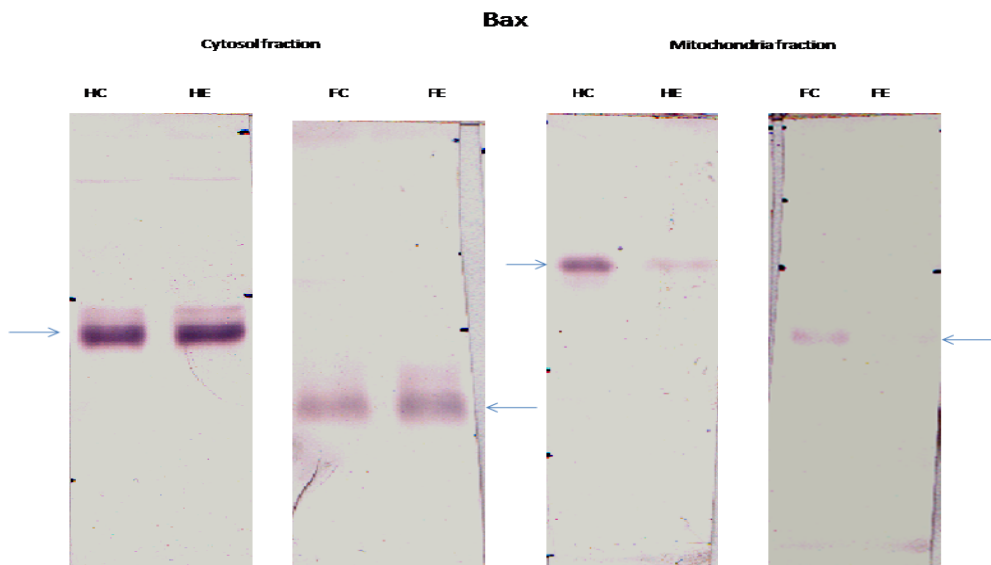


Fig 13. Immunoblot analysis of Bax (21 k Da) from cytosol and mitochondria fractions of control (HC-control hippocampus, FC-control frontal cortex) and ethanol-treated rat (HE- ethanol treated hippocampus, FE- ethanol treated frontal cortex).

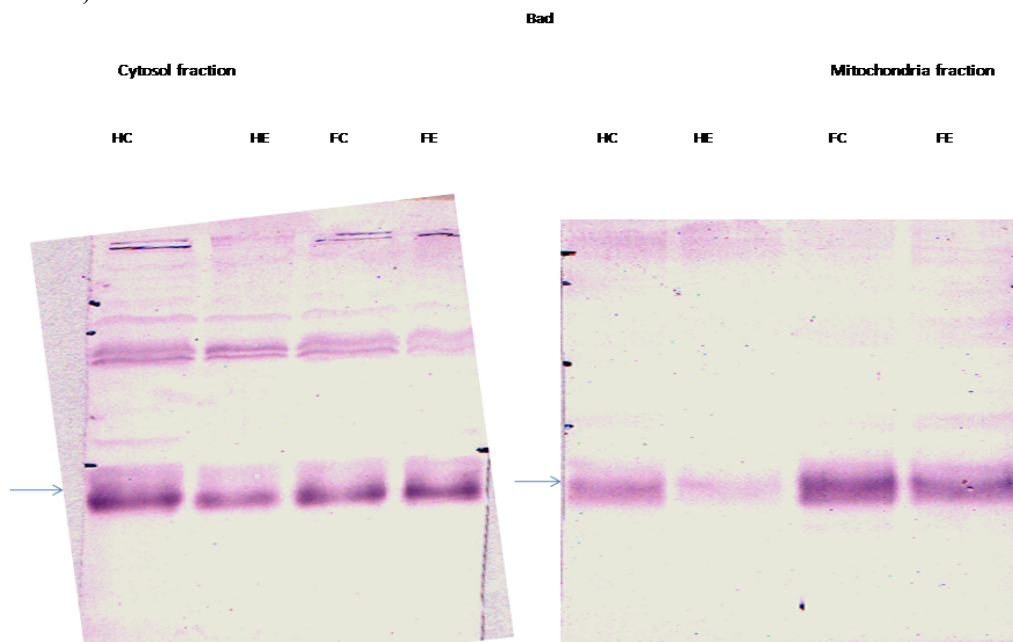


Fig 14. Immunoblot analysis of Bad (23 k Da) from cytosol and mitochondria fractions of control (HC-control hippocampus, FC-control frontal cortex) and ethanol-treated rat (HE- ethanol treated hippocampus, FE- ethanol treated frontal cortex).

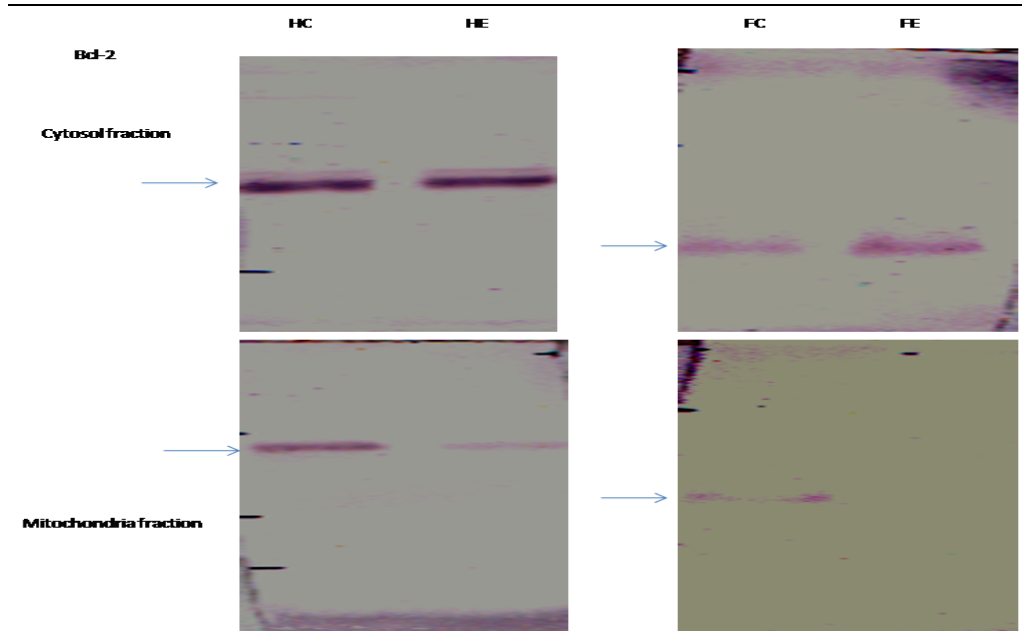


Fig 15. Immunoblot analysis of Bcl-2 (26 k Da) from cytosol and mitochondria fractions of control (HC-control hippocampus, FC-control frontal cortex) and ethanol-treated rat (HE- ethanol treated hippocampus, FE- ethanol treated frontal cortex).

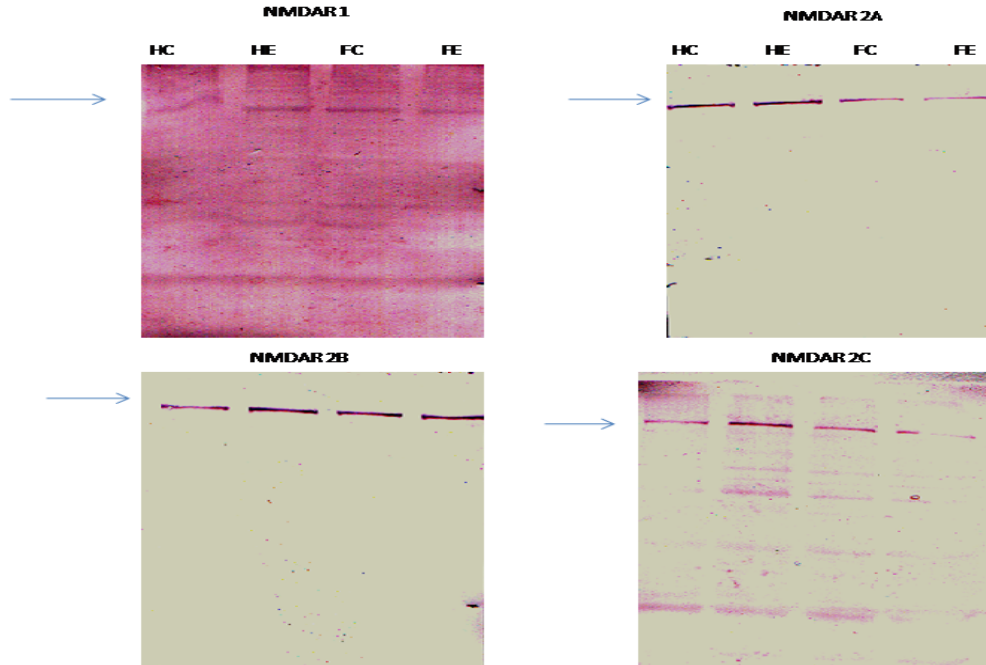


Fig 16. Immunoblot analysis of NMDA receptor subunits, namely NMDAR1 (180 k Da), NMDAR2A (180 k Da), NMDAR2B (180 k Da) and NMDAR2C (140 k Da).

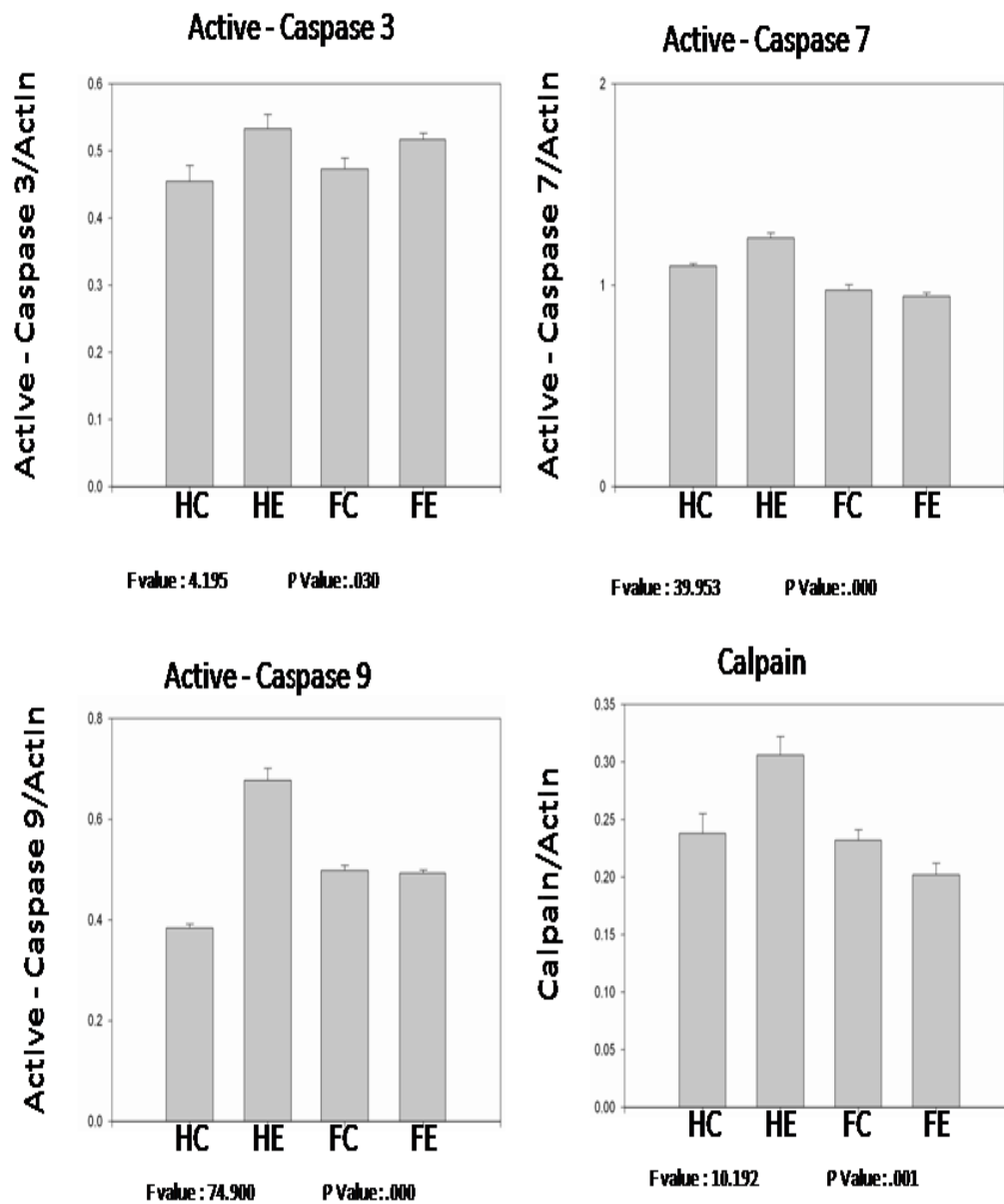


Fig 17. Densitometric scans of the immunoblots of active caspase-3, active caspase-7, active caspase-9 and calpain as arbitrary units. Each data point represents the mean from four analyses.

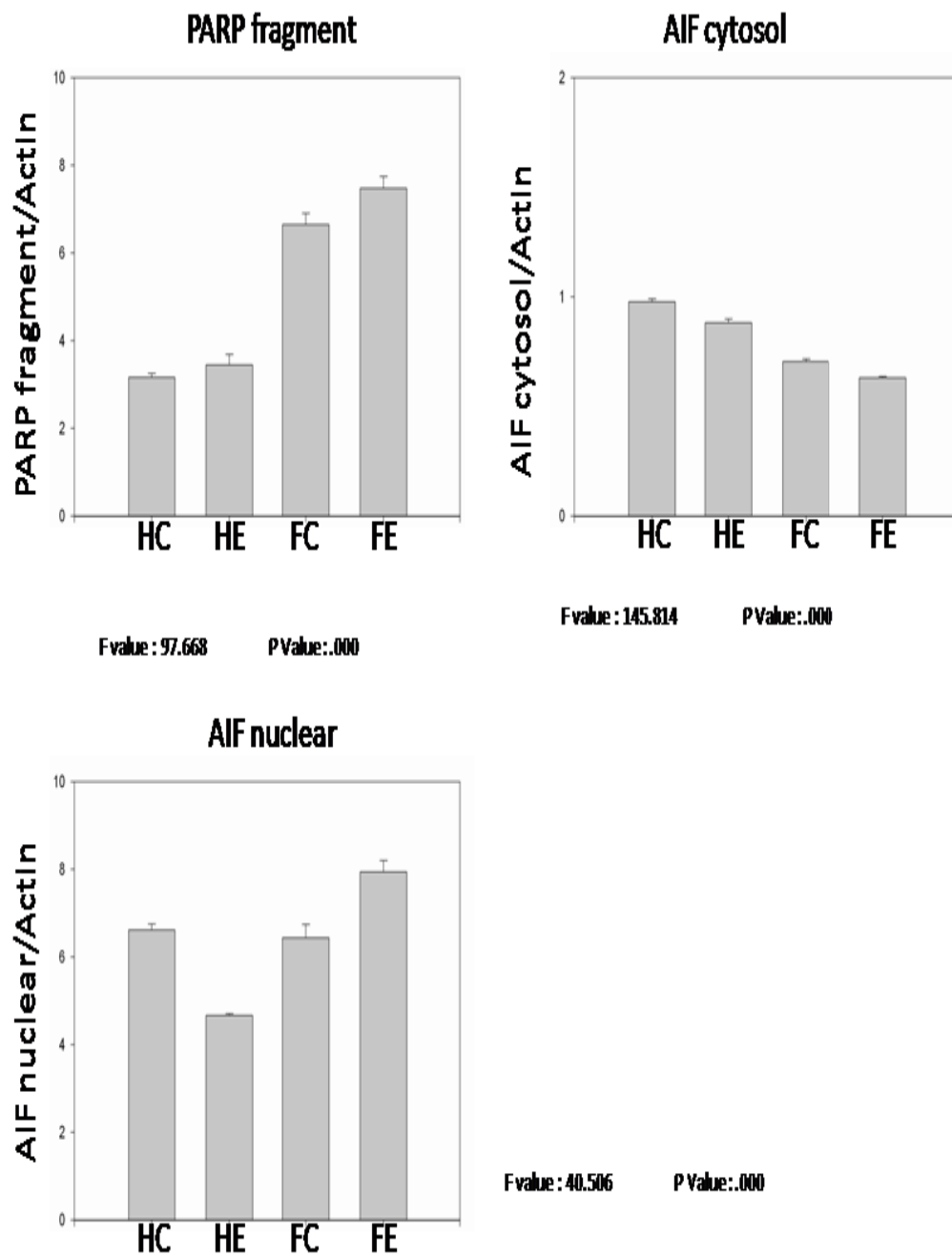


Fig 18. Densitometric scans of the immunoblots of PARP fragment, AIF cytosol and nuclear fractions as arbitrary units. Each data point represents the mean from four analyses.

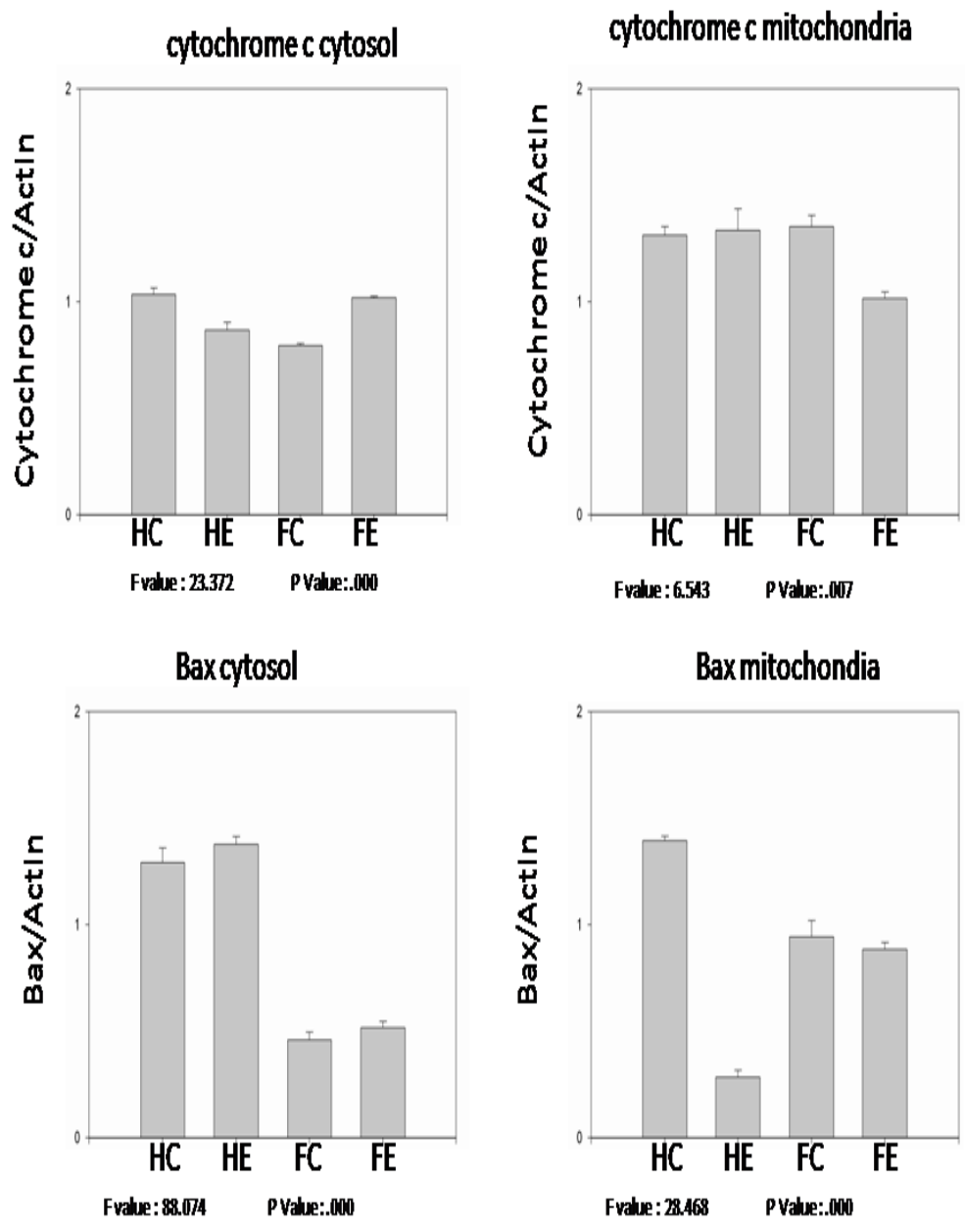


Fig 19. Densitometric scans of the immunoblots of Cytochrome c and Bax, Cytosol and mitochondria fractions as arbitrary units. Each data point represents the mean from four analyses.

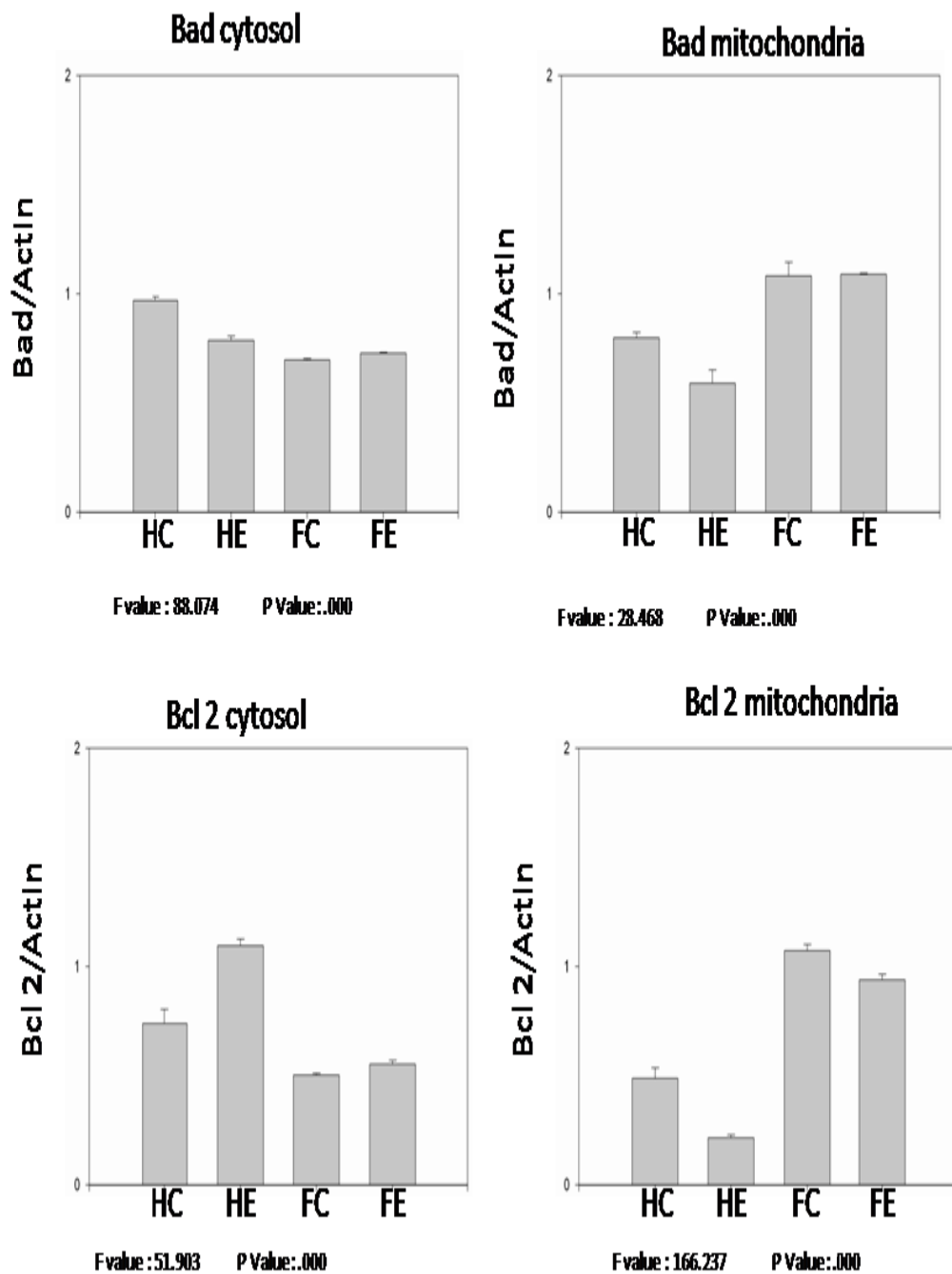


Fig 20. Densitometric scans of the immunoblots of Bad and Bcl-2, Cytosol and mitochondria fractions as arbitrary units. Each data point represents the mean from four analyses.

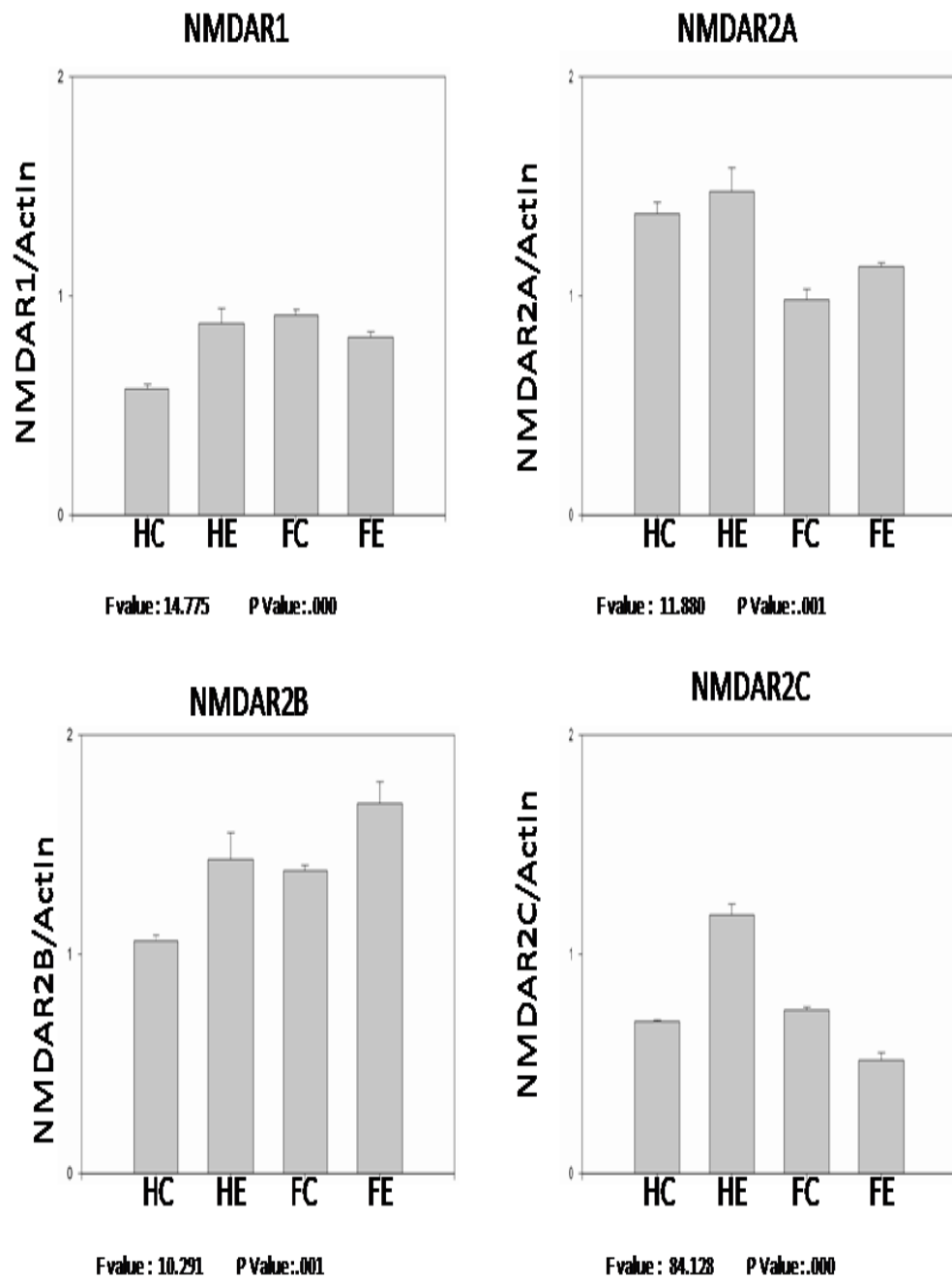


Fig 21. Densitometric scans of the immunoblots of NMDAR1, NMDAR2A, NMDAR2B, and NMDAR2C as arbitrary units. Each data point represents the mean from four analyses.

Table 3

Oneway Anova

1=HC; 2=FC; 3=HE; 4=FE

Descriptives									
		N	Mean	Std. Deviation	Std. Error	95% Confidence Interval for Mean		Minimum	Maximum
						Lower Bound	Upper Bound		
NMDAR2B	1	4	1.061	.048	.024	.984	1.138	1.019	1.110
	2	4	1.381	.048	.024	1.306	1.457	1.332	1.445
	3	4	1.433	.241	.121	1.050	1.817	1.276	1.792
	4	4	1.687	.201	.100	1.368	2.006	1.413	1.895
	Total	16	1.391	.271	.068	1.246	1.535	1.019	1.895
AIF cytosol	1	4	.977	.029	.014	.931	1.023	.948	1.016
	2	4	.704	.022	.011	.669	.738	.680	.732
	3	4	.882	.037	.018	.823	.940	.833	.919
	4	4	.631	.012	.006	.612	.650	.616	.643
	Total	16	.798	.144	.036	.721	.875	.616	1.016
AIF nuclear	1	4	6.620	.257	.129	6.210	7.029	6.412	6.986
	2	4	6.436	.619	.309	5.452	7.420	5.539	6.867
	3	4	4.665	.083	.041	4.533	4.797	4.591	4.754
	4	4	7.941	.509	.255	7.130	8.751	7.486	8.663
	Total	16	6.415	1.262	.315	5.743	7.088	4.591	8.663
Bad cytosol	1	4	.970	.033	.016	.918	1.022	.924	1.000
	2	4	.697	.012	.006	.678	.715	.681	.708
	3	4	.786	.038	.019	.725	.846	.731	.818
	4	4	.727	.008	.004	.714	.740	.716	.735
	Total	16	.795	.112	.028	.735	.854	.681	1.000
Bad mitochondria	1	4	.798	.048	.024	.721	.875	.753	.866
	2	4	1.082	.124	.062	.886	1.279	.898	1.159
	3	4	.591	.122	.061	.396	.786	.456	.753
	4	4	1.089	.010	.005	1.073	1.105	1.082	1.104
	Total	16	.890	.230	.058	.767	1.013	.456	1.159
Bax cytosol	1	4	1.292	.133	.067	1.080	1.504	1.103	1.416

	2	4	.459	.074	.037	.341	.577	.350	.515
	3	4	1.377	.075	.037	1.259	1.496	1.307	1.464
	4	4	.517	.056	.028	.428	.607	.433	.550
	Total	16	.911	.446	.111	.674	1.149	.350	1.464
Bax mitochondria	1	4	1.394	.042	.021	1.328	1.461	1.347	1.429
	2	4	.942	.154	.077	.697	1.187	.745	1.089
	3	4	.284	.065	.032	.181	.387	.229	.359
	4	4	.883	.068	.034	.775	.991	.791	.944
	Total	16	.876	.416	.104	.654	1.098	.229	1.429
Bcl 2 mitochondria	1	4	.487	.095	.048	.336	.639	.361	.585
	2	4	1.072	.058	.029	.979	1.164	1.015	1.150
	3	4	.215	.027	.014	.172	.258	.194	.255
	4	4	.940	.045	.023	.868	1.011	.881	.991
	Total	16	.678	.360	.090	.487	.870	.194	1.150
Bcl 2 cytosol	1	4	.738	.130	.065	.530	.946	.574	.865
	2	4	.503	.017	.008	.476	.530	.486	.519
	3	4	1.095	.062	.031	.997	1.193	1.015	1.163
	4	4	.552	.034	.017	.499	.606	.504	.575
	Total	16	.722	.249	.062	.589	.855	.486	1.163
Calpain	1	4	.238	.035	.017	.183	.293	.192	.266
	2	4	.232	.019	.009	.202	.262	.206	.251
	3	4	.306	.032	.016	.255	.357	.259	.331
	4	4	.202	.020	.010	.170	.235	.173	.220
	Total	16	.244	.046	.012	.220	.269	.173	.331
Active-caspase 3	1	4	.455	.046	.023	.383	.528	.395	.498
	2	4	.473	.031	.016	.423	.523	.435	.505
	3	4	.533	.041	.021	.467	.599	.483	.570
	4	4	.517	.018	.009	.489	.545	.493	.532
	Total	16	.495	.046	.011	.470	.519	.395	.570
Active-caspase 7	1	4	1.095	.024	.012	1.057	1.134	1.075	1.124
	2	4	.975	.052	.026	.893	1.057	.914	1.021
	3	4	1.234	.051	.025	1.153	1.315	1.186	1.303
	4	4	.945	.033	.017	.892	.998	.906	.986
	Total	16	1.062	.124	.031	.996	1.128	.906	1.303
Active-caspase 9	1	4	.384	.016	.008	.358	.409	.368	.401
	2	4	.498	.020	.010	.465	.530	.471	.514
	3	4	.677	.048	.024	.600	.754	.610	.720

	4	4	.493	.012	.006	.475	.512	.481	.504
	Total	16	.513	.112	.028	.454	.572	.368	.720
cytochrome c cytosol	1	4	1.034	.062	.031	.936	1.133	.943	1.081
	2	4	.794	.019	.010	.764	.825	.766	.805
	3	4	.866	.072	.036	.751	.980	.804	.962
	4	4	1.020	.009	.005	1.005	1.036	1.010	1.033
	Total	16	.929	.114	.028	.868	.989	.766	1.081
cytochrome c mitochondria	1	4	1.313	.079	.040	1.186	1.439	1.218	1.408
	2	4	1.352	.106	.053	1.184	1.521	1.202	1.449
	3	4	1.335	.204	.102	1.011	1.660	1.204	1.639
	4	4	1.016	.057	.029	.924	1.107	.947	1.069
	Total	16	1.254	.181	.045	1.157	1.351	.947	1.639
NMDAR1	1	4	.576	.037	.019	.516	.636	.539	.626
	2	4	.913	.048	.024	.835	.990	.845	.956
	3	4	.874	.135	.068	.658	1.089	.755	1.065
	4	4	.811	.051	.025	.731	.892	.736	.846
	Total	16	.793	.152	.038	.712	.874	.539	1.065
NMDAR2A	1	4	1.376	.101	.051	1.214	1.537	1.272	1.474
	2	4	.983	.095	.048	.831	1.135	.902	1.120
	3	4	1.476	.218	.109	1.129	1.824	1.343	1.801
	4	4	1.134	.032	.016	1.083	1.185	1.087	1.155
	Total	16	1.242	.232	.058	1.118	1.366	.902	1.801
NMDAR2C	1	4	.694	.012	.006	.674	.713	.682	.706
	2	4	.745	.025	.013	.704	.785	.722	.770
	3	4	1.179	.098	.049	1.024	1.335	1.103	1.315
	4	4	.517	.068	.034	.409	.626	.462	.615
	Total	16	.784	.257	.064	.647	.921	.462	1.315
PARP, 89	1	4	3.163	.175	.087	2.885	3.441	2.993	3.381
	2	4	6.651	.512	.256	5.837	7.465	6.027	7.220
	3	4	3.448	.474	.237	2.693	4.203	2.965	4.099
	4	4	7.479	.525	.262	6.643	8.314	6.970	8.209
	Total	16	5.185	2.007	.502	4.116	6.255	2.965	8.209

Test of Homogeneity of Variances				
	Levene Statistic	df1	df2	Sig.
NMDAR2B	2.658	3	12	.096
AIF cytosol	.963	3	12	.442

AIF nuclear	2.108	3	12	.153
Bad cytosol	2.047	3	12	.161
Bad mitochondria	2.301	3	12	.129
Bax cytosol	.926	3	12	.458
Bax mitochondria	3.812	3	12	.040
Bcl 2 mitochondria	1.479	3	12	.270
Bcl 2 cytosol	5.469	3	12	.013
Calpain	.912	3	12	.464
Active-caspase 3	1.736	3	12	.213
Active-caspase 7	1.336	3	12	.309
Active-caspase 9	2.159	3	12	.146
cytochrome c cytosol	3.680	3	12	.043
cytochrome c mitochondria	2.157	3	12	.146
NMDAR1	1.973	3	12	.172
NMDAR2A	3.337	3	12	.056
NMDAR2C	2.719	3	12	.091
PARP, 89	.859	3	12	.489

ANOVA						
		Sum of Squares	df	Mean Square	F	Sig.
NMDAR2B	Between Groups	.795	3	.265	10.291	.001
	Within Groups	.309	12	.026		
	Total	1.104	15			
AIF cytosol	Between Groups	.303	3	.101	145.814	.000
	Within Groups	.008	12	.001		
	Total	.311	15			
AIF nuclear	Between Groups	21.728	3	7.243	40.506	.000
	Within Groups	2.146	12	.179		
	Total	23.873	15			
Bad cytosol	Between Groups	.180	3	.060	88.074	.000
	Within Groups	.008	12	.001		
	Total	.188	15			
Bad mitochondria	Between Groups	.698	3	.233	28.468	.000
	Within Groups	.098	12	.008		

	Total	.796	15			
Bax cytosol	Between Groups	2.887	3	.962	120.573	.000
	Within Groups	.096	12	.008		
	Total	2.983	15			
Bax mitochondria	Between Groups	2.494	3	.831	97.040	.000
	Within Groups	.103	12	.009		
	Total	2.597	15			
Bcl 2 mitochondria	Between Groups	1.896	3	.632	166.237	.000
	Within Groups	.046	12	.004		
	Total	1.942	15			
Bcl 2 cytosol	Between Groups	.866	3	.289	51.903	.000
	Within Groups	.067	12	.006		
	Total	.932	15			
Calpain	Between Groups	.023	3	.008	10.192	.001
	Within Groups	.009	12	.001		
	Total	.032	15			
Active-caspase 3	Between Groups	.016	3	.005	4.195	.030
	Within Groups	.015	12	.001		
	Total	.031	15			
Active-caspase 7	Between Groups	.208	3	.069	39.953	.000
	Within Groups	.021	12	.002		
	Total	.229	15			
Active-caspase 9	Between Groups	.177	3	.059	74.900	.000
	Within Groups	.009	12	.001		
	Total	.187	15			
cytochrome c cytosol	Between Groups	.166	3	.055	23.372	.000
	Within Groups	.028	12	.002		
	Total	.195	15			
cytochrome c mitochondria	Between Groups	.306	3	.102	6.543	.007
	Within Groups	.187	12	.016		
	Total	.493	15			
NMDAR1	Between Groups	.273	3	.091	14.775	.000
	Within Groups	.074	12	.006		
	Total	.347	15			
NMDAR2A	Between Groups	.606	3	.202	11.880	.001
	Within Groups	.204	12	.017		
	Total	.810	15			

NMDAR2C	Between Groups	.948	3	.316	84.128	.000
	Within Groups	.045	12	.004		
	Total	.993	15			
PARP, 89	Between Groups	58.058	3	19.353	97.668	.000
	Within Groups	2.378	12	.198		
	Total	60.435	15			

Post Hoc Tests

Multiple Comparisons LSD						
Dependent Variable	(I) group	(J) group	Mean Difference (I-J)	Std. Error	Sig.	
			Lower Bound	Upper Bound	Lower Bound	
NMDAR2B	1	3	8.645	10.998	.447	
		2	-.321(*)	.113	.015	
		3	-.373(*)	.113	.007	
	2	4	-.626(*)	.113	.000	
		1	.321(*)	.113	.015	
		3	-.052	.113	.655	
	3	4	-.306(*)	.113	.020	
		1	.373(*)	.113	.007	
		2	.052	.113	.655	
	4	4	-.254(*)	.113	.045	
		1	.626(*)	.113	.000	
		2	.306(*)	.113	.020	
	AIF cytosol	1	3	.254(*)	.113	.045
			2	.273(*)	.019	.000
			4	.095(*)	.019	.000
		2	4	.346(*)	.019	.000
1			-.273(*)	.019	.000	
3			-.178(*)	.019	.000	
3		4	.073(*)	.019	.002	
		1	-.095(*)	.019	.000	
		2	.178(*)	.019	.000	
4		4	.251(*)	.019	.000	
		1	-.346(*)	.019	.000	
		2	-.073(*)	.019	.002	
		3	-.251(*)	.019	.000	

AIF nuclear	1	2	.184	.299	.551
		3	1.955(*)	.299	.000
		4	-1.321(*)	.299	.001
	2	1	-.184	.299	.551
		3	1.771(*)	.299	.000
		4	-1.505(*)	.299	.000
	3	1	-1.955(*)	.299	.000
		2	-1.771(*)	.299	.000
		4	-3.276(*)	.299	.000
	4	1	1.321(*)	.299	.001
		2	1.505(*)	.299	.000
		3	3.276(*)	.299	.000
Bad cytosol	1	2	.273(*)	.018	.000
		3	.184(*)	.018	.000
		4	.243(*)	.018	.000
	2	1	-.273(*)	.018	.000
		3	-.089(*)	.018	.000
		4	-.030	.018	.130
	3	1	-.184(*)	.018	.000
		2	.089(*)	.018	.000
		4	.059(*)	.018	.008
	4	1	-.243(*)	.018	.000
		2	.030	.018	.130
		3	-.059(*)	.018	.008
Bad mitochondria	1	2	-.284(*)	.064	.001
		3	.207(*)	.064	.007
		4	-.291(*)	.064	.001
	2	1	.284(*)	.064	.001
		3	.491(*)	.064	.000
		4	-.007	.064	.914
	3	1	-.207(*)	.064	.007
		2	-.491(*)	.064	.000
		4	-.498(*)	.064	.000
	4	1	.291(*)	.064	.001
		2	.007	.064	.914
		3	.498(*)	.064	.000
Bax cytosol	1	2	.833(*)	.063	.000

		3		-.085	.063	.202	
		4		.775(*)	.063	.000	
		2	1		-.833(*)	.063	.000
			3		-.918(*)	.063	.000
			4		-.058	.063	.375
		3	1		.085	.063	.202
	2			.918(*)	.063	.000	
	4			.860(*)	.063	.000	
	4	1		-.775(*)	.063	.000	
		2		.058	.063	.375	
		3		-.860(*)	.063	.000	
	Bax mitochondria	1	2		.452(*)	.065	.000
3				1.110(*)	.065	.000	
4				.511(*)	.065	.000	
2		1		-.452(*)	.065	.000	
		3		.658(*)	.065	.000	
		4		.059	.065	.383	
3		1		-1.110(*)	.065	.000	
		2		-.658(*)	.065	.000	
		4		-.599(*)	.065	.000	
4		1		-.511(*)	.065	.000	
		2		-.059	.065	.383	
		3		.599(*)	.065	.000	
Bcl 2 mitochondria	1	2		-.584(*)	.044	.000	
		3		.272(*)	.044	.000	
		4		-.452(*)	.044	.000	
	2	1		.584(*)	.044	.000	
		3		.856(*)	.044	.000	
		4		.132(*)	.044	.011	
	3	1		-.272(*)	.044	.000	
		2		-.856(*)	.044	.000	
		4		-.725(*)	.044	.000	
	4	1		.452(*)	.044	.000	
		2		-.132(*)	.044	.011	
		3		.725(*)	.044	.000	
Bcl 2 cytosol	1	2		.235(*)	.053	.001	
		3		-.357(*)	.053	.000	

		4	.186(*)	.053	.004
	2	1	-.235(*)	.053	.001
		3	-.592(*)	.053	.000
		4	-.049	.053	.368
	3	1	.357(*)	.053	.000
		2	.592(*)	.053	.000
		4	.543(*)	.053	.000
	4	1	-.186(*)	.053	.004
		2	.049	.053	.368
		3	-.543(*)	.053	.000
Calpain	1	2	.006	.019	.763
		3	-.068(*)	.019	.004
		4	.035	.019	.093
	2	1	-.006	.019	.763
		3	-.074(*)	.019	.002
		4	.029	.019	.155
	3	1	.068(*)	.019	.004
		2	.074(*)	.019	.002
		4	.103(*)	.019	.000
	4	1	-.035	.019	.093
		2	-.029	.019	.155
		3	-.103(*)	.019	.000
Active-caspase 3	1	2	-.018	.025	.496
		3	-.078(*)	.025	.009
		4	-.061(*)	.025	.031
	2	1	.018	.025	.496
		3	-.060(*)	.025	.034
		4	-.044	.025	.109
	3	1	.078(*)	.025	.009
		2	.060(*)	.025	.034
		4	.017	.025	.522
	4	1	.061(*)	.025	.031
		2	.044	.025	.109
		3	-.017	.025	.522
Active-caspase 7	1	2	.120(*)	.029	.002
		3	-.139(*)	.029	.001
		4	.150(*)	.029	.000

	2	1	-.120(*)	.029	.002
		3	-.259(*)	.029	.000
		4	.030	.029	.328
	3	1	.139(*)	.029	.001
		2	.259(*)	.029	.000
		4	.289(*)	.029	.000
	4	1	-.150(*)	.029	.000
		2	-.030	.029	.328
		3	-.289(*)	.029	.000
Active-caspase 9	1	2	-.114(*)	.020	.000
		3	-.294(*)	.020	.000
		4	-.110(*)	.020	.000
	2	1	.114(*)	.020	.000
		3	-.180(*)	.020	.000
		4	.004	.020	.832
	3	1	.294(*)	.020	.000
		2	.180(*)	.020	.000
		4	.184(*)	.020	.000
	4	1	.110(*)	.020	.000
		2	-.004	.020	.832
		3	-.184(*)	.020	.000
cytochrome c cytosol	1	2	.240(*)	.034	.000
		3	.168(*)	.034	.000
		4	.014	.034	.699
	2	1	-.240(*)	.034	.000
		3	-.071	.034	.060
		4	-.226(*)	.034	.000
	3	1	-.168(*)	.034	.000
		2	.071	.034	.060
		4	-.155(*)	.034	.001
	4	1	-.014	.034	.699
		2	.226(*)	.034	.000
		3	.155(*)	.034	.001
cytochrome c mitochondria	1	2	-.040	.088	.661
		3	-.023	.088	.802
		4	.297(*)	.088	.006
	2	1	.040	.088	.661

		3	.017	.088	.850
		4	.337(*)	.088	.002
	3	1	.023	.088	.802
	3	2	-.017	.088	.850
	3	4	.320(*)	.088	.004
	4	1	-.297(*)	.088	.006
	4	2	-.337(*)	.088	.002
	4	3	-.320(*)	.088	.004
NMDAR1	1	2	-.336(*)	.055	.000
		3	-.298(*)	.055	.000
		4	-.235(*)	.055	.001
	2	1	.336(*)	.055	.000
		3	.039	.055	.498
		4	.101	.055	.093
	3	1	.298(*)	.055	.000
		2	-.039	.055	.498
		4	.062	.055	.283
	4	1	.235(*)	.055	.001
		2	-.101	.055	.093
		3	-.062	.055	.283
NMDAR2A	1	2	.393(*)	.092	.001
		3	-.101	.092	.295
		4	.242(*)	.092	.022
	2	1	-.393(*)	.092	.001
		3	-.494(*)	.092	.000
		4	-.151	.092	.127
	3	1	.101	.092	.295
		2	.494(*)	.092	.000
		4	.342(*)	.092	.003
	4	1	-.242(*)	.092	.022
		2	.151	.092	.127
		3	-.342(*)	.092	.003
NMDAR2C	1	2	-.051	.043	.264
		3	-.486(*)	.043	.000
		4	.176(*)	.043	.002
	2	1	.051	.043	.264
		3	-.435(*)	.043	.000

		4	.227(*)	.043	.000
	3	1	.486(*)	.043	.000
		2	.435(*)	.043	.000
		4	.662(*)	.043	.000
	4	1	-.176(*)	.043	.002
		2	-.227(*)	.043	.000
		3	-.662(*)	.043	.000
PARP, 89	1	2	-3.488(*)	.315	.000
		3	-.285	.315	.384
		4	-4.315(*)	.315	.000
	2	1	3.488(*)	.315	.000
		3	3.203(*)	.315	.000
		4	-.827(*)	.315	.022
	3	1	.285	.315	.384
		2	-3.203(*)	.315	.000
		4	-4.031(*)	.315	.000
	4	1	4.315(*)	.315	.000
		2	.827(*)	.315	.022
		3	4.031(*)	.315	.000
* The mean difference is significant at the .05 level.					

Multiple Comparisons

	HC*FC	HC*HE	HC*FE	FC*HE	FC*FE	HE*FE
NMDAR2B	S	S	S	NS	S	S
AIF cytosol	S	S	S	S	S	S
AIF nuclear	NS	S	S	S	S	S
Bad cytosol	S	S	S	S	NS	S
Bad mitochondria	S	S	S	S	NS	S
Bax cytosol	S	NS	S	S	NS	S
Bax mitochondria	S	S	S	S	NS	S
Bcl 2 mitochondria	S	S	S	S	S	S
Bcl 2 cytosol	S	S	S	S	NS	S
Calpain	NS	S	NS	S	NS	S
Active-caspase 3	NS	S	S	S	NS	NS
Active-caspase 7	S	S	S	S	NS	S
Active-caspase 9	S	S	S	S	NS	S
cytochrome c cytosol	S	S	NS	NS	S	S
cytochrome c	NS	NS	S	NS	S	S

mitochondria						
NMDAR1	S	S	S	NS	NS	NS
NMDAR2A	S	NS	S	S	NS	S
NMDAR2C	NS	S	S	S	S	S
PARP, 89	S	NS	S	S	S	S

Discussion

Mechanism of cell death in Hippocampus

Brain has selective vulnerability to different toxins, hence we wanted to determine the mechanism of cell death in hippocampus and frontal cortex (which are important regions involved in memory and higher cognitive functions) after chronic ethanol treatment. Caspase 3 is known for its role in chromatin condensation and DNA fragmentation in dismantling a cell with ultimate formation of apoptotic bodies (Janicke *et al.* 1998). Results of the current study revealed that increased caspase-3 activation was associated with activation of caspase 7, caspase 9 and calpain in comparison with findings for controls and that the cell death mechanism involves caspase 3 activation. Earlier studies have reported that NMDA receptor excitotoxicity leads to activation of caspase 3 and caspase 7 (Jordan *et al.* 2003). An increase in intracellular Ca²⁺ can occur either through voltage gated calcium channels or NMDA receptor. Increases in intracellular calcium may occur in response to diverse necrosis-initiating stimuli such as excess glutamate, acidosis or reactive oxygen/ nitrogen species (ROS). It is conceivable that the degree of Ca²⁺ elevation and ensuing calpain activation will determine whether cells die by apoptosis or necrosis. Mild Ca²⁺ elevation favours apoptosis, whereas acute calpain activation precipitates necrosis probably via catastrophic cleavage of regulatory and structural proteins. However, caspases might be activated by calpain proteases (Artal-Sanz *et al.* 2005). Chronic ethanol treatment in our study resulted in up regulation of NMDAR1, NMDAR2B, NMDAR2C subunits along with activation of caspase 3, caspase 7, caspase 9, calpain in hippocampal region. Bax and Bad were largely present within the cytoplasm of hippocampal region. Similar observations of

these proteins were made within the cytoplasm before and after seizures in seizure-induced neuronal death. (Schindler *et al.* 2004). However, Bcl-2 translocation to cytosol further activates the caspase cascade in this model. To our knowledge, this is the first study to show sub cellular alterations of Bcl-2 family members in adult chronic alcohol paradigm. Our Lab has previously reported regional heterogeneity of plasma membrane associated proteins in rat cerebral cortex and cerebellum (Babu 1997). Because the brain is heterogenous, we report here that different cascades might be activated in the two different regions observed in this study.

Mechanism of cell death in frontal cortex

Inflammation during necrosis involves microglia and reactive astrocytes, which release the neurotoxic mediators nitric oxide, IL1 β (interleukin 1 β) and TNF α (Benn and Woolf 2004). TNF α induced cell death in ethanol-exposed cells depends on p38 MAPK signaling, which brings about accumulation of cytochrome c in the cytosol (Pastorino *et al.* 2003). Consistent with these observations translocation of cytochrome c to cytosol was found in frontal cortex of alcohol treated rat. In previous studies, loss of mitochondrial cytochrome c was correlated with an increased production of reactive oxygen species by mitochondria, which may contribute to cellular damage (Luetjens *et al.* 2000). Regardless of whether cytochrome c serves to activate downstream caspases the loss of cytochrome c from mitochondria was regarded to impair respiration in myocardial ischemia reperfusion (Chen *et al.* 2001). Similarly translocation of cytochrome c from mitochondria to cytosol in frontal cortex of ethanol treated rat in our studies might be responsible for the impairment of respiration. Release of additional resident proteins of the intermembrane space including AIF may contribute to apoptosis in ethanol treated frontal cortex as observed by translocation of AIF to nucleus in ethanol treated frontal cortex. The present study has shown, for the first time that AIF is a key player in caspase-independent cell death in this region. Similar AIF translocations to the nucleus were reported in several paradigms of apoptosis (Lorenzo *et al.* 1999; Daugas *et al.* 2000; Joza *et al.* 2001; Cande *et al.* 2002) where it promotes peripheral

chromatin condensation and DNA fragmentation. These findings suggest that activation of caspase independent pathways of apoptosis occur in frontal cortex of rat chronically treated with ethanol. The cell death in ethanol treated frontal cortex was Caspase, Calpain, Bax and Bad independent.

The specific death-signaling pathways that lead to degeneration of adult neurons are difficult to define. The molecular pathways seem to depend on the neuronal population that is affected, as well as the nature, stage, cause and extent of the death-inducing insult (Benn and Woolf 2004). In agreement with this we have found significant differences in the pathways of apoptotic cascade activation in both regions. Taken together our results imply that different pathways of cell death are activated in hippocampus and frontal cortex. Our results are in agreement with previous experiments with the same chronic alcohol treatment model (Rajgopal and Vemuri. 2002) and support studies of Herrera *et al.* (2003) in which chronic alcoholism is proved to disrupt neurogenesis by retarding cell proliferation and increasing cell death. Taken together, ethanol induced cell death might involve a broad range of biochemical mechanisms. Despite the efforts of numerous investigators, most of the information on molecular players has remained in the dark. Clearly, these studies are important, but many important questions regarding the functions of genes, proteins, and other mechanisms in determining cell survival or death following ethanol treatment need to be addressed.

CHAPTER 2

***In situ detection of cell death in hippocampus and frontal cortex of rats treated
with ethanol chronically***

The present model has been used to analyze selective vulnerability in the hippocampal and frontal cortex of chronic ethanol treated rats. Since caspase 3 (involved in apoptotic cell death) and calpain (involved in necrotic cell death) were activated differentially in both the regions, we proceeded to look for cellular evidence of the type of cell death involved in this paradigm. As reported by Jordan and Harrison (2003) apoptosis was originally identifiable only by morphological criteria; however, subsequent developments have led to an expanding variety of detection methods, each with particular drawbacks that often resort to morphological criteria for confirmation or corroboration of those results. Morphology is still believed to be the gold standard for detection of apoptosis, albeit accepting that not all apoptotic cells will be detected by this approach (Jordan and Harrison 2003). Also, any measure of apoptosis is a snapshot in time, and it is difficult to assess the rate of apoptosis within a given system (Darzynkiewicz *et al.* 1998) and even more difficult in a chronic condition, as is in this model. There are at least three widely accepted criteria for detecting nervous system damage regardless of the nature of the damage-inducing insult to cause cell death, and we have used majority of these in establishing the neurotoxicity of ethanol. They are (1) evidence of cell loss based on classical histological stains (e.g. Nissl stains, or H&E), (2) astrogliosis and (3) an argyrophilia reaction using silver degeneration stains (O'Callaghan and Jensen 1992). Light Microscopic appearance of dying cells involves observation for nuclear and cytoplasmic abnormalities (Smith 1972), as discussed below

Changes in the nucleus:

- a) Pyknosis: Common manifestation of death of cells. The pyknotic nucleus is decreased in size but round. The nucleus is black when stained by hematoxylin and eosin. This is because it is more acid in its reaction and attracts the basic hematoxylin; its nucleic acid is being set free. The pyknotic nucleus is homogeneous; it lacks the nucleolus and chromatin granules.

Pyknosis is one of the earlier changes in point of time; ultimately the dead nucleus disappears altogether.

- b) Karyorrhexis: Literally a flowing of the nucleus, this term is used to designate the dead nucleus which is reduced to many tiny fragments, barely visible, and these may remain to mark the original position of the nucleus or they may be scattered over a considerable space. It is a step in the development of caseous necrosis.
- c) Karyolysis: This is dissolution of the nuclear material. When complete the nucleus is not seen, but the term is used to refer to the incomplete stages, when the nucleus appears as a hollow sphere, a ghost with only the nuclear membrane remaining. A corollary process to karyolysis is chromatolysis. The stainable material of the nucleus including the nucleolus, the chromosomes, and other visible structures is known as chromatin because it gives the nucleus its color (blue by hematoxylin). In karyolysis it is the chromatin which is dissolved. The dissolved chromatin does not vanish but is in solution in the intercellular fluids of the vicinity, carrying its blue color with it.

Changes in the cytoplasm:

Acidophilic (eosinophilic) cytoplasm: The cytoplasm is acidophilic because its reaction is more basic than during life, hence it takes the acid stain, which is red (Eosin). The cytoplasm is, then, a deeper red than usual. Cytoplasmic structure is obscured, the nucleus being concomitantly pyknotic.

Adequate detection of cytologically apoptotic neurons can usually be obtained from fixed paraffin-embedded brain sections cut at a thickness of 3-5 μ m (Roth 2002) and observing under a light microscope, which provides a quick, convenient, and on-site method for monitoring the progression of apoptosis. It can be semi-quantitative, if the images of representative fields of cells are captured (Bai 2003). An advantage of using morphological over biochemical methods for identifying cell death is that these techniques allow independent recognition of apoptosis and necrosis when the processes occur simultaneously, as in our model. Apoptosis typically involves scattered individual cells in a tissue, whereas necrosis

involves groups of adjoining cells (Kerr *et al.* 1995). Different morphological criteria have been established to identify apoptosis and necrosis. Table 3 shows the features displayed by dying cells in a chronological sequence.

Table 4. Morphological comparison of necrosis and apoptosis in chronological sequence

Apoptosis	Necrosis
<p><i>Cell and cytosol shrinkage</i></p> <ul style="list-style-type: none"> • Functional alteration of ion flux and buildup of intracellular calcium • Mitochondrial permeability transition, release of AIF, Cytochrome C, Procaspases. • Effector enzyme activation, e.g. caspase <p><i>Nuclear changes</i></p> <ul style="list-style-type: none"> • Chromatin condensation and clumping • Modified transcription/translation • Site-specific cleavage of DNA by a cation-dependent endonuclease, aided by numerous factors • Nuclear fragmentation (Karyohexis) <p><i>Cytoplasmic blebbing</i></p> <ul style="list-style-type: none"> • Consequence of modified 	<p><i>Plasma membrane alterations</i></p> <ul style="list-style-type: none"> • Blebbing, blunting, distortion of microvilli, failed integrity causing cellular oedema, loss of intercellular attachments. (Functional-loss of ion flux control, Ca⁺² build up) • Cytoplasmic protein denaturation and clumping <p><i>Variable mitochondrial changes</i></p> <ul style="list-style-type: none"> • Swelling, rarefaction, formation of phospholipids-rich amorphous densities. (Functional loss of ATP production, impairing Na⁺K⁺ ATPase pump contributing to cellular swelling <p><i>Dilatation of endoplasmic reticulum</i></p> <ul style="list-style-type: none"> • Detachment of ribosomes <p><i>Nuclear changes</i></p> <ul style="list-style-type: none"> • Disaggregation of nuclear

<p>cytoskeleton produced by caspase/tTG action</p> <p><i>Variable endoplasmic reticulum changes</i></p> <p><i>Condensation or no alteration of mitochondria</i></p> <p><i>Cytoplasmic budding</i></p> <ul style="list-style-type: none"> • Packaging: production of vesicles or apoptotic bodies containing chromatin/organelles (Function of cytoskeletal modification) <p><i>Clearance</i></p> <ul style="list-style-type: none"> • Phagocytosis by surrounding cells without inducing an inflammatory response(ideal situation) • Relies on expression of external marker moieties, e.g phosphatidyl-serine • Energy required 	<p>skeleton and chromatin clumping</p> <ul style="list-style-type: none"> • Karyolysis or Karryohexis • Random dissociation and cleavage of DNA(uncontrolled enzymic release including those of lysosomal origin) <p><i>Cellular dissociation</i></p> <p><i>Clearance</i></p> <ul style="list-style-type: none"> • Probable activation of inflammatory pathways • No energy requirement
---	---

(Adapted from Jordan and Harrison 2003).

Apart from these observations, some studies have taken advantage of astroglial responses in assessing the toxicity of a particular compound to cause brain damage. One of the most widely documented cellular reactions to nervous system damage is hypertrophy of astrocytes (Lindsay 1986; Eng 1988; O'Callaghan 1991). This response, often termed reactive gliosis or astrogliosis (Lindsay 1986; Eng 1988), can be induced by a diversity of insults, including those resulting from

physical damage, disease or chemicals (Eng 1988; O'Callaghan 1988; O'Callaghan 1991). Moreover, damage to all neuronal and glial cell types examined to date appears to elicit this specific cellular response (O'Callaghan 1991). The hallmark of reactive gliosis is the accumulation of glial filaments (Eng 1988), the major component of which is glial fibrillary acidic protein (GFAP) (Eng 1985). Indeed, immunocytochemical studies of GFAP have firmly established the existence of reactive gliosis as the dominant response to CNS damage (Eng 1988). Most studies that have characterized astrogliosis by examining changes in GFAP have used various forms of brain trauma or animal models of neurological disease states as the source of injury (e.g., Eng 1988; Hatten *et al.* 1991). Some studies have used immunohistological techniques to characterize cell death.

Immunohistological techniques involving the direct binding of antibodies to specific proteins to enable subsequent visualization by fluorescence or peroxidase reactions are probably the most rapidly increasing method used for apoptotic marker detection. Specific antibodies are used against caspases (Jordan and Harrison 2003), to check for their activation and relate them to apoptotic cell death. Apoptotic nuclear phenotype typically requires caspase activity for its occurrence (Zheng *et al.* 1998; Keramaris *et al.* 2000). Caspase 3 is an effector caspase and targeted disruption of caspase-3 has been shown to have a marked effect on nervous system development and neuronal apoptosis (Kuida *et al.* 1996). Caspases are cysteine proteases that exist in cells at baseline as inactive zymogens (Nicholson 1999). Upon receipt of an apoptosis stimulus, the caspase zymogen becomes cleaved at specific aspartic residues and generates large and small subunits that together constitute the active caspase. Because of this cleavage event, antibodies can be generated against the carboxyl terminus of the large caspase subunit that will not recognize the inactive zymogen form of the caspase. A number of antibodies have now been generated against various active caspases, including caspase 3 (Srinivasan *et al.* 1998; Velier *et al.* 1999). Immunohistochemical studies of neuronal apoptosis have been performed with active caspase antibodies and they have proven to be sensitive indicators of caspase activation and neuronal apoptosis (Roth 2002). There are many methods for localizing antibody binding in tissue sections, the simplest being usage

of secondary antibodies that are either fluorescently labeled or conjugated to an enzyme such as horseradish peroxidase (HRP), which can then be used to deposit a chromogenic substrate e.g., diaminobenzidine (DAB) (Roth 2002). Apoptotic nuclear changes can also be detected *in situ* with TdT-dependent incorporation.

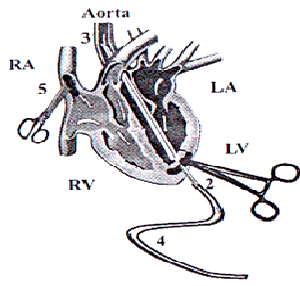
The TUNEL method relies on the *in situ* labeling of DNA breaks in individual nuclei in tissue sections processed through procedures of histopathology. TUNEL stands for TdT-mediated dUTP-biotin nick end labeling and relies on the specific binding of terminal deoxynucleotidyl transferase (TdT) to exposed 3'-OH ends of DNA followed by the synthesis of a labeled polydeoxynucleotide molecule. Nuclear DNA on histological sections is first exposed by proteolytic treatment; then TdT is used to incorporate biotinylated deoxyuridine into the sites of DNA breaks (Ben-Sasson *et al.* 1995). However, the major caveat to TUNEL detection is that it may lack specificity, i.e., it may label necrotic cells and/or cells that are not obviously undergoing apoptosis (McCarthy and Evan 1998; Ishimaru *et al.* 1999; de Torres *et al.* 1997). For routine screening and assessment, light microscopy is to be preferred for the rapid ability to survey large areas. In new experimental paradigms or complex tissues with multiple cell classes (example: brain) ultrastructural demonstration should be supported with light microscopy. For better understanding of apoptosis one should use a combination of histological analysis, TUNEL staining for DNA cleavage, electrophoretic analysis of DNA for laddering pattern supportive of internucleosomal DNA breaks and ultrastructural analysis using electron microscopy. The more current approach is to grade nuclear and cytoplasmic changes independently and to consider other experimental data on internucleosomal DNA cleavage, gene activation, calcium influx, protease activation with regard to establishing evidence for apoptotic cell death in a given experimental paradigm. Current literature suggests that apoptosis and necrosis often co-exist in adult tissues during injury or degeneration and that a full continuum of morphological changes is often observed between apoptosis and necrosis. The major changes that have to be keenly observed are nuclear and cytoplasmic morphology, organelle (particularly mitochondria) and membrane integrity (Schmechel 1999) if one uses electron microscopy for the detection of cell death.

Ultrastructurally, apoptotic cells are characterized by condensation of nucleus and cytoplasm with early nuclear changes in chromatin. They may also display convoluted nuclear membrane, relative preservation of cell membrane and of organelles such as mitochondria and cytoplasmic structures whereas necrotic cells show swelling of cytoplasm and nucleus with retention of the shape of the nucleus; vacuolation and loss of ultrastructural integrity of cell membrane, organelles, cytoplasmic membranes, and nucleus. (Piantadosi *et al.* 1997). For a detailed description of nuclear and cytoplasmic ultrastructure of dying or injured cells the reader may refer Schmechel (1999). Electron microscopy provides the definitive morphological evidence of apoptosis; however, it has a limitation. The limitation being not to provide quantitative data to assess cell death (Bai 2003).

In brief, the morphological changes of brain cells were extensively characterized using light microscopy staining techniques limited to haematoxylin & eosin staining and Toluidine blue. This study also characterizes the type of cell death in hippocampus and frontal cortex of ethanol treated rat by a combination of immunohistochemistry (active caspase-3), TUNEL assay (to assess the DNA damage) and electron microscopy (to observe ultrastructural features of dying cells and characterize the type of cell death).

Materials and Methods

Fig 22 Perfusion technique



Cavalier (2000), described schematically in Figure 14 and the sections were stained with haematoxylin & eosin after preparation of brain sections.

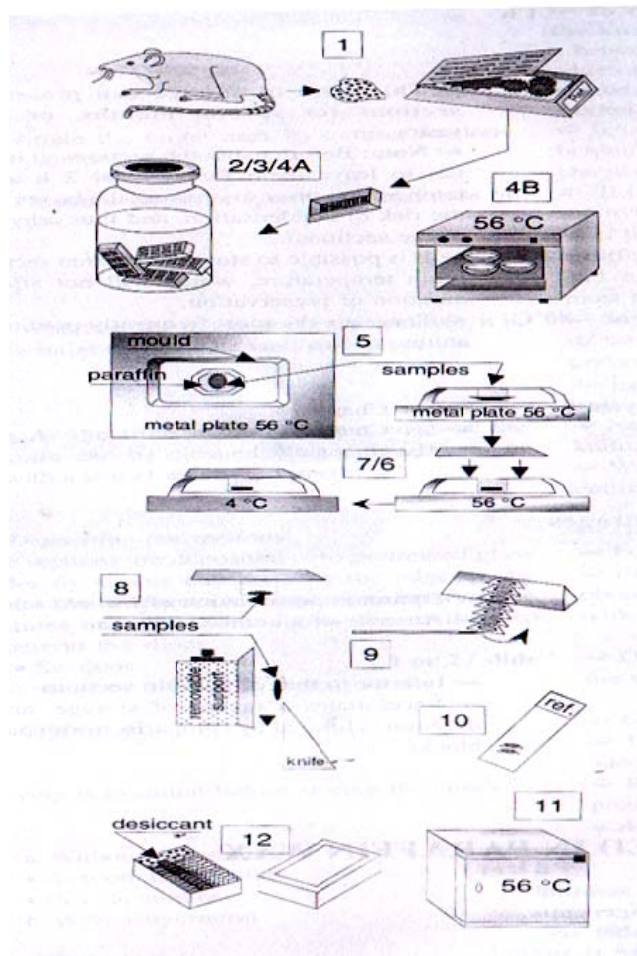
Transcardial perfusion

1=Opened the thoracic cage and the pericardium; 2=Small incision in the left ventricle near the tip of the heart; 3=Introduced cannula delicately up to the aorta; 4=Clamped the cannula with the aid of artery clamps; 5=Opened the right auricle (RA)

This procedure is aimed to fix the antigens in brain by cross linking the molecules, rendering them insoluble and holding them in their natural place. Briefly, rats were anesthetized with pentobarbital (100 mg/Kg, i.p). Anesthesia was confirmed by lack of pain response. Chest wall

For histological assessment of damage to hippocampus and frontal cortex, the brains were fixed using transcardial perfusion as described by Morel and

Fig.23 The schematic represents method of preparation of brain sections



was opened, heart exposed and pericardium was removed. Right auricle was incised and a cannula was placed in the left ventricle and perfused with room temperature normal saline (1ml/gm body weight). Perfusion was carried till blood return from right auricle was clear. Then, freshly prepared ice cold solution of 4% (w/v) paraformaldehyde in 0.1 M sodium phosphate buffer pH 7.4 was infused (3 ml/ g body weight) to fix the organs in vivo. Perfusion was confirmed by observing Liver, Spleen and kidneys which turned grayish white and muscle tremor was seen on limbs and tail. After perfusion rat was left undisturbed for 1-2 h. Hippocampus and frontal cortex was dissected and post fixation was done in the same fixative used for perfusion, for 24 hours. Thereafter tissue storage was done in refrigerated phosphate buffer solution having thymol crystal to avoid microbial propagation (Schmechel 1999).

Preparation of brain sections:

Fig. 15 shows the method of preparation of brain sections. 1=Dissection after fixation by perfusion- placed in a cassette, 2= Fixation by immersion – Rinsing, 3= Dehydration (baths of alcohol of increasing concentrations); 4= “Clearing” impregnation: 4A: solvent for paraffin 4B: liquid paraffin at 56 ° C; 5= Embedding (56 ° C) embedding mold; 6= Closure of the cassette; 7= Cooling of the block; 8= Removal from the mold; 9= Cutting the sections–Microtome (5-10 μ m); 10=Depositing the sections- on pretreated slides; 11=Dried (56 ° C); 12= Stored at 4 ° C.

The post-fixed regions of brain were placed in 20 ml snap cap glass vials dehydrated through increasing concentrations of ethanol (50%, 70%, 95%, 100%) each 20 minutes and 3 changes, followed by Xylene (10 minutes, 2 changes). Then, 1:1 xylene and molten wax was infiltrated overnight into tissue blocks at room temperature. Samples were then transferred to 60 ° C oven to melt wax/Xylene mixture and removed. Immediately fresh molten wax was infiltrated for 1 hour at 60 ° C. Embedding was done in paraffin wax using embedding ring on mold, labeled and left at room temperature to harden. Cast blocks were removed from embedding

molds and stored in a dry place at room temperature.

Wax blocks containing samples were cut into trapezoidal shape and the wide edge of it was facing the knife of Leica microtome (Model: RM2145). Sections of 5 μm were cut and the sections ribbon was transferred to microscopic slides precoated with gelatin (0.5 % w/v gelatin, 0.05% w/v chrome alum).

Subbing slides

To ensure that the section sticks to the slide, slides were covered with a thin layer of gelatin (Subbing). Rack containing slides were cleaned in cleaning solution (potassium dichromate-60g, sulfuric acid-60 ml and dH₂O-600ml) for 2 hours and rinsed in running tap water for 2 hours. The rack was then placed in gelatin containing solution (0.5 % w/v gelatin, 0.05% w/v chrome alum) for 5-10 minutes, removed and placed in warm oven to dry or left it covered with foil at Room Temperature (RT) overnight. Slides were stored in covered slide box in the refrigerator for up to 6 months until needed. Subbing was done according to Paul *et al.* 1997.

Then, the sections were fixed on to slides by keeping them at 56⁰ C for few minutes to remove wrinkles. Slides were dried at room temperature and incubated at 42^o C for 1-2 days to firmly attach sections to subbed slides. Sections were stored at -20^oC in a slide box with dessicant for several weeks (Watkins 1993).

Haematoxylin and eosin staining (H&E)

H&E staining was performed according to Herde *et al* (2003). The sections were dewaxed in 2 changes of xylene (7 min each), and stained with Harris Haematoxylin for 2-10 minutes, rinsed in running water for 5 min, differentiated in 1% HCl for 3 seconds, rinsed in running water for 5-10 min. Transferred to 1% eosin yellow for 1-2 min, rinsed in running water for 5 min, dehydrated in 70%, 96%, 100%, 100%, 100% ethanol (2 min each), cleared in xylene and mounted on DPX. Slides were

dried overnight prior to microscopic examination. Nuclei appeared blue and cytoplasm appeared pink.

Immunohistochemistry

After sections were deparaffinized in xylene, antigen retrieval was carried out by microwaving sections in 10 mM citrate buffer, pH 6.0, for 1 min at full power followed by 9 min at medium power. Blocking was carried out in 10% normal goat serum in Phosphate buffered saline (PBS) for 1 h at room temperature in a humidified chamber, to reduce back ground (it blocks sticky sites so that secondary antibody binds to primary antibody only). Primary antibody, Rabbit polyclonal antibody against Glial Fibrillary Acidic Protein (Sigma Chemical Company, St Louis, USA) and Rabbit polyclonal antibody against cleaved caspase-3 (Asp 175) antibody (Cell Signaling Technology, USA) was diluted 1:100 in blocking solution and incubated for overnight at 4⁰C. Peroxidase-conjugated anti-rabbit secondary antibody (1:250) was used for incubation time of 1 h at room temperature followed by PBS washes (3x5 min each). 3, 3'-Diaminobenzidine tetrahydrochloride (DAB) at a final concentration of 0.25 mg/ml with 0.05% H₂O₂ in PBS was used for developing till the section turned brown (typically for 3–5 min at RT). Sections were counter stained with methyl green for 10s. Sections were then washed with dH₂O followed by dehydration in graded ethanol and xylene and cover slipped with DPX mount.

In situ labeling of DNA fragmentation

In situ detection of DNA fragmentation was done using the TUNEL method according to Gavrieli *et al.* (1992) using ApoAlertTM DNA Fragmentation Assay Kit (BD Biosciences, USA). In brief, hippocampal and frontal cortex sections were deparaffinised sequentially washed in 100, 95, 85, 70 and 50% ethanol, 0.85% NaCl, phosphate buffered saline (PBS), 4% formaldehyde/PBS for 15 min, PBS twice and incubated for 15 min at RT with 20 µg/ml of proteinase K and washed sequentially

in PBS, 4% formaldehyde/PBS and PBS. Sections were then incubated in equilibration buffer (200 mM Potassium cacodylate, pH 6.6; 25 mM Tris-HCl, pH 6.6; 0.2 mM DTT; 0.25 mg/ml BSA; 2.5 mM Cobalt chloride) for 10 min, followed by TdT incubation buffer (45 μ l Equilibration buffer; 5 μ l nucleotide mix; 1 μ l TdT enzyme) for 60 minutes at 37⁰ C in a dark, humidified chamber. The reaction was stopped by incubating the sections with 2x SSC (3 M NaCl; 300 mM Na₃Citrate.H₂O) for 15 minutes at RT, followed by two washes in PBS and further incubated with propidium iodide (PI) for 5-10 min. This was followed by two washes in dH₂O and visualized under Fluorescence microscope. Aluminium foil was wrapped around the slide and stored at 4⁰ C until photographed. Apoptotic cells exhibited strong, nuclear green fluorescence using a standard fluorescein filter set (520 \pm 20 nm).

Transmission Electron microscopy

Electron microscopy was performed according to the method of Kerr *et al* (1995). Freshly removed tissue, placed in a pool of fixative (5% Glutaraldehyde + 4% paraformaldehyde in 0.067 M sodium cacodylate buffer, pH 7.2) was diced into blocks approximately 1mm³ in size, fixed in fresh fixative for 3 h, rinsed in 0.1 M Sodium cacodylate buffer, pH 7.2 for 15 min, postfixed in 1% osmium tetroxide in 0.1 M cacodylate buffer for 2 h, rinsed in distilled H₂O for 15 minutes, and stained en bloc in 5% uranyl acetate for 30 minutes. Sections were washed in distilled H₂O, dehydrated in ethanol, cleared with propylene oxide. Overnight infiltration was carried out in 50% Epoxy resin: 50 % Propylene oxide, subsequently 100% Epoxy resin was infiltrated for 2 h. Embedding was done in plastic capsules for 1-2 days with polymerization which took place at 60⁰ C. Blocks were trimmed and 1 μ m thick sections were cut and stained with toluidine blue for light microscopy. Toluidine blue stained the nuclei deep blue violet and the cytoplasm in a lighter tone of the same colour. Ultrathin sections of 50-70 nm were cut on a Leica Ultra cut UCT-GA-D/E-1/00 ultra microtome and picked up on copper grids. Then the sections were stained with saturated aqueous Uranyl acetate and counter stained with 4% lead

citrate and observed at various magnifications under a transmission electron microscope (Model: Hitachi, H-7500). Sections were examined and photographed at different magnifications.

Results

Histopathology

Hematoxylin and Eosin staining of control hippocampus (Fig. 24a) had normal cell morphology (including large nucleus and nucleolus) with intact neuropile, whereas ethanol treated hippocampus (Figs 24 b-f) displayed definite lethal changes such as eosinophilic cytoplasm with break up neuropile and Pyknosis (Fig. 24b), degenerating cell and eosinophilic cytoplasm (Figs. 24c), Pyknosis (Figs. 24d and e), and Karyorrhexis (Fig. 24f), whereas ethanol treated frontal cortex (Figs. 24g-i) displayed pyknosis (Figs. 24g-i) along with eosinophilic cytoplasm and chromatolysis (Fig. 24h). Fig 24 d, g, h, i demonstrate near end stage apoptotic cells, the cells are shrunken and condensed. The blood vessel in Fig 24g is free of cells indicating proper tissue fixation, the cell lining the vessel is endothelial cell.

Light microscopic examination of Toluidine blue stained sections demonstrated that control hippocampus exhibiting normal cell structure with intact neuropile. (Fig. 25a) whereas ethanol treated hippocampus demonstrated dark cells with break up neuropile. (Figs. 25b and c). However ethanol treated frontal cortex demonstrated no significant alterations (Fig. 25d).

Immunohistochemistry

Immunohistochemistry using Anti GFAP (Figs. 26a-d) and cleaved caspase-3 (Asp 175) antibody, (Figs. 27a-d) revealed increased immunoreactivity in ethanol treated hippocampus and frontal cortex (Figs. 26b and d, 27b and d). Intense staining of GFAP antibody around blood vessel was evident in ethanol treated hippocampus (Fig. 26b).

In situ labeling of DNA fragmentation

DNA nick end labeling of apoptotic cells (TUNEL) in representative sections of hippocampus (Figs 28a and b) and frontal cortex (Figs 28c and d) of control (Figs 28a and c) and ethanol treated rats (Figs 28b and d) clearly showed cell death in alcohol treated rats.

Transmission Electron microscopy indicating necrosis and apoptosis.

Cell death exhibited apoptotic as well as necrotic features in ethanol treated hippocampus (Fig 29 c and d respectively) and early necrosis features in frontal cortex (Figs 29 g). Cell in hippocampus of ethanol treated rat (Fig 29 c) showing watery and condensed cytoplasm, electronlucent with disruption of cellular organelles, abnormal nuclear shape with crenelation of nuclear membrane, margination of chromatin (early signs of apoptosis). Fig 29 d shows a cell in hippocampus displaying swollen, watery, electronlucent cytoplasm, disruption of cellular organelles with irregular nuclear profile of nuclear membrane, swollen mitochondria, and normal rough endoplasmic reticulum (early signs of necrosis). Cell in frontal cortex of ethanol treated rat (Fig 29 g and h) showing swollen cytoplasm, irregular nuclear profile of nuclear membrane, presence of abundant lysosomes, normal mitochondria and rough endoplasmic reticulum, cytoplasm is watery and electronlucent (early signs of necrosis).

Fig 24

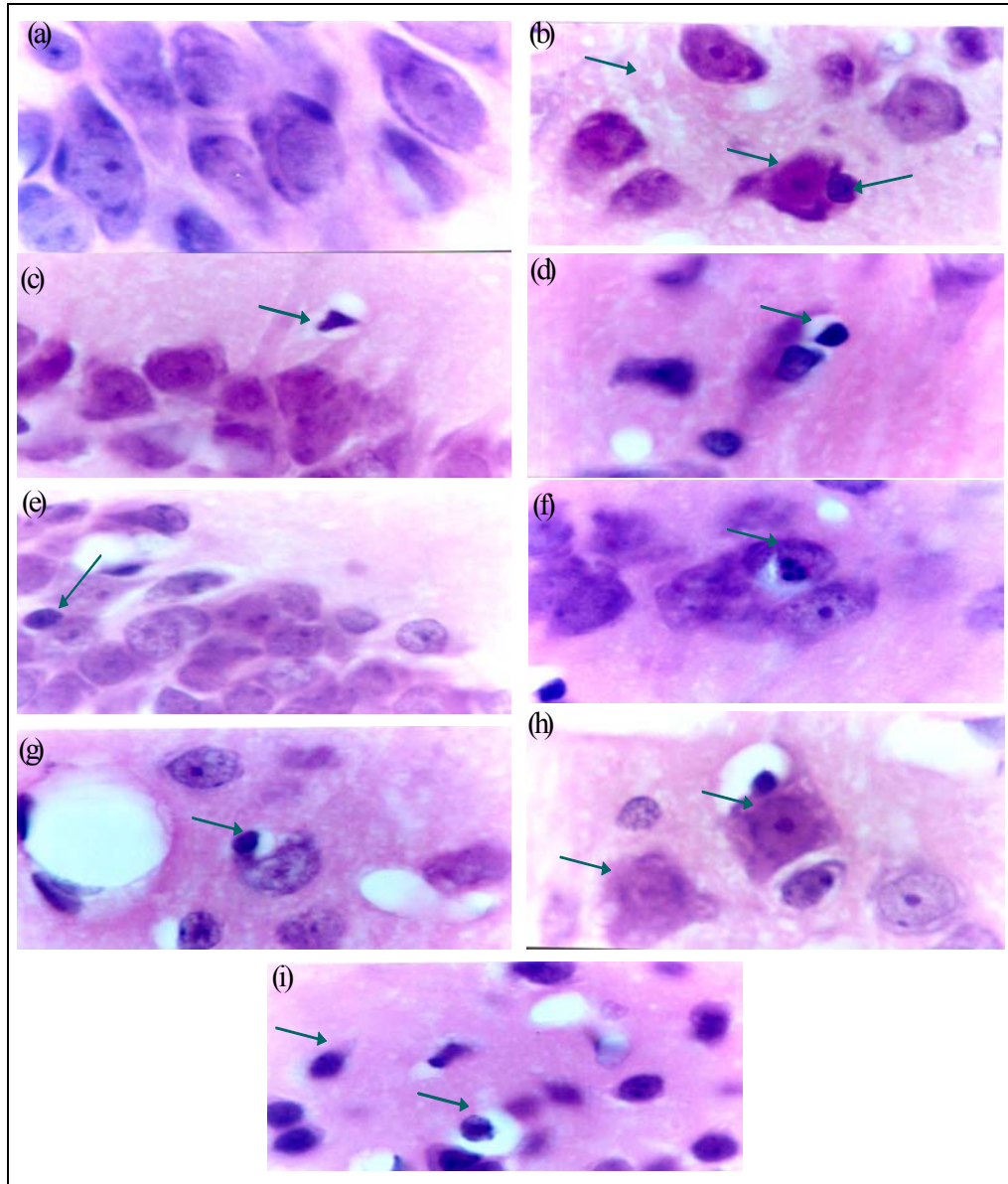


Fig 24. Paraffin embedded representative sections of hematoxylin-eosin (HE) stain demonstrating the histopathological observations in control and ethanol treated rat. (a) Control hippocampus demonstrating normal cells with large nucleus and nucleolus, and intact neuropile. (b-f) ethanol treated hippocampus, (b) demonstrating eosinophilic cytoplasm with break up neuropile and pyknosis (c) degenerating cell and eosinophilic cytoplasm (d & e) Pyknotic cells (f) Karyorrhexis, whereas (g, h, i) ethanol treated frontal cortex displayed (g-i) pyknosis along with (h) eosinophilic cytoplasm and chromatolysis. d,g,h,i demonstrate near end stage apoptotic cells, the cells are shrunken and condensed. Magnification: 100x

Fig. 25

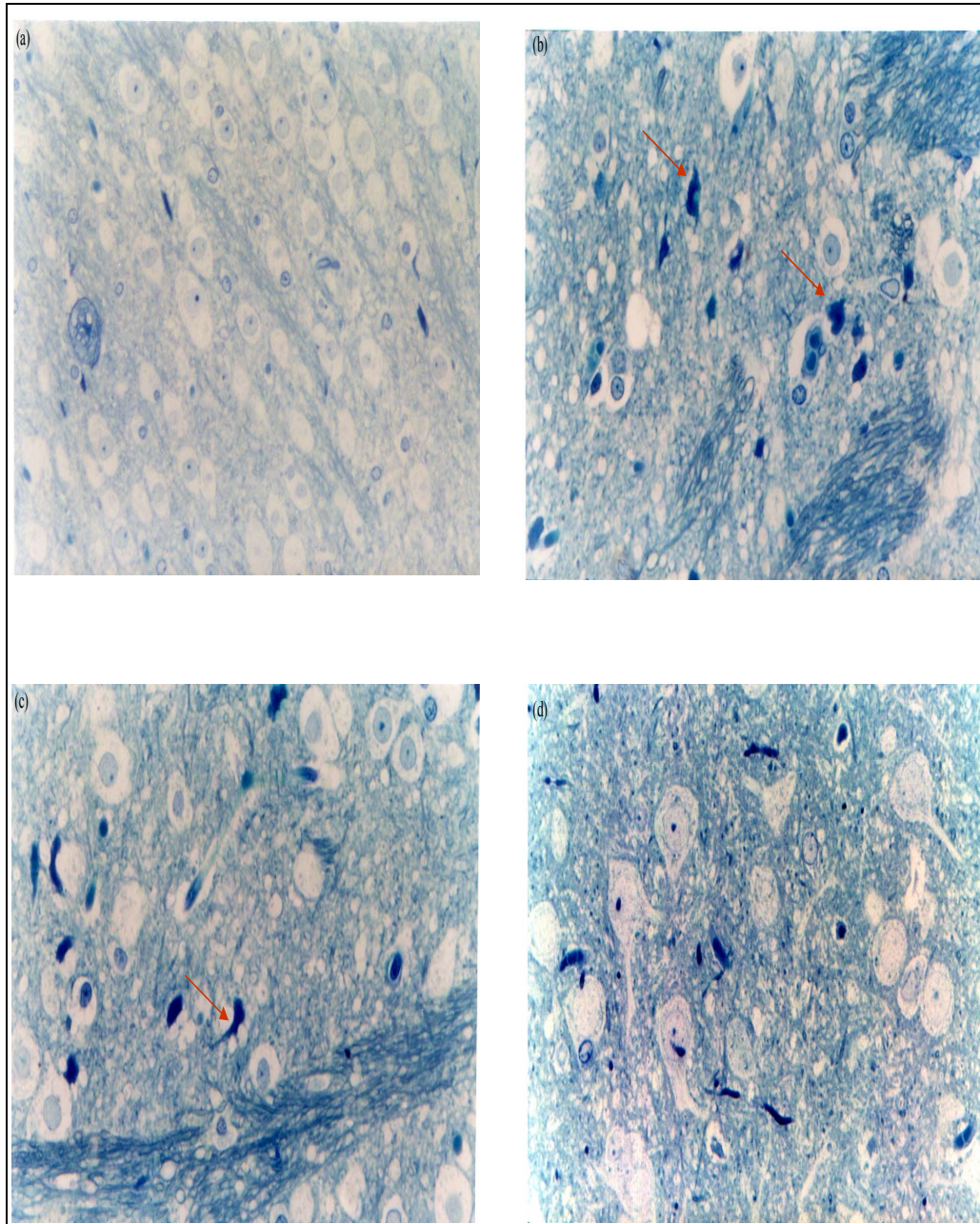


Fig 25. Representative sections of Resin embedded Toluidine blue stain demonstrating the histopathological observations in control and ethanol treated rat. (a) Control hippocampus demonstrating normal neurons with intact neuropile, (b, c) ethanol treated hippocampus demonstrating dark neurons with break up neuropile, (d) ethanol treated frontal cortex demonstrating normal cells. Magnification: (a) 100x. (b, c) 150x. (d) 169x.

Fig.26

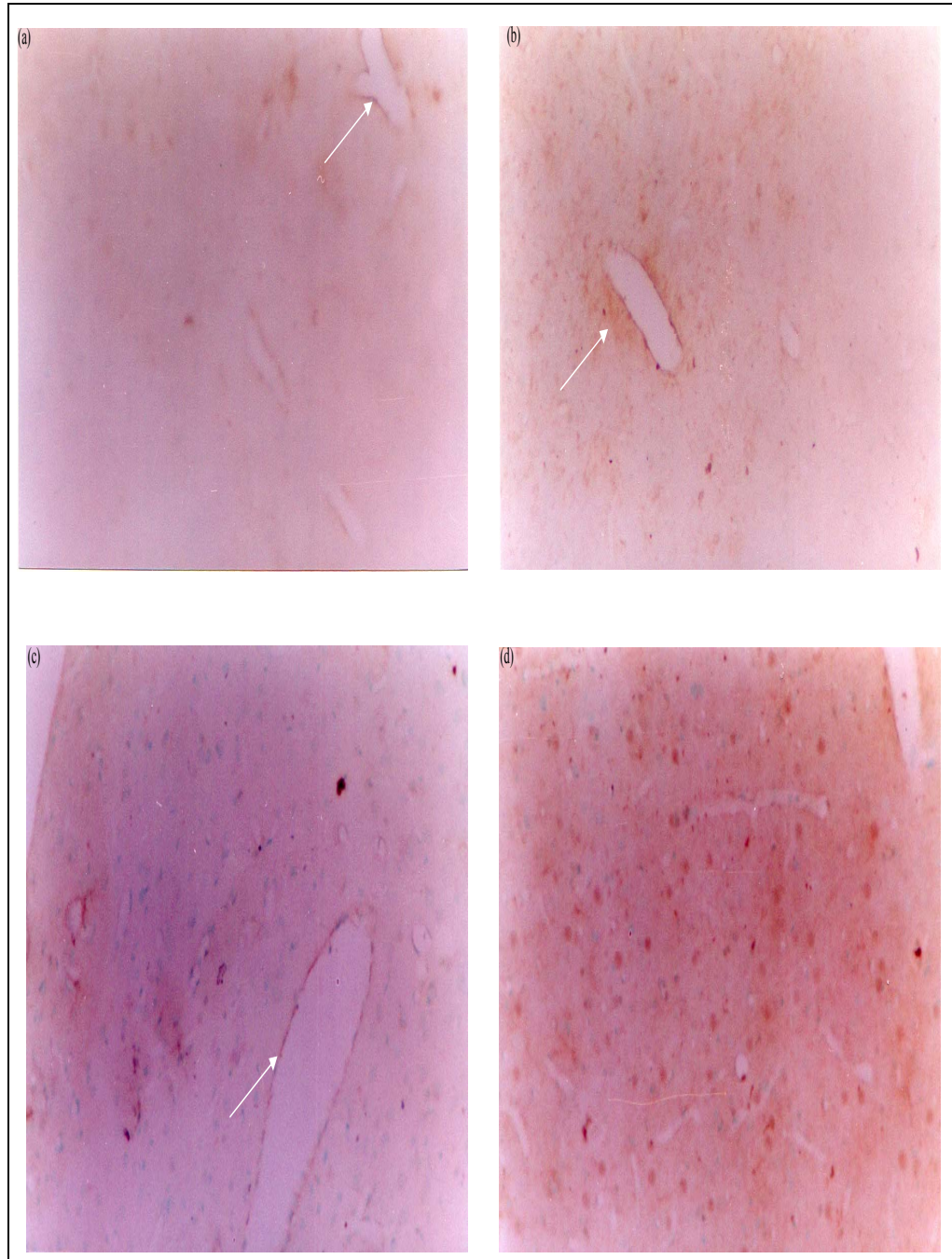


Fig 26. Immunostaining for GFAP in sections of hippocampus (a, b) and frontal cortex (c, d) of control (a, c) and ethanol treated rats (b, d). Note the increase in immunoreaction in ethanol treated rats. Magnification: 10x.

Fig. 27

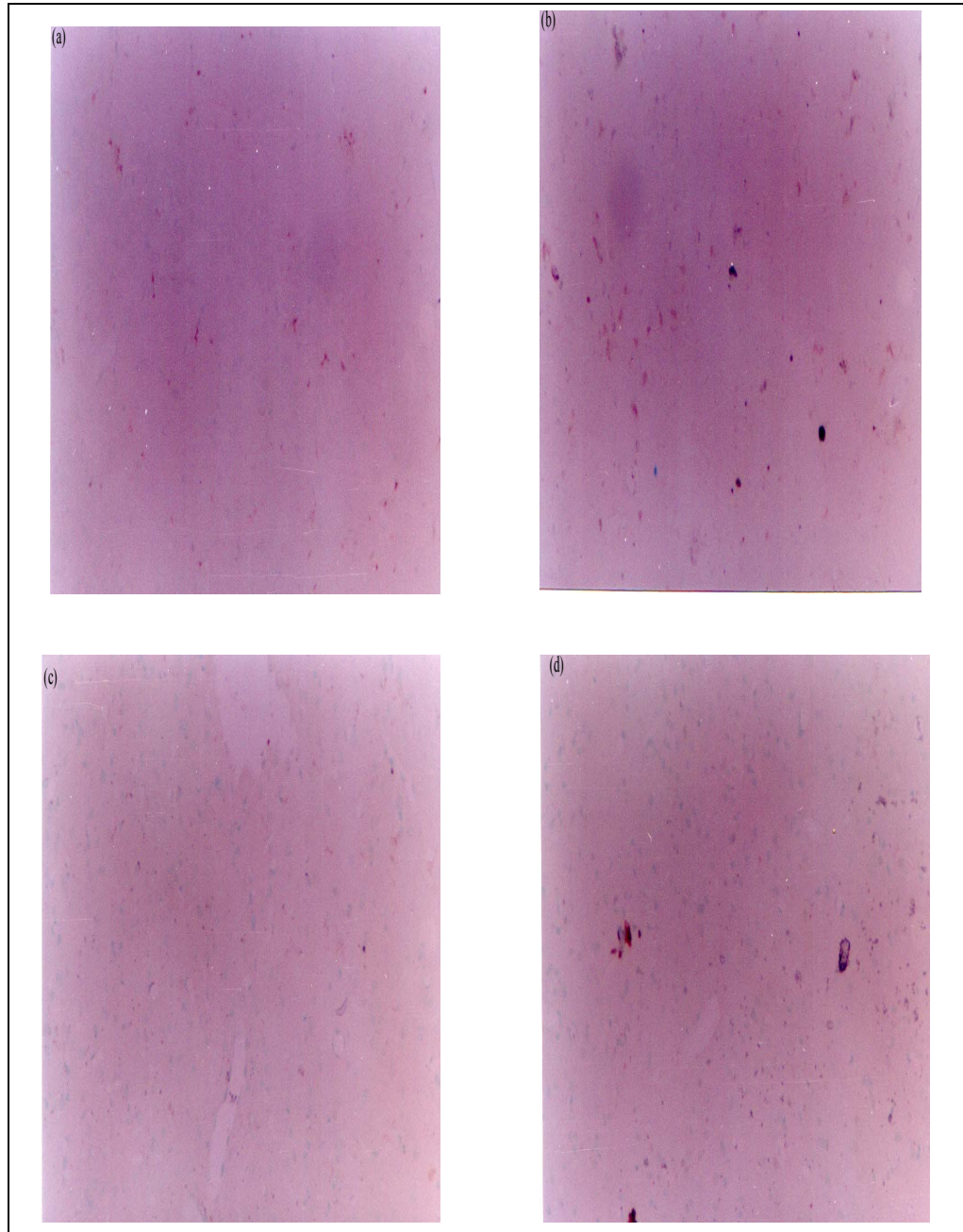


Fig 27. Immunostaining for active caspase-3 in sections of hippocampus (a, b) and frontal cortex (c, d) of control (a, c) and alcohol treated rats (b, d). Note the increase in immunoreaction in alcohol treated rats. Magnification: 10x.

Fig. 28

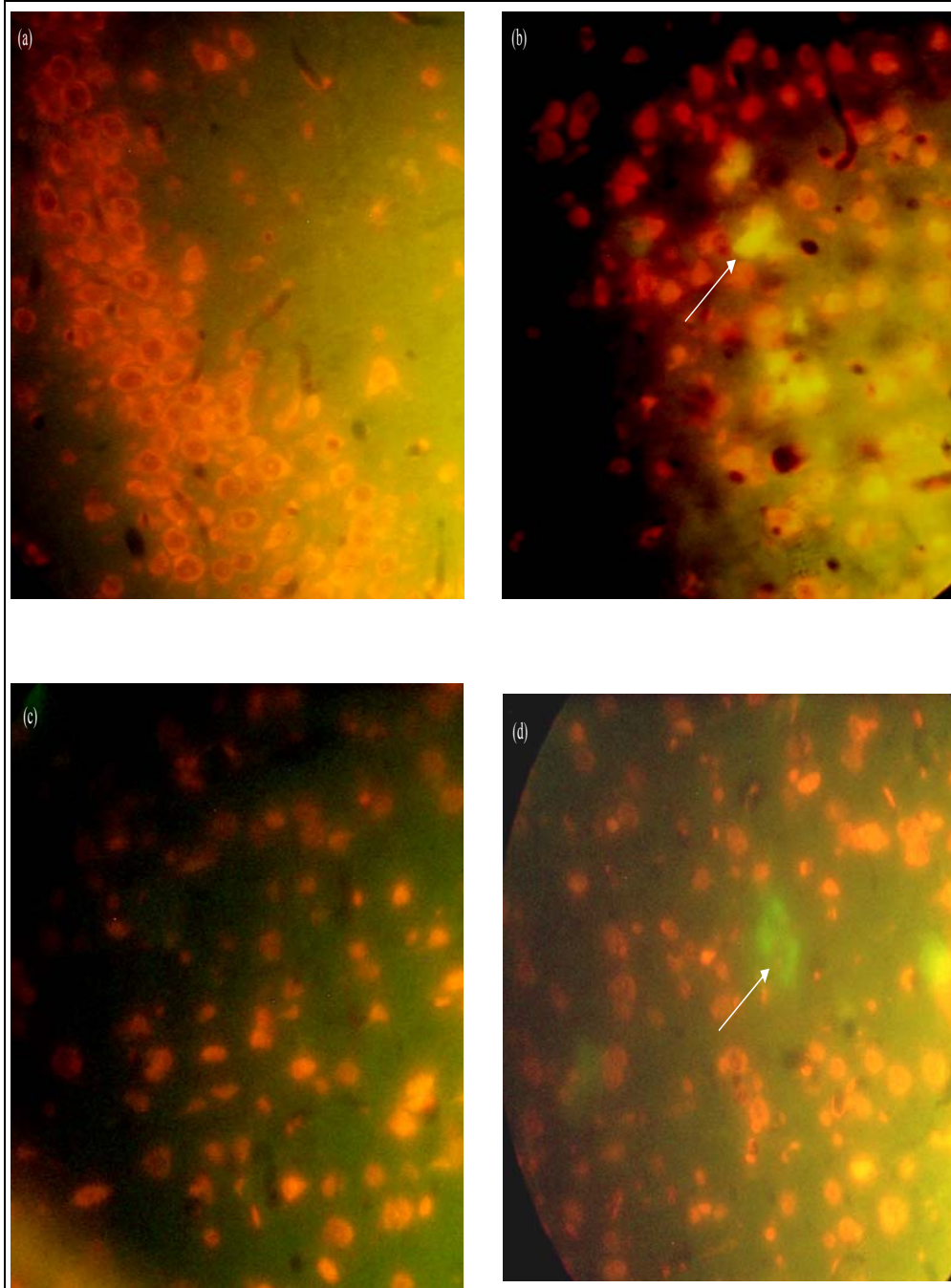


Fig 28. DNA nick end labeling of apoptotic cells (TUNEL). Sections of hippocampus (a, b) and frontal cortex (c, d) of control (a, c) and alcohol treated rats (b, d). Note the increase in labeling of DNA fragmentation in alcohol treated rats. Magnification: 40x

Fig.29

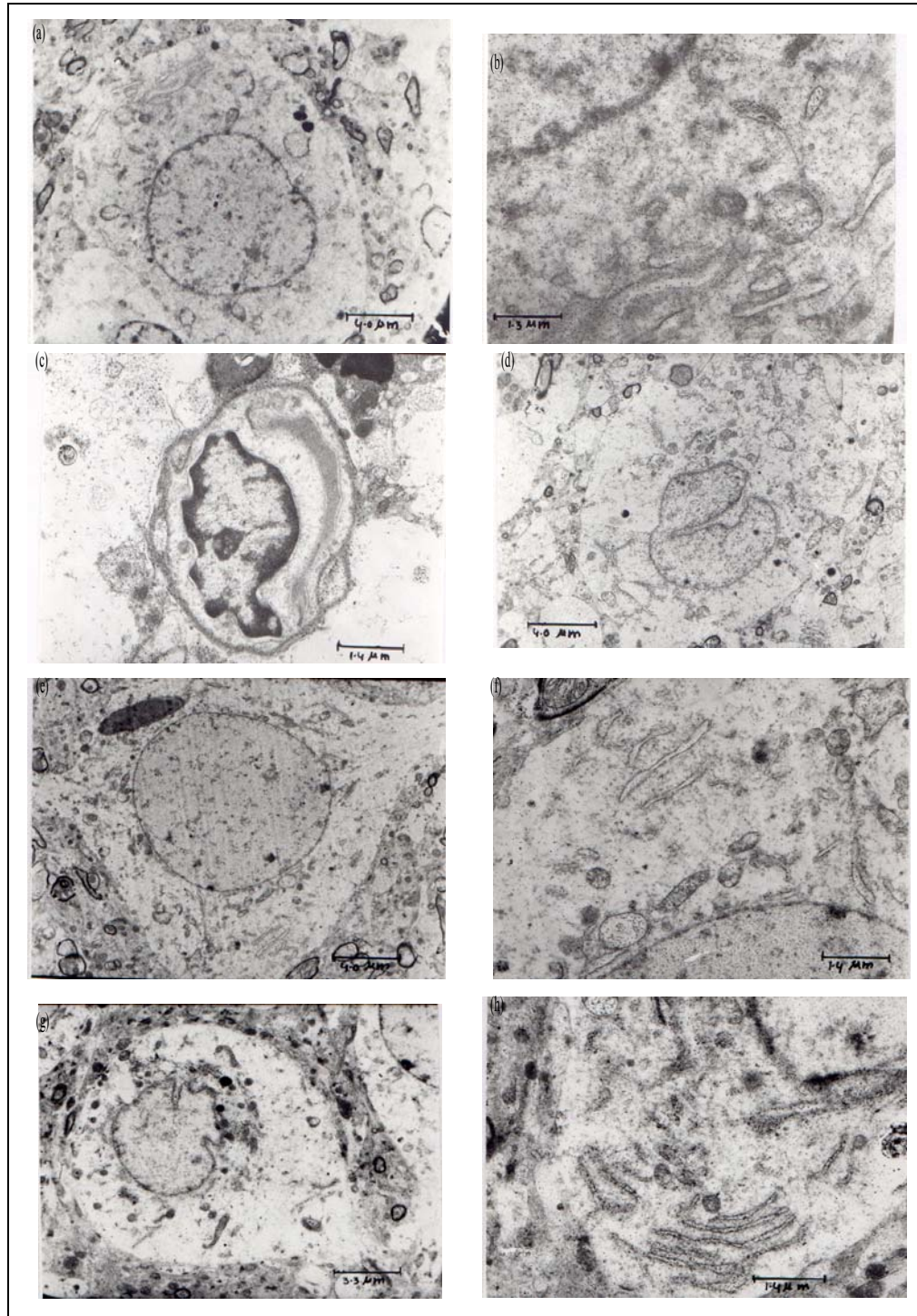


Fig 29. (a) Normal hippocampal cell. Hippocampal cell of control rat having

normal, oval nuclear morphology, cytoplasmic density and neuropile. Magnification. 2500x. (b) Detail of hippocampal cell in (a), showing normal nuclear membrane, nuclear pores, mitochondria and rough endoplasmic reticulum. Nuclear pores are easily visible and mitochondria and rough endoplasmic reticulum appear normal. Magnification 8000x.

(c) Cell displaying early signs of apoptosis Cell in hippocampus of ethanol treated rat showing watery and condensed cytoplasm, electronlucent with disruption of cellular organelles, abnormal nuclear shape with crenelation of nuclear membrane and margination of chromatin. Magnification 7000x.

(d) Swollen cell with early signs of necrosis. A cell in hippocampus of ethanol treated rat showing swollen, watery, electronlucent cytoplasm, disruption of cellular organelles with irregular nuclear profile of nuclear membrane. Mitochondrion is swollen, and rough endoplasmic reticulum is relatively normal. Magnification 2500x.

(e) Normal cell in frontal cortex of rat showing normal, oval nuclear morphology, cytoplasmic density and neuropile. Magnification 2500x.

(f) Detail of cell in frontal cortex showing normal nuclear membrane, nuclear pores, rough endoplasmic reticulum and golgi apparatus. Nuclear pores are easily visible and mitochondria and rough endoplasmic reticulum appear normal. Magnification 7000x.

(g) Cell displaying early signs of necrosis. A cell in frontal cortex of ethanol treated rat showing swollen cytoplasm and irregular nuclear profile of nuclear membrane and presence of abundant lysosomes. Magnification 3000x.

(h) Detail of frontal cortex cell in (g) showing normal mitochondria and rough endoplasmic reticulum. Cytoplasm is watery and electronlucent Magnification 7000x.

Discussion

To further support the biochemical observations with *in situ* detection techniques, morphological methods were employed. Apoptosis is relatively easy to detect in the developing nervous system, where programmed cell death predictably occurs in specific neuroanatomical sites and cell sub populations. Similarly acute neurotoxic injury in the adult brain may effect large subpopulations of neurons in a relatively synchronous fashion. More difficult to detect, however is neuronal apoptosis in the setting of chronic injury or neurodegenerative conditions, when neurons might be expected to undergo apoptosis in a sporadic or asynchronous fashion. (Roth 2002). Direct morphological evidence for apoptotic cell death is lacking in several chronic neurological diseases, including Amyotrophic Lateral Sclerosis, Huntington's disease, Parkinson's disease, Alzheimer's disease and HIV dementia, however this may simply reflect the fact that only a very small number of neurons are dying at any point of time in these chronic diseases (Raymond and Susana 2003). The asynchronous apoptosis and rapidity of phagocytosis of apoptotic bodies and their subsequent intracellular digestion further reduced the likelihood of detection of large numbers of apoptotic cells in H&E and Toluidine blue stained sections, but indirect evidence like break up neuropile, scanty and diffused degenerating cells, eosinophilic cells, karyorrhexis, chromatolysis, pyknosis, shrunken condensed cells, dark neurons (DN) and enhanced immunoreactivity of GFAP provided substantial evidence of injury. Both pyknosis and karyorrhexis were considered to characterize necrotic cell death in neoplastic cells of a canine malignant lymphoma after treatment with nitrogen mustard (Smith 1972). Tetramethyllead induced brain stem neurons and spinal motoneurons to undergo chromatolysis (Chang and Dyer 1995) in the same manner as observed in our study further supporting toxic potential of ethanol in causing cell death. Typical necrotic change was characterized as having eosinophilic cytoplasm or red neuron by Mackey *et al.* (1997). The observation of eosinophilic cytoplasm in both the regions in this study clearly indicates activation of necrotic cell death; however we could not detect large number of necrotic cells as expected since the dosage used in this study was not sufficient to trigger massive

necrosis. The specific death-signaling pathways that lead to degeneration of adult neurons are difficult to define. The molecular pathways seem to depend on the neuronal population that is affected, as well as the nature, stage, cause and extent of the death-inducing insult (Benn and Woolf 2004). Some cells in both the regions demonstrated near end stage apoptotic cells characterized by shrinking and condensation. “Near end stage apoptotic neurons” have been reported previously by Martin (2002) during motor neuron degeneration in Amyotrophic lateral sclerosis. Previously our lab has reported observation of broken neuropil and pyknotic cells during post-ischemic neuronal death (Phanithi *et al.* 2000) similar results are being reported in this study, to indicate pathology of brain tissue during chronic ethanol consumption. We also detected the appearance of dark neuron profiles, which may degenerate over a period of time either by apoptosis or necrosis. Similar observations of DN have been well characterized in ischemia (Czurko and Nishino 1993) and injury (Gallyas *et al.* 1992) poisoning with toxins such as kainic acid (Kiernan *et al.* 1998). The detection of DN profiles in histological sections has been interpreted as a sign of neuronal atrophy, probably representing a degenerative step previous to cell death, which occurs later by necrotic or apoptotic phenomenon.

One of the well-known functions of the astrocyte is concerned with repair. Subsequent to trauma, astrocytes invariably proliferate, swell, accumulate glycogen and undergo fibrosis by the accumulation of filaments, expressed neurochemically as an increase in GFAP (Cedric 1989), which can be used as a marker for neurotoxic evaluation. (O'Callaghan and Jensen 1992). Since astrocytes invest blood vessels (Cedric 1989), clear increase in immunoreactivity of GFAP around the blood vessel in alcohol treated hippocampus and also alcohol treated frontal cortex confirmed neurotoxic potential of alcohol.

Since commitment to cell death occurs prior to the caspase-3 activation step, immunohistochemical detection of neurons positive for caspase-3 activation provides a reliable means of mapping the cell death responses (Farber and Olney 2003). The observed increased immunoreactivity in alcohol treated sections implies that these cells are destined to die. This study provides evidence of activation of apoptotic cascade supported by immunohistochemistry of cleaved caspase-3 and

TUNEL assay.

It has also been suggested that mature neurons may not express a classic apoptotic phenotype or may undergo non-apoptotic form of cell death in neurodegenerative diseases (Raymond *et al.* 2003). It is known that oxidative stress induces a form of programmed cell death with characteristics of both apoptosis and necrosis in neuronal cells (Tan *et al.* 1998) and chronic ethanol administration is known to induce oxidative stress (Fadda and Rossetti 1998). It was previously reported that chronic ethanol consumption activates some inflammatory mediators and different pathways, which could participate in the transcriptional induction of genes implicated in the inflammatory injury, cell death and neurodegeneration. However, necrotic cell death is not excluded during chronic alcohol consumption (Valles *et al.* 2004). Since calpain activation represents a critical step in, apoptotic and necrotic neuronal death (Artal-Sanz *et al.* 2005), the present study was designed to characterize the type of cell death. Our ultrastructural studies have identified the existence of necrosis as well as apoptosis in chronic ethanol treated rat hippocampus and early necrosis in frontal cortex. It has also been suggested that apoptosis and necrosis often coexist in adult tissues during injury or degeneration and that a full continuum of morphological changes is often observed between apoptosis and necrosis (Schmechel 1999). Kaminski (2002) and co-workers, reported co existence of apoptotic and necrotic features in one single cell, however we could not detect both features in a single cell but were able to observe two independent cells displaying features of apoptosis and necrosis. Taken together our results imply that apoptosis and necrosis co-exist in rat brain during chronic ethanol consumption.

CHAPTER 3

Oxidative stress and Base excision repair in hippocampus and frontal cortex of rats treated with ethanol chronically

Ethanol and oxidative stress

Brain is susceptible to oxidative damage. In spite of the high rate of reactive oxygen species (ROS) production, due to high rate of oxidative metabolism and abundance of polyunsaturated fatty acids in cell membrane, brain has a relatively low antioxidant defense system. Oxygen species are key participants in damage caused by neurodegenerative processes, including cell death, motor neuron diseases and axonal injury (Fig 22) (Mates 2000). Chronic ethanol administration to rats for up to 18 months and subsequent withdrawal for 6 months has been reported to accelerate the formation of lipofuscin (which are reaction products of peroxidized lipids and denatured proteins) in the cerebellum, hippocampus and prefrontal cortex. A single dose of ethanol can elevate lipid

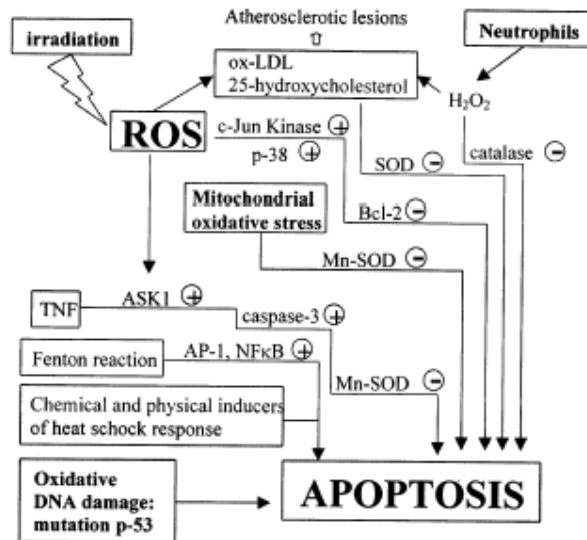


Fig. 30 Main critical steps in the signal transduction cascade leading to apoptosis that are sensitive to oxidants and antioxidants. AP-1, activated protein-1; ASK1, apoptosis signal-regulating kinase 1; NFκB, nuclear transcription factor kappa B; ox-LDL, oxidized low-density lipoproteins; TNF, tumor necrosis factor. (Adapted from Mates 2000)

hydroperoxide levels and reduce glutathione levels in rat brain homogenates; however no effects are observed after chronic ethanol treatment. Chronic administration of ethanol increases the concentration of free iron in the rat brain (Hunt and Nixon 1993). Activation of NMDA receptors can lead to neurodegeneration through the formation of ROS. It is known that acute or chronic

ethanol exposure produces lipid peroxidation as a consequence of free radical formation. The formation of the hydroxyl radical OH has been detected in the brain of ethanol-dependent rats at various times after withdrawal and shown to correlate with spontaneous seizure activity and with indices of cell degeneration. Cytosolic calcium appears to play a pivotal role in the generation of the superoxide anion and hydrogen peroxide H_2O_2 which in turn, can form the hydroxyl radical OH in the presence of Fe^{2+} by the fenton reaction. Chronic consumption of ethanol induces extracellular glutamate levels. Increased extracellular glutamate levels can generate OH radicals *in vivo* in the brain of rats through the activation of NMDA receptors. The calcium dependent activation of Phospholipase A_2 releases Arachidonic acid which leads to the generation of ROS (Fadda and Rossetti 1998).

Catalase

Living organisms have evolved antioxidant defenses to remove excess H_2O_2 . Catalase (EC 1.11.1.6) is present in the peroxisomes of mammalian cells and probably serves to destroy H_2O_2 generated by oxidase enzymes located within these subcellular organelles. Catalases convert H_2O_2 to water and O_2 . Catalase is a tetrameric haemin enzyme consisting of four identical tetrahedrally arranged subunits of 60 k Da. Therefore, it contains four ferriprotoporphyrin groups per molecule, and its molecular mass is about 240 k Da. Catalase is one of the most efficient enzymes known. It is so efficient that it cannot be saturated by H_2O_2 at any concentration. In animals, Catalase and Glutathione peroxidase (GPX) detoxify H_2O_2 . Further catalase protects cells from hydrogen peroxide generated within them. Even though catalase is not essential for some cell types under normal conditions, it plays an important role in the acquisition of tolerance to oxidative stress in the adaptive response of cells. (Mates 2000).

Glutathione

More important H_2O_2 removing enzymes in mammalian cells are the GPX, enzymes that require selenium (a selenocysteine residue, essential for enzyme activity, is present at the active site) (Halliwell 2004). GSH is synthesized from amino acids in selenium (Se)-dependent pathway (Segner and Braunbeck 1998). GPX enzymes remove H_2O_2 by using it to oxidize reduced glutathione (GSH) to oxidized glutathione (GSSG) (Halliwell 2004). Oxidized glutathione (GSSG) is reduced to GSH by glutathione reductase (GR); the NADPH required for the GR reaction is usually derived from the pentose shunt (Fig 23) (Segner and Braunbeck 1998). Small molecule free radical scavenger like GSH can scavenge various free radicals and ONOOH directly, as well as being substrate for GPX enzymes (Halliwell 2004). GSH functions in biotransformation: in the glutathione $-S$ -transferase (GST) reaction, electrophilic xenobiotics are conjugated to reduced GSH and thereby prepared for elimination from the cell. GSH protects against increased levels of peroxidants such as oxyradicals or lipid peroxyradicals from lipid peroxidation processes. The protective role of GSH in oxidative stress is based either on a direct function as a scavenger similar to eg ascorbate, or on its function as a co-substrate in the GPX reaction (Segner and Braunbeck 1998).

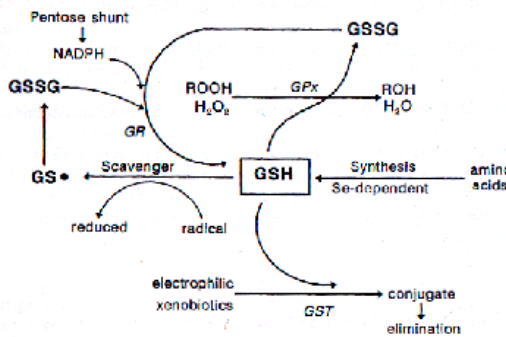


Fig. 31. Involvement of reduced glutathione (GSH) in protective cellular reactions towards toxic compounds adapted from Segner and Braunbeck (1998)

DNA damage and repair

DNA is the master molecule and serves as the blue print for the formation of all proteins and enzymes in every organism. The proteins then generate all the other substances in our cells. Thus it is essential for reproduction, growth and maintenance, and for sustaining normal living, that the DNA remains intact so that the genetic code can be read correctly. The stability and intactness of the DNA is a prerequisite for normal cellular functions, and there is good evidence that damage to

the DNA can lead to cellular dysfunction, or cell death. A major theory of aging holds that much of the aging phenotype is caused by the gradual accumulation of DNA damage over a life span. DNA damage occurs at a high frequency due to metabolic processes and environmental factors such as various types of exposures and the intake of food and drugs. The prevention or repair of DNA damage is thus a major concern in biology and medicine.

DNA damage

The long, thin DNA molecules contain three components: nitrogen-rich bases, sugar groups, and phosphate groups. The composition of the four types of bases – adenine, guanine, cytosine and thymidine-makes up the genetic code. Damage to DNA can occur to any of its three components. The bases are the most reactive. Many chemicals form adducts with new chemical groups being attached to existing DNA bases.

Base modifications in DNA after exposures

Living organisms are constantly exposed to stress from environmental agents and from endogenous metabolic processes. An important factor is exposure to oxidative reagents or oxidative stress. The resulting reactive oxygen species (ROS) attack proteins, lipids, and DNA. Since proteins and lipids are readily degraded and resynthesized, the most significant consequence of oxidative stress is thought to be DNA modifications, which can become permanent via the formation of mutations and other types of genomic instability.

Ethanol-induced DNA strand breaks have been demonstrated in neurons (Lamarche *et al.* 2003). Ikegami *et al.* (2003) identified possible DNA damage occurring in the superior frontal cortex and hippocampus of the human alcoholic brain, which is selectively localized to glial cells. These studies indicate that ethanol-induced genotoxicity contributes to neuronal cell death in the CNS.

Many different DNA base changes have been observed following oxidative

stress, and these lesions are widely considered to instigate the development of cancer, aging, and neurological degradation. The attack on DNA by ROS generates a low steady state level of DNA adducts that have been detected in the DNA from human cells. DNA base damage also can occur after direct attack by external sources. Irradiation from various sources can directly damage bases in DNA. For example, ultraviolet irradiation from exposure to sunlight creates certain DNA lesions. Irradiation from γ -ray sources, such as X-rays, leads to many different kinds of lesions in DNA, including base modifications, sites with a loss of base, and breaks in the DNA strand. Since DNA contains two strands running in parallel but opposite directions, breaks can be either single stranded or double stranded. A large number of components of food intake can directly damage DNA. These include carcinogens and chemicals that cause DNA damage, either by direct reactions or via metabolic modification. For example, aromatic amines are found in variety of foods and are known to cause DNA damage and to be highly mutagenic. A number of poisons work by attacking the DNA and damaging it. An example of this is the poisonous gas nitrogen mustard, which causes modification of DNA bases and also can link DNA bases on opposite DNA strands. These cause serious havoc in the cell by completely blocking the progression of polymerases.

Consequences of DNA damage

DNA damage can be induced by external or internal sources. Ultraviolet (UV) irradiation and ionizing irradiation are examples of exogenous sources of stress. ROS generated by the oxidative phosphorylation that occurs in mitochondria, and thus via cellular metabolism, is an example of an endogenous type of stress. Mutations in DNA can occur via replication of the damaged DNA whereby they become fixed. Lesion bypass or replication errors can give rise to other forms of genomic instability. A lesion in DNA can block transcription completely, it may truncate the transcript, or it may cause errors in the transcription. Alternatively, the DNA damage may induce new transcripts, and a number of genes have been shown to be inducible by various forms of cellular stress. These changes in transcription

patterns that are caused by DNA damage may be part of the origin of the malignant phenotype; many changes in transcription have been reported in cancers. They are also likely to be a cause of some of the changes seen in aging, where reductions or in some cases increases, in transcriptional activity are well established. Lesions in DNA also can lead to cell cycle arrest, or they can cause strand breaks in DNA. It is estimated that there are several thousand DNA alterations in each cell in the human organism per day, caused by both exogenous and endogenous stresses. Were it not for an efficient DNA repair process, genetic material would be destroyed by these processes over a normal human lifetime

Repair of damage to DNA

Major types of DNA damage repair are shown in table 4 along with their functions.

Mechanism	Mismatch repair	Base excision repair	Nucleotide excision	Recombination
Damage repaired	A-G or T-C Mismatch	Base modifications, single strand breaks	Large adducts, pyrimidine dimers	Interstrandcrosslinks, double strand breaks
Potential source of damage	Normal DNA replication	ROS, alkylating agents, X-rays	Reactiveintermediates, UV radiation	Clastogens, X-rays

Table 5. DNA repair mechanisms (adapted from Plant, 2003)

Mismatch repair is the basic repair system of the cell, removing nucleotides incorrectly incorporated during replication and replacing them with the correct nucleotide. Base excision repair (BER) and nucleotide excision repair (NER) are the main systems to deal with chemical-mediated damage to DNA. Both systems remove one or more damaged nucleotides and replace them with the correct nucleotide. BER is targeted towards small adducts or DNA lesions (e.g. ROS-mediated damage) whereas NER is a more flexible system that can remove larger

adducts, such as those formed by interactions of reactive chemical intermediates with DNA. Finally large chromosomal aberrations are repaired by recombination repair systems (Bohr 2005).

Brain is composed of two major heterogeneous populations of cells – neurons and astroglia, which have different characteristics. A large number of studies have documented that developmental ethanol exposure causes loss of specific neuronal populations. Neuronal cell populations that are reduced by developmental ethanol exposure include neurons in the CA1 region of the hippocampus and granule and Purkinje cells in the cerebellum (Bonthius and West *et al.* 1990; Miller 1995; Pauli *et al.* 1995; Bonthius *et al.* 2001). In addition to affecting neurons, developmental exposure to ethanol has also been shown to affect glial cells (Phillips *et al.* 1992). Reduction in glial cell number has been reported in rat models of FAS (Miller and Potempa 1990; Perez-Torrero *et al.* 1997). Ethanol has also been shown to cause apoptotic cell death of hippocampal, cerebellar, and cortical neurons *in vitro* and *in vivo* (Oberdoerster and Rabin 1999; Ikonomidou *et al.* 2000; Climent *et al.* 2002). Increased TUNEL-positive cells indicate DNA damage induced by ethanol-related overproduction of reactive oxygen species (Ikegami *et al.* 2003). Base Excision Repair (BER) is performed by DNA-polymerase beta in response to different insults. BER may differ in both populations under chronic treatment.

All these observations clearly indicate oxidative stress during alcohol consumption, however very few reports exist on ethanol induced oxidative stress in hippocampus and frontal cortex. It is well known that oxidative stress leads to apoptosis (Figure 22) (Mates 2000). In the previous chapters we have shown the activation of apoptotic cascade and hence we looked for upstream events in causing cell death, namely oxidative stress. We wanted to test whether oxidative stress has any role in apoptotic events by reducing Base excision repair. The aim of this study was to determine activities of certain antioxidant enzymes namely Catalase, Glutathione Peroxidase (GPX), Glutathione S transferase (GST), GSH and GSSG levels, along with the status of base excision repair in neurons and astrocytes of ethanol treated rats. The half-lives of ROS is extremely short, hence, it is technically difficult to measure their concentrations in the brain. One way to overcome this

problem is to measure the antioxidant levels of the tissue as an indicator of oxidative stress. The cellular antioxidant status determines the susceptibility to oxidative damage and is usually altered in response to oxidative stress and the changes in levels of antioxidant enzyme activities in a disease condition would explain the degree of oxidative stress. Since Catalase, GST, and GPX constitute the primary line of defense against the intracellularly generating free radicals; the present study was designed to investigate the changes in activities of Catalase, GST, and GPX in different regions of rat brain after chronic alcohol administration.

Materials and methods

Chemicals

Bovine serum albumin, glutathione (reduced form), glutathione (oxidized form), glutathione reductase, N-ethylmaleimide (NEM), o-phthalaldehyde (OPT), 1-chloro-2, 4, -dinitrobenzene (CDNB), Tween-20, Phenylmethyl-sulfonyl fluoride (PMSF), Highly polymerized calf thymus DNA, 'activated' calf thymus DNA (may be defined as the DNA partially digested with small amounts of DNase1 to induce nicks), ATP and deoxynucleotide triphosphates were purchased from Sigma Chemical St Louis, USA. NADH-reduced form (disodium salt), NADPH-reduced form (tetrasodium salt), Hydrogen peroxide solution (30%), Folin & Ciocalteu's phenol reagent, dithiothreitol (DTT), Nitroblue tetrazolium (NBT), 5-bromo-4-chloro-3-indoyl phosphate (BCIP), Ethylene Diamine tetra acetic acid (EDTA), di-Potassium Hydrogen Ortho Phosphate (K_2HPO_4), Magnesium Chloride ($MgCl_2$), Sodium Chloride (NaCl), Potassium Chloride (KCl) were purchased from Sisco Research Laboratories Pvt. Ltd, Mumbai, India. Nitrocellulose sheet was from Millipore (Billerica, MA, USA) and secondary antibodies were purchased from Bangalore Genei Pvt. Ltd. (Bangalore, India). All other chemicals were of analytical grade and purchased locally.

Sub fractionation for measuring GSH and GSSG

Sub fractionation and estimation of GSH and GSSG levels was done according to Hissin and Hilf (1976) with slight modification. GSH and GSSG were prepared daily in 0.1 M sodium phosphate-0.005M EDTA buffer (pH-8.0) and kept on ice until used. O-phthaldehyde (OPT) solution was prepared daily in reagent grade absolute methanol just prior to use. Rats were killed by cervical dislocation; brains were removed, blotted, weighed, and used immediately or frozen in liquid nitrogen and stored at -80° C until assayed. A portion of tissue (250 mg) was homogenized on ice using a polytron homogenizer. The solution used for homogenization consisted of 3.5 ml of the phosphate-EDTA buffer and 1ml of 25% HPO₃, which was used as a protein precipitant. The total homogenate was centrifuged at 4° C at 16,000Xg for 30 min to obtain the supernatant for the assay of GSH and GSSG assay.

GSH Assay

To 0.5 ml of the 16,000Xg supernatant, 4.5 ml of the phosphate-EDTA buffer, pH-8.0, was added. The final assay mixture 2.0 ml contained 100 µl of the diluted tissue supernatant, 1.8 ml of phosphate-EDTA buffer, and 100 µl of the OPT solution, containing 100 µg of OPT(1% solution in methanol). After thorough mixing and incubation at room temperature for 15 min, the solution was transferred to a quartz cuvette. Fluorescence at 420 nm was determined (activation at 350 nm). GSH was shown to react specifically with OPT at pH 8.0, yielding a highly fluorescent product that could be activated at 350 nm with emission peak of 420 nm. An increase above pH 8.0 caused the conversion of GSH to GSSG. The fluorescence intensity for the OPT-GSH reaction was directly related to GSH concentration and was linear over the concentration range of 10 ng to 2 µg.

GSSG Assay

A 0.5 ml portion of original 16,000Xg supernatant was incubated at room temperature with 200 µl of 40 nm NEM for 30 min to interact with GSH present in

the tissue. To this mixture, 4.3 ml of 0.1N NaOH was added. A 100 μ l portion of this mixture was taken for measurement of GSSG, using the procedure outlined above for GSH assay, except that 0.1 N NaOH was employed as diluent rather than phosphate-EDTA buffer. Protein Estimation was done by the method of Lowry (1951). O-phthaldehyde reacted with GSSG, yielding readily measurable fluorescent intensity at pH-12. The fluorescence intensity was observed to be linear over the concentration range of 5 ng to 2 μ g of GSSG. The absorbance and emission spectra for the OPT-GSSG reaction were similar to that for GSH, namely 350 and 420 nm, respectively.

Antioxidant enzyme assays

Sub fractionation for enzyme assays

Sub fractionation for enzyme assays was carried out as described by Baskaran *et al* (1999). Rats were sacrificed at the end of experimental period by cervical dislocation and the brain was dissected. It was washed in ice cold PBS and frozen immediately in -80° C until further use. The brains were minced and 10% homogenate in 50 mM phosphate buffer (pH 7.4), in ice cold was prepared using teflon-glass homogenizer. The homogenate was centrifuged at 1000Xg for 15 min; the supernatant was stored at 4° C and used for various biochemical assays. Total protein in the homogenate was assayed by the Lowry's method (1951).

Glutathione S-Transferase (GST) (2.5.1.18) activity assay:

Glutathione S-transferase activity was measured according to the method of Habig and Jakoby (1981) by using CDNB as substrate. The standard assay mixture contained CDNB 1mM, reduced glutathione 1mM and potassium phosphate buffer (100 mM; pH 6.5) in a volume of 1 ml. The reaction was monitored at 340 nm. The Thioether formed was determined by reading the absorbance at 340 nm and quantification was done using $9.6 \text{ mM}^{-1} \text{ cm}^{-1}$ as the extinction coefficient. Activity

was calculated according to the following equation.

Difference in absorbance for 1 min x Volume of the reaction mixture in ml

$$\varepsilon \text{ CDNB}(9.6) \times \text{Volume of the enzyme in ml}$$

Specific activity is expressed as units per mg of protein. One unit of enzyme activity was defined as 1 μM of product formed or 1 μM of substrate consumed per minute. Specific activities were calculated in units per milligram of protein.

Glutathione Peroxidase Assay

Glutathione peroxidase (GSH: H_2O_2 oxidoreductase, EC 1.11.1.9) activity was measured according to the method of Nakamura *et al.* (1981). The activity was assayed by following the oxidation of NADPH at 340 nm in the presence of glutathione reductase which catalyzed the reduction of GSSG formed by the peroxidase in a shimadzu UV-Vis spectrophotometer. The standard reaction mixture was composed of 50 mM sodium phosphate buffer (pH 7.0), 0.16 mM NADPH, 1mM NaN_3 , 0.4 mM EDTA, 1 mM GSH, 0.2 mM H_2O_2 , 4 μg of yeast glutathione reductase and 10 μl of enzyme in a total volume of 2 ml. The reaction was started by the addition of H_2O_2 and measured at 25° C .The non enzymatic oxidation of GSH was measured by using water instead of the enzyme fraction in the standard reaction mixture, and its reaction rate was subtracted from that of the former system in order to determine the true enzymatic activity. Protein concentration was estimated by the method of Lowry *et al* (1951) using crystalline bovine serum albumin as a standard. Activity was calculated according to the following equation.

Difference in absorbance for 1 min x Volume of the reaction mixture in ml

$$\varepsilon \text{ NADPH} (6.2) \times \text{Volume of the enzyme in ml}$$

Specific activities were calculated in units per milligram of protein. Extinction coefficient of NADPH was taken as 6.2 $\text{mM}^{-1} \text{cm}^{-1}$. One unit of enzyme activity is the amount of the enzyme required to oxidize 1 μM of NADPH/min.

Catalase (E.C 1.11.1.6) activity assay:

Catalase activity was measured as described by Chance and Maechly (1955). 1 ml of reaction mixture contained 20 μ l of enzyme in phosphate buffer pH 7.0 and 10 mM H_2O_2 . H_2O_2 was added last to start the reaction. The absorbance was read at 240 nm against a blank, which decreased every 15 s. Blank tube did not contain H_2O_2 . For standardization a value of OD between 0.02 - 0.10 was considered and recorded for a period of 180 seconds. Light path was 1 cm. To check the purity of H_2O_2 , which was prepared freshly, the absorbance of 30 mM H_2O_2 was taken between 0.5 & 1.0, and the difference in optical density was found to be between 0.02 - 0.10 (normal range). Phosphate buffer was stored at 4° C. Extinction coefficient of H_2O_2 was taken as 43.6 $mM^{-1} cm^{-1}$. Activity was calculated according to the following equation.

Difference in absorbance for 1 min x Volume of the reaction mixture in ml

$$\epsilon H_2O_2 (43.6) \times \text{Volume of the enzyme in ml}$$

Specific activities were calculated in units per milligram of protein. One unit of enzyme activity is the amount of the enzyme required to disproportionate hydrogen peroxide at the rate of 0.1 μ M/min.

Isolation of neurons and astrocytes

Animals were killed by decapitation. Neurons and astroglia from rat brain cerebral cortex and cerebellum of control and ethanol treated rats were prepared essentially as described by Rani *et al* (1983). All the procedure was carried out at 4° C and autoclaved water was used for preparation of solutions. Brains were collected into ice cold isolation medium (2% medium, 4g ficoll/200 ml medium). Cerebral cortex and cerebellum was dissected. Gray matter was used for isolation of Neurons and Astrocytes. White matter, fat and blood vessels were completely removed. Gray matter was minced and incubated in isolation medium containing 0.1% Trypsin (10 ml per gram of tissue for 1 hour at 37° C for adult brains). After incubation the Trypsin containing medium is removed (decanted carefully) and equal volume of isolation medium containing 0.1% Soyabean Trypsin inhibitor was added and left on

ice for 5 min. Trypsin inhibitor was removed and washed the tissue thrice with ice cold isolation medium using a flat bottom glass rod gently. The tissue was then passed through 103 μm , 80 μm , and 48 μm nylon meshes each 3 times. Tissue was kept moist always with isolation medium. Filtrate was centrifuged at 800Xg for 15 min. Supernatant was discarded and the pellet was suspended in 7% Isolation medium (7g ficoll/100 ml Isolation medium) (10 ml per gram of tissue) and centrifuged at 300Xg for 20 min. The pellet contained neurons and supernatant consisted astrocytes. Further processing of neuronal pellet was performed by suspending it in isolation medium (5 ml/gm) and centrifuged at 1500Xg for 10 min. Supernatant was discarded and the pellet was suspended in medium (1.095 g KH_2PO_4 , 64 g glucose, 40 g fructose, pH adjusted to 6 with NaOH, and made up to 800 ml)(5 ml/gm) and centrifuged at 1500Xg for 10 min. The supernatant was discarded and the pellet was suspended in medium and centrifuged once again at 1500Xg for 10 min. The supernatant was discarded and the pellet was suspended in extraction buffer after cell counting.

The supernatant from the 7% step (astrocyte fraction) was diluted with isolation medium in the ratio of 1:1.125 and centrifuged at 1100Xg for 15 min. The supernatant was discarded and pellet was suspended in isolation medium and centrifuged at 1500Xg for 10 min. The supernatant was discarded and pellet was suspended in medium and centrifuged at 1500Xg for 10 min. The supernatant was again discarded and pellet was suspended in medium and centrifuged at 1500Xg for 10 min. The supernatant was discarded and pellet was suspended in extraction buffer after cell counting.

Preparation of cell extracts

The final preparation of cells were suspended at a concentration of 10 million cells per ml in extraction medium consisting of 20 mM Tris pH 7.5, 0.1 mM DTT, 1 mM EGTA, 10% glycerol, 0.5% CHAPS, 0.1 mM PMSF (just before use), 5mM β -mercaptoethanol, 1mM MgCl_2 , 1 $\mu\text{g/ml}$ leupeptin and 1 $\mu\text{g/ml}$ pepstatin A (both just before use) and 0.5 M KCl and sonicated for 5 s, three times with the setting of five

in a Branson sonifier. The suspension was kept at 0-4° C for 30 min and then centrifuged at 100,000Xg for 1 h in a Sorvall ultracentrifuge and the clear supernatant was used as the source for DNA-polymerases.

DNA polymerase assay

Polymerase assay was performed as described earlier (Raji *et al.* 2002) performed with 'activated' calf thymus DNA. The incubation mixture (total volume 50µl) contained 40mM Tris-HCl (pH7.5), 8mM MgCl₂, 1mM β-mercaptoethanol, 4mM ATP, 100 µM each dATP, dGTP, dTTP, 25µM dCTP, 5 µg 'activated' DNA, 1µCi α⁻³² P-dCTP (4000 Ci/mmol) and cell extract as enzyme source (10 µg protein). The mixture was incubated for 20 min at 37° C, 200 µg each of DNA and BSA were added and the reaction stopped with 1M : 10mM perchloric acid : tetra sodium pyrophosphate, respectively. The samples were kept on ice and centrifuged at 3000Xg for 10 min. The supernatant was aspirated carefully and the precipitate was dissolved in 0.5 ml of 0.2M NaOH. A 2 ml volume of stop solution was again added and centrifuged after 10 min. The alkali solubilization step and reprecipitation with stop solution was repeated. The whole solution along with the precipitate was transferred to 2.5 cm glass fiber filters (Schleicher & Schuell) and washed three times with ice-cold stop solution and twice with 95% ethanol. The washed filters were directly taken into counting vials and dried by keeping in oven at 40° C for 20 min or keeping in a hood overnight. Then toluene-based scintillation fluid having Triton-X 100 was added and the radioactivity was counted in a Wallac 1409 counter. Activity is expressed as picomoles of radio activity incorporated into acid insoluble fraction.

Gel electrophoresis and Western blotting

Fifty micrograms of neuronal and astrocyte extracts were separated by reducing sodium dodecyl sulphate polyacrylamide gel electrophoresis (SDS-PAGE). Protein transfer was performed according to the method of Towbin *et al* (1979). Briefly,

proteins were transferred onto nitrocellulose membrane overnight at 30 V in Towbin buffer (25 mM Tris-HCl (pH 8.3), 192 mM glycine, 20% methanol). The non-specific binding sites were blocked with 5% (w/v) non-fat milk for 2 h. The blots were probed with 1: 1000 dilution of Rabbit polyclonal antibody against DNA polymerase beta (39 k Da). The blots were further processed with Alkaline Phosphatase-conjugated anti-rabbit secondary antibody (Bangalore Genei, India). After developing, the membrane was dried, and densitometry analysis was performed using a color scanner (HP Scanjet 3200C) and the NIH Image software, ImageJ 1.34s (available for Windows through NIH: <http://rsb.info.nih.gov/ij/download.html>).

Data analysis

Data were analysed by one-way analysis of variance (ANOVA). When a significant F value was found, Fisher's least difference (LSD) multiple comparison was performed to test the differences between the means. Data are reported as mean \pm S.E.M. of n experiments. A level of $P < 0.05$ was considered statistically significant and was determined using SPSS for windows version.

Results

Glutathione: Reduced glutathione (GSH) content showed significant variation in HE compared to control HC, where it is increased. However GSH levels were decreased in frontal cortex of ethanol treated rats when compared to that of control samples (Fig 32). The levels were calculated using standard graph shown in Fig 32.

Oxidized glutathione: Oxidized glutathione (GSSG) content also showed significant variation in HE, where it was found to be increased. However GSSG levels were decreased in FE when compared to that of control samples (Fig 32). The levels were calculated using standard graph shown in Fig 32.

Glutathione S- transferase: GST activity was measured in control and ethanol treated rats using CDNB as substrate and the data is presented in “Fig. 33”. GST activity did not show any significant change in activity compared to that of control in HE, however activity increased in FE

Glutathione peroxidase (GPX): Glutathione peroxidase (GPX) activity was measured in control and ethanol treated rats and the data is presented in “Fig 33”. GPX activity increased in both HE and FE, more so in FE, indicating GSH consumption, which could be the possible reason for induction of oxidative stress in these regions.

Catalase: Catalase activity was measured in control and ethanol treated rats using H₂O₂ as substrate and the data is presented in “Fig. 33”. Catalase activity did not show any significant change in activity compared to that of control in both the regions observed, suggesting that ethanol administration did not affect the catalase activity.

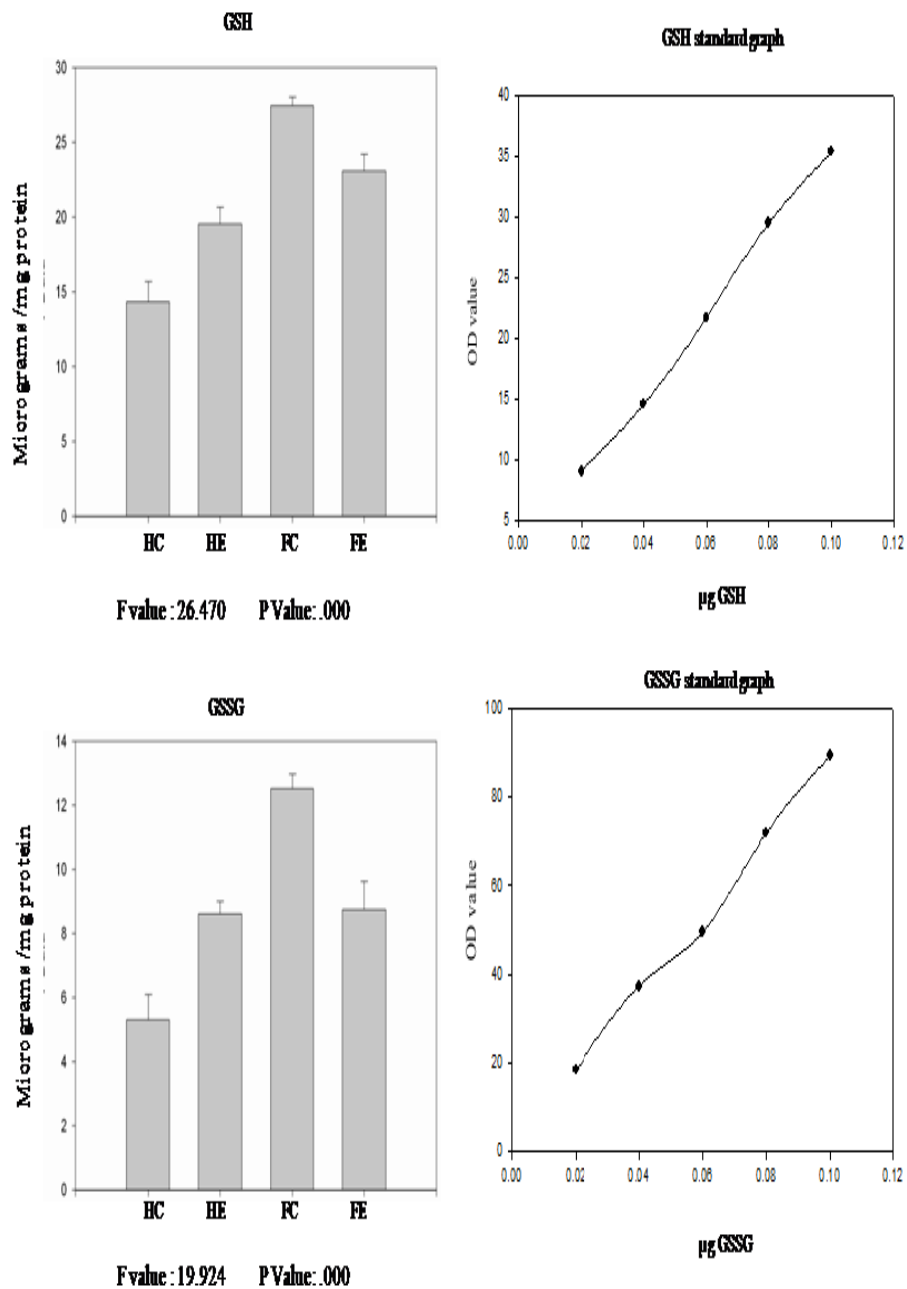
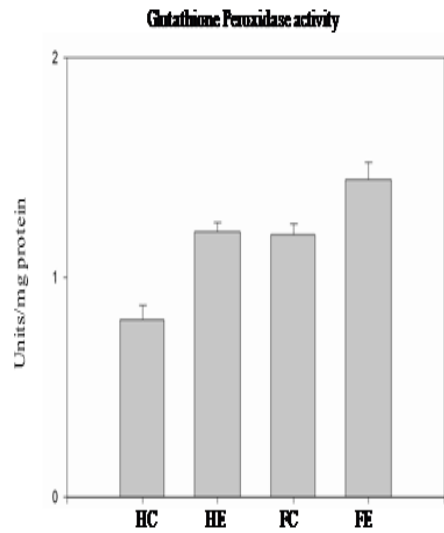
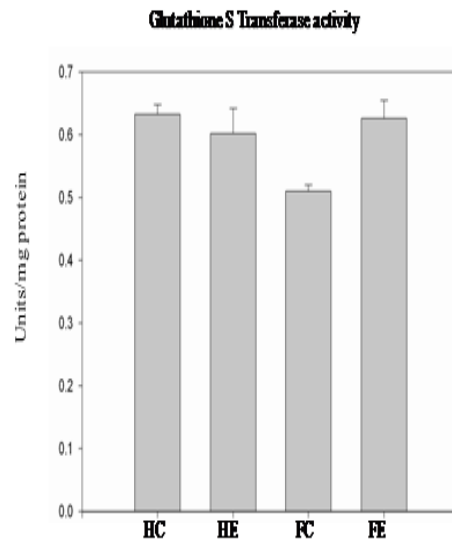


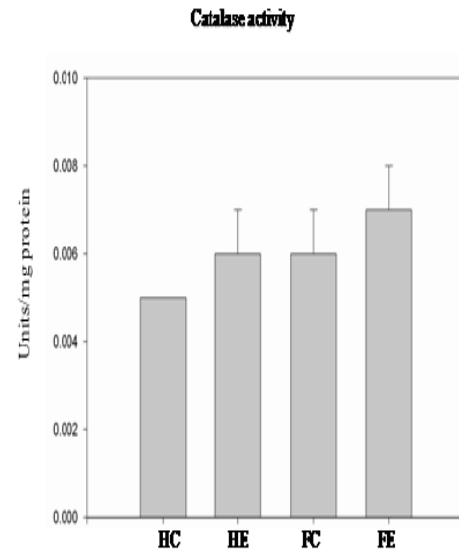
Fig. 32 Reduced glutathione (GSH) content showed significant increases in HE; however GSH levels were decreased in FE. Oxidized glutathione (GSSG) content also showed significant variation in HE, where it was found to be increased, however it was decreased in FE. The levels were calculated using standard graph shown in the figure. The graph was linear. Each data point represents the mean from four analyses. Crude cytosolic fractions were used (HC-control hippocampus, HE-ethanol treated hippocampus, FC- control frontal cortex and FE-ethanol treated frontal cortex).



Fvalue :19.305 PValue:.000



Fvalue :3.349 PValue: .069



Fvalue :1.135 PValue: .386

Fig 33 Glutathione Peroxidase activity, Glutathione S Transferase activity and Catalase activity

Table 6

Oneway Anova

1=HC; 2=FC; 3=HE; 4=FE

Descriptives									
		N	Mean	Std. Deviation	Std. Error	95% Confidence Interval for Mean		Minimum	Maximum
		Lower Bound	Upper Bound	Lower Bound	Upper Bound	Lower Bound	Upper Bound	Lower Bound	Upper Bound
GST	1	3	.633	.025	.015	.570	.695	.605	.653
	2	3	.510	.017	.010	.468	.552	.493	.527
	3	4	.602	.080	.040	.474	.729	.490	.672
	4	3	.626	.050	.029	.501	.751	.568	.655
	Total	13	.593	.068	.019	.552	.634	.490	.672
Catalase	1	3	.005	.001	.000	.003	.007	.004	.006
	2	3	.006	.001	.001	.002	.009	.005	.007
	3	3	.006	.001	.001	.003	.010	.005	.008
	4	4	.007	.001	.001	.005	.009	.005	.008
	Total	13	.006	.001	.000	.005	.007	.004	.008
GPX	1	4	.807	.133	.066	.596	1.018	.686	.981
	2	3	1.194	.087	.050	.977	1.411	1.101	1.274
	3	3	1.208	.073	.042	1.028	1.389	1.133	1.278
	4	3	1.445	.137	.079	1.106	1.784	1.335	1.598
	Total	13	1.136	.268	.074	.974	1.298	.686	1.598
GSH	1	3	14.336	2.345	1.354	8.512	20.160	11.638	15.880
	2	3	27.441	1.029	.594	24.885	29.997	26.253	28.040
	3	3	19.550	1.889	1.091	14.857	24.243	17.380	20.830
	4	3	23.072	1.953	1.128	18.220	27.924	20.846	24.500
	Total	12	21.100	5.262	1.519	17.756	24.443	11.638	28.040
GSSG	1	3	5.305	1.356	.783	1.936	8.675	3.750	6.243
	2	3	12.512	.795	.459	10.536	14.488	11.683	13.269
	3	3	8.619	.657	.380	6.986	10.252	7.900	9.189
	4	3	8.742	1.523	.879	4.958	12.526	6.986	9.711
	Total	12	8.795	2.837	.819	6.992	10.597	3.750	13.269

Test of Homogeneity of Variances

	Levene Statistic	df1	df2	Sig.
--	------------------	-----	-----	------

GST	1.663	3	9	.243
Catalase	.261	3	9	.852
GPX	.864	3	9	.494
GSH	1.258	3	8	.352
GSSG	1.892	3	8	.209

ANOVA						
		Sum of Squares	df	Mean Square	F	Sig.
GST	Between Groups	.029	3	.010	3.349	.069
	Within Groups	.026	9	.003		
	Total	.055	12			
Catalase	Between Groups	.000	3	.000	1.135	.386
	Within Groups	.000	9	.000		
	Total	.000	12			
GPX	Between Groups	.745	3	.248	19.305	.000
	Within Groups	.116	9	.013		
	Total	.860	12			
GSH	Between Groups	276.750	3	92.250	26.470	.000
	Within Groups	27.881	8	3.485		
	Total	304.631	11			
GSSG	Between Groups	78.075	3	26.025	19.924	.000
	Within Groups	10.450	8	1.306		
	Total	88.525	11			

Post Hoc Tests

Multiple Comparisons LSD					
Dependent Variable	(I) group	(J) group	Mean Difference (I-J)	Std. Error	Sig.
			Lower Bound	Upper Bound	Lower Bound
GST	1	2	.123(*)	.044	.021
		3	.031	.041	.466
		4	.007	.044	.881
	2	1	-.123(*)	.044	.021
		3	-.092	.041	.052
		4	-.116(*)	.044	.027
	3	1	-.031	.041	.466
		2	.092	.041	.052

		4		-.025	.041	.566
	4	1		-.007	.044	.881
		2		.116(*)	.044	.027
		3		.025	.041	.566
Catalase	1	2		.000	.001	.657
		3		-.001	.001	.366
		4		-.002	.001	.115
	2	1		.000	.001	.657
		3		.000	.001	.634
		4		-.001	.001	.241
	3	1		.001	.001	.366
		2		.000	.001	.634
		4		-.001	.001	.485
	4	1		.002	.001	.115
		2		.001	.001	.241
		3		.001	.001	.485
GPX	1	2		-.387(*)	.087	.002
		3		-.401(*)	.087	.001
		4		-.638(*)	.087	.000
	2	1		.387(*)	.087	.002
		3		-.014	.093	.880
		4		-.251(*)	.093	.024
	3	1		.401(*)	.087	.001
		2		.014	.093	.880
		4		-.237(*)	.093	.031
	4	1		.638(*)	.087	.000
		2		.251(*)	.093	.024
		3		.237(*)	.093	.031
GSH	1	2		-13.105(*)	1.524	.000
		3		-5.214(*)	1.524	.009
		4		-8.736(*)	1.524	.000
	2	1		13.105(*)	1.524	.000
		3		7.891(*)	1.524	.001
		4		4.369(*)	1.524	.021
	3	1		5.214(*)	1.524	.009
		2		-7.891(*)	1.524	.001
		4		-3.522(*)	1.524	.050
	4	1		8.736(*)	1.524	.000

		2	-4.369(*)	1.524	.021
		3	3.522(*)	1.524	.050
GSSG	1	2	-7.206(*)	.933	.000
		3	-3.314(*)	.933	.007
		4	-3.436(*)	.933	.006
	2	1	7.206(*)	.933	.000
		3	3.892(*)	.933	.003
		4	3.770(*)	.933	.004
	3	1	3.314(*)	.933	.007
		2	-3.892(*)	.933	.003
		4	-.122	.933	.899
	4	1	3.436(*)	.933	.006
		2	-3.770(*)	.933	.004
		3	.122	.933	.899
* The mean difference is significant at the .05 level.					

Multiple comparisons

	HC*FC	HC*HE	HC*FE	FC*HE	FC*FE	HE*FE
GPX	S	S	S	NS	S	S
GSH	S	S	S	S	S	S
GSSG	S	S	S	S	S	NS
GST	S	NS	NS	NS	S	NS
catalase	NS	NS	NS	NS	NS	NS

S- Significant, NS- Non Significant

Effect on Base excision repair in neurons and astrocytes

DNA polymerase activity in rat neuronal and astroglial fractions (Fig. 34) of control and ethanol treated cerebral cortex and cerebellum of rat, showed a significant loss of Base Excision Repair in ethanol treated cortex and cerebellum. Note the decrease in activity of DNA polymerase beta in ethanol treated cortex neurons (ECN) and

cerebellum neurons (EBN) when compared to control cortex neurons (CCN) and control cerebellum neurons (CBN). Similar decrease in activity of DNA polymerase beta in ethanol treated cortex astrocytes (ECA) and cerebellum astrocytes (EBA) was observed when compared to control cortex astrocytes (CCA) and control cerebellum astrocytes (CBA). The loss in repair was more pronounced in astrocytes than neurons in cerebral cortex. Loss in activity was further confirmed by immunoblot analysis, which also showed reduced expression levels in ethanol treated samples. Reduced immunoreactivity of DNA polymerase beta in ethanol treated samples (Fig 35) indicated reduced BER

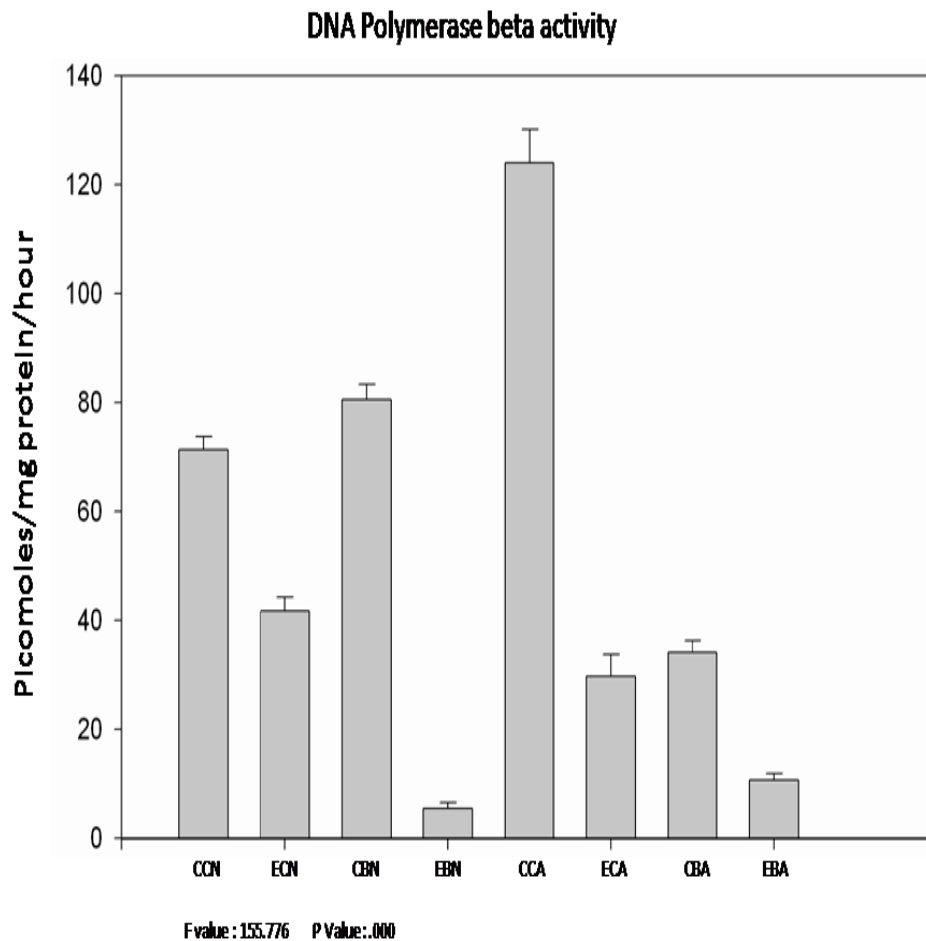


Fig 34. DNA polymerase activity in rat neuronal and astroglial fractions of control and ethanol treated cerebral cortex and cerebellum, showed a significant loss of Base

Excision Repair in ethanol treated cortex and cerebellum. Note the decrease in activity of DNA polymerase beta in ethanol treated cortex neurons (ECN) and ethanol treated cerebellum neurons (EBN) when compared to control cortex neurons (CCN) and control cerebellum neurons (CBN). Similar decrease in activity was observed in ethanol treated cortex astrocytes (ECA) and ethanol treated cerebellum astrocytes (EBA) when compared to control cortex astrocytes (CCA) and control cerebellum astrocytes (CBA). The loss in repair was more pronounced in astrocytes than neurons in cerebral cortex.

DNA Polymerase beta Immunoblot

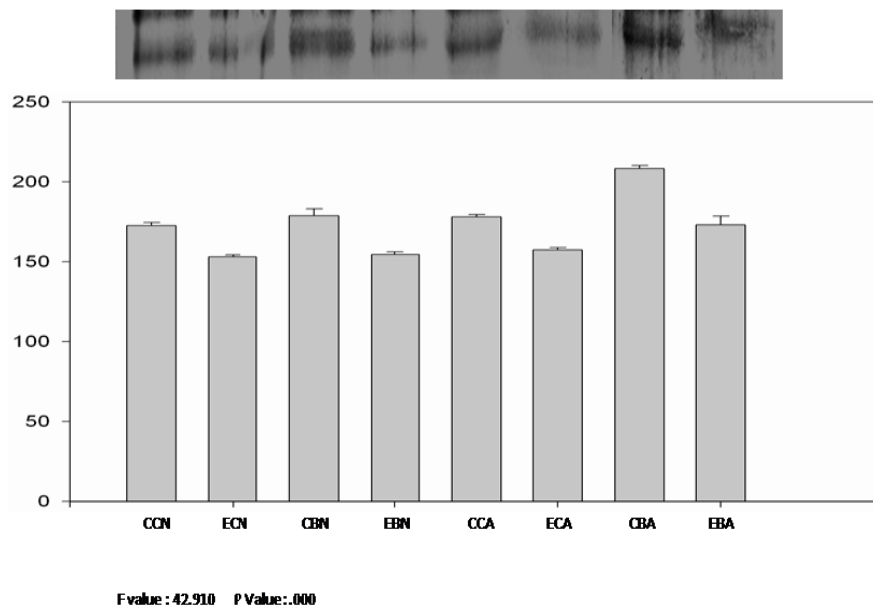


Fig 35. DNA polymerase beta immunoblot analysis of rat neuronal and astroglial fractions of control and ethanol treated cerebral cortex and cerebellum, showed a significant loss of Base Excision Repair in ethanol treated cortex and cerebellum.

Table 7

Oneway Anova

1=Control cortex neurons (CCN); 2=Ethanol treated cortex neurons (ECN); 3=Control cerebellum neurons (CBN); 4=Ethanol treated cerebellum neurons (EBN); 5=Control cortex astrocytes (CCA); 6=Ethanol treated cortex astrocytes

(ECA); 7=Control cerebellum astrocytes (CBA); 8=Ethanol treated cerebellum astrocytes (EBA)

Descriptives									
		N	Mean	Std. Deviation	Std. Error	95% Confidence Interval for Mean		Minimum	Maximum
		Lower Bound	Upper Bound	Lower Bound	Upper Bound	Lower Bound	Upper Bound	Lower Bound	Upper Bound
DNA Polymerase Activity	1.00	3	71.3740	3.93788	2.27353	61.5918	81.1562	67.85	75.62
	2.00	3	41.7592	4.32496	2.49702	31.0154	52.5030	37.48	46.12
	3.00	3	80.4572	4.84352	2.79641	68.4252	92.4892	76.60	85.89
	4.00	3	5.4272	2.01957	1.16600	.4103	10.4440	4.24	7.76
	5.00	3	123.9230	10.62960	6.13700	97.5176	150.3284	111.65	130.06
	6.00	3	29.6409	7.13557	4.11972	11.9152	47.3666	21.51	34.88
	7.00	3	34.0971	3.82383	2.20769	24.5981	43.5960	31.35	38.46
	8.00	3	10.6554	2.10511	1.21539	5.4260	15.8848	8.31	12.39
	Total	24	49.6667	38.35995	7.83019	33.4688	65.8647	4.24	130.06
DNA Polymerase Beta immunoblot	1.00	3	172.6730	3.30408	1.90761	164.4652	180.8808	169.18	175.75
	2.00	3	153.0613	1.91759	1.10712	148.2978	157.8249	151.28	155.09
	3.00	3	178.8233	7.24553	4.18321	160.8244	196.8222	170.47	183.32
	4.00	3	154.6403	2.82617	1.63169	147.6197	161.6609	152.35	157.80
	5.00	3	178.0277	2.48045	1.43209	171.8659	184.1894	175.74	180.66
	6.00	3	157.4553	2.17523	1.25587	152.0518	162.8589	155.12	159.42
	7.00	3	208.2930	3.54656	2.04761	199.4829	217.1031	204.35	211.21
	8.00	3	173.1827	9.11670	5.26353	150.5355	195.8298	165.65	183.32
	Total	24	172.0196	17.67313	3.60751	164.5569	179.4823	151.28	211.21

Test of Homogeneity of Variances				
	Levene Statistic	df1	df2	Sig.
DNA Polymerase Activity	3.272	7	16	.023
DNA Polymerase Beta immunoblot	3.205	7	16	.025

ANOVA						
		Sum of Squares	df	Mean Square	F	Sig.
DNA Polymerase Activity	Between Groups	33354.756	7	4764.965	155.776	.000
	Within Groups	489.417	16	30.589		
	Total	33844.172	23			
DNA Polymerase Beta immunoblot	Between Groups	6820.499	7	974.357	42.910	.000
	Within Groups	363.311	16	22.707		
	Total	7183.810	23			

Post Hoc Tests

Multiple Comparisons LSD					
Dependent Variable	(I) group	(J) group	Mean Difference (I-J)	Std. Error	Sig.
			Lower Bound	Upper Bound	Lower Bound
DNA Polymerase Activity	1.00	2.00	29.61477(*)	4.51579	.000
		3.00	-9.08320	4.51579	.061
		4.00	65.94683(*)	4.51579	.000
		5.00	-52.54900(*)	4.51579	.000
		6.00	41.73310(*)	4.51579	.000
		7.00	37.27693(*)	4.51579	.000
		8.00	60.71860(*)	4.51579	.000
	2.00	1.00	-29.61477(*)	4.51579	.000
		3.00	-38.69797(*)	4.51579	.000
		4.00	36.33207(*)	4.51579	.000
		5.00	-82.16377(*)	4.51579	.000
		6.00	12.11833(*)	4.51579	.016
		7.00	7.66217	4.51579	.109
		8.00	31.10383(*)	4.51579	.000
	3.00	1.00	9.08320	4.51579	.061
		2.00	38.69797(*)	4.51579	.000
		4.00	75.03003(*)	4.51579	.000
		5.00	-43.46580(*)	4.51579	.000
		6.00	50.81630(*)	4.51579	.000
		7.00	46.36013(*)	4.51579	.000
		8.00	69.80180(*)	4.51579	.000
4.00	1.00	-65.94683(*)	4.51579	.000	

		2.00	-36.33207(*)	4.51579	.000	
		3.00	-75.03003(*)	4.51579	.000	
		5.00	-118.49583(*)	4.51579	.000	
		6.00	-24.21373(*)	4.51579	.000	
		7.00	-28.66990(*)	4.51579	.000	
		8.00	-5.22823	4.51579	.264	
	5.00	1.00	52.54900(*)	4.51579	.000	
		2.00	82.16377(*)	4.51579	.000	
		3.00	43.46580(*)	4.51579	.000	
		4.00	118.49583(*)	4.51579	.000	
		6.00	94.28210(*)	4.51579	.000	
		7.00	89.82593(*)	4.51579	.000	
	6.00	8.00	113.26760(*)	4.51579	.000	
		1.00	-41.73310(*)	4.51579	.000	
		2.00	-12.11833(*)	4.51579	.016	
		3.00	-50.81630(*)	4.51579	.000	
		4.00	24.21373(*)	4.51579	.000	
		5.00	-94.28210(*)	4.51579	.000	
	7.00	7.00	-4.45617	4.51579	.338	
		8.00	18.98550(*)	4.51579	.001	
		1.00	-37.27693(*)	4.51579	.000	
		2.00	-7.66217	4.51579	.109	
		3.00	-46.36013(*)	4.51579	.000	
		4.00	28.66990(*)	4.51579	.000	
	8.00	5.00	-89.82593(*)	4.51579	.000	
		6.00	4.45617	4.51579	.338	
		8.00	23.44167(*)	4.51579	.000	
		1.00	-60.71860(*)	4.51579	.000	
		2.00	-31.10383(*)	4.51579	.000	
		3.00	-69.80180(*)	4.51579	.000	
	DNA Polymerase Beta immunoblot	1.00	4.00	5.22823	4.51579	.264
			5.00	-113.26760(*)	4.51579	.000
6.00			-18.98550(*)	4.51579	.001	
7.00			-23.44167(*)	4.51579	.000	
	1.00	2.00	19.61167(*)	3.89075	.000	
		3.00	-6.15033	3.89075	.133	
		4.00	18.03267(*)	3.89075	.000	
		5.00	-5.35467	3.89075	.188	

		6.00	15.21767(*)	3.89075	.001
		7.00	-35.62000(*)	3.89075	.000
		8.00	-.50967	3.89075	.897
	2.00	1.00	-19.61167(*)	3.89075	.000
		3.00	-25.76200(*)	3.89075	.000
		4.00	-1.57900	3.89075	.690
		5.00	-24.96633(*)	3.89075	.000
		6.00	-4.39400	3.89075	.275
		7.00	-55.23167(*)	3.89075	.000
		8.00	-20.12133(*)	3.89075	.000
		3.00	1.00	6.15033	3.89075
	2.00		25.76200(*)	3.89075	.000
	4.00		24.18300(*)	3.89075	.000
	5.00		.79567	3.89075	.841
	6.00		21.36800(*)	3.89075	.000
	7.00		-29.46967(*)	3.89075	.000
	8.00		5.64067	3.89075	.166
	4.00	1.00	-18.03267(*)	3.89075	.000
		2.00	1.57900	3.89075	.690
		3.00	-24.18300(*)	3.89075	.000
		5.00	-23.38733(*)	3.89075	.000
		6.00	-2.81500	3.89075	.480
		7.00	-53.65267(*)	3.89075	.000
		8.00	-18.54233(*)	3.89075	.000
	5.00	1.00	5.35467	3.89075	.188
		2.00	24.96633(*)	3.89075	.000
		3.00	-.79567	3.89075	.841
		4.00	23.38733(*)	3.89075	.000
		6.00	20.57233(*)	3.89075	.000
		7.00	-30.26533(*)	3.89075	.000
		8.00	4.84500	3.89075	.231
	6.00	1.00	-15.21767(*)	3.89075	.001
		2.00	4.39400	3.89075	.275
		3.00	-21.36800(*)	3.89075	.000
		4.00	2.81500	3.89075	.480
		5.00	-20.57233(*)	3.89075	.000
		7.00	-50.83767(*)	3.89075	.000
		8.00	-15.72733(*)	3.89075	.001

	7.00	1.00	35.62000(*)	3.89075	.000
		2.00	55.23167(*)	3.89075	.000
		3.00	29.46967(*)	3.89075	.000
		4.00	53.65267(*)	3.89075	.000
		5.00	30.26533(*)	3.89075	.000
		6.00	50.83767(*)	3.89075	.000
		8.00	35.11033(*)	3.89075	.000
	8.00	1.00	.50967	3.89075	.897
		2.00	20.12133(*)	3.89075	.000
		3.00	-5.64067	3.89075	.166
		4.00	18.54233(*)	3.89075	.000
		5.00	-4.84500	3.89075	.231
		6.00	15.72733(*)	3.89075	.001
		7.00	-35.11033(*)	3.89075	.000
* The mean difference is significant at the .05 level.					

Discussion

Brain is considered highly vulnerable to oxidative stress than other organs of the body as it consumes high amounts of oxygen, contains high amounts of PUFA and low levels of antioxidant enzymes. Redistribution of cellular GSH is another event that may be critical during apoptosis. Although GSH is synthesized in the cytosol, it is transported into organelles, including mitochondria and the nucleus, where it can be used as a cofactor in glutathione peroxidase and glutathione-S-transferase mediated reactions (Bellomo *et al.* 1992). Notably even in this study GSH was used as a cofactor as observed by increase in activity of glutathione peroxidase in HE and FE. In the present study high activity of GPX in HE and FE compared to controls, indicates enhanced biochemical defenses to scavenge the over production of H₂O₂. Catalase showed no significant differences in ethanol treated hippocampus and frontal cortex, indicating cells in these regions can adapt to mild oxidative stress during a chronic paradigm. Glutathione S Transferase activity did not show any difference from controls in HE region however increased activity was found in FE compared to controls. GSH was used as a cofactor as observed by increase in activity of glutathione peroxidase in FE, compared to controls.

Several mechanisms for ROS induction of apoptosis have been proposed; however, an integrated model has yet to be established. Stridh favoured a scheme in which ROS, for example H₂O₂, act upon mitochondria, causing a disruption of mitochondrial membrane potential and the release of cytochrome C; this, in turn, is followed by the activation of caspase cascade (Stridh *et al.* 1998). An alternative model for ROS induced apoptosis involves up regulation of the Fas/FasLsystem (Dumont *et al.* 1999). The observation that various chemotherapeutic drugs cause intracellular ROS production and Fas up-regulation has perpetuated this paradigm; however other studies contend that H₂O₂ induced apoptosis is Fas-independent. Finally, transcription factors can be modulated by oxidative stress. Nuclear translocation of p53 and the ubiquitous transcription factors, NFκB and AP-1, are activated by ROS (Pinkus *et al.* 1996). Once activated, these transcription factors might drive transcription of pro-apoptotic genes or perhaps cause expression of inhibitors of survival-related proteins. Ethanol withdrawal hyperactivity is associated with the expression of the early genes c-fos and c-jun and with transient selective increases in the DNA-binding activity of immediate early genes (IEGs)-encoded transcription factors AP-1 and Egz-1 in the brain. The induction of early gene-encoded transcription factors has been implicated in the mechanisms leading to programmed cell death in the nervous system during chronic alcohol consumption (Fadda and Rossetti 1998).

Enhanced ROS production as well as decreased antioxidant capacity have been claimed to be important in apoptosis during chronic alcohol exposure (Hajnoczky *et al.* 2005). Significant strand breaks were induced primarily in the hippocampus and cerebellum during chronic ethanol treatment (Renis *et al.* 1996). Chronic ethanol exposure produces lipid peroxidation as a consequence of free radical formation (Nordmann *et al.* 1990; Montoliu *et al.* 1994). Nuclear pools of glutathione appear to be more resistant to depletion by agents like buthionine sulfoximine (BSO), diethyl maleate (DEM), and NEM than cytosolic stores of GSH, suggesting that GSH is an important guardian against oxidative damage to DNA and nuclear proteins (Bellomo *et al.* 1992). We also looked for the status of DNA repair selectively in neurons and astrocytes of cerebral cortex and cerebellum of control

and ethanol treated rats. Base Excision Repair (BER) protects mammalian cells against single-base DNA damage by methylating agents, most oxidative damages, and a large number of spontaneous depurinations (Bernstein and Bernstein 2004). Studies over the years have revealed that DNA-polymerase β (pol β), which is involved in BER, is the most predominant DNA-polymerase in rat brain (Rao 1997). It is observed that the activity and immunoreactivity of DNA polymerase β , rate limiting factor for BER, is markedly decreased in cerebral cortex and cerebellar neurons and astrocytes, indicating impaired activity of this mode of DNA repair under the experimental conditions. Further, the loss in repair was more pronounced in astrocytes than neurons in cerebral cortex of ethanol treated rats.

Taken together our results imply that different pathways of cell death are activated in hippocampus and frontal cortex, which are associated with reduced DNA repair.

Chapter 1 (Cell death associated proteins) Summary and conclusions

(Data are derived from cell sub-fractionation and western blot analysis.)

	HE		FE	
Active Caspase 3 (cytosol) (17 k Da)	↑ (activation)		=	
Active Caspase 7 (cytosol) (20 k Da)	↑ (activation)		=	
Active Caspase 9 (cytosol) (17 k Da)	↑ (activation)		=	
PARP (nuclear) (89 k Da)	=		↑ (Repair lost)	
NMDAR1 (membrane) (180 k Da)	↑ (Upregulation)		=	
NMDAR2A (membrane) (180 k Da)	=		=	
NMDAR2B (membrane) (180 k Da)	↑ (Upregulation)		↑ (Upregulation) (FE>HE)	
NMDAR2C (membrane) (140 k Da)	↑ (Upregulation)		↓ (down regulation)	
Calpain (cytosol) (80 k Da)	↑ (activation)		=	
	HE	FE	HE	FE
AIF(57 k Da)	↓ (Cytosol)	↓ (Cytosol)	↓ (nuclear)	↑(nuclear translocation)
Cytochrome C (14 k Da)	↓ (Cytosol)	↑ (Cytosol translocation)	=(mitochondria)	↓(mitochondria)
Bcl-2 (26 k Da)	↑(Cytosol translocation)	=	↓(mitochondria)	↓(mitochondria)
Bax (21 k Da)	= (Cytosol)	= (Cytosol)	↓(mitochondria)	= (mitochondria) Bax independent
Bad (23 k Da)	↓ (Cytosol)	= (Cytosol)	↓(mitochondria)	= (mitochondria) Bad independent

All modifications are compared to controls

Chapter 2 (*In-situ* detection of cell death) Summary and conclusions

	HC	HE	FC	FE
Hematoxylin-eosin (HE)	Intact neuropil	Eosinophilic cytosol (necrosis), Break up neuropile Degenerating cells, Pyknotic cells and Karyorrhexis (apoptosis/necrosis), shrunken and condensed cells (apoptosis).	Intact neuropil	Pyknosis, Eosinophilic cytoplasm (necrosis), chromatolysis, shrunken and condensed cells (apoptosis).
Toluidine blue	Normal cells intact neuropile	Dark neurons with break up neuropile (apoptosis/necrosis)		
GFAP	Normal	Increased immunoreactivity (hypertrophy)	Normal	Increased immunoreactivity (hypertrophy)
Caspase-3	Normal	Increased immunoreactivity	Normal	Increased immunoreactivity
TUNEL	Normal	Increased positivity	Normal	Increased positivity
Electron microscopy	Normal •Oval nucleus •Normal cytoplasmic density •Normal neuropil • Normal nuclear membrane • Normal nuclear pores • Normal mitochondria •Normal rough endoplasmic reticulum. •Nuclear pores visible.	<u>Early signs of apoptosis</u> •Watery and condensed cytoplasm •electronlucent with disruption of cellular organelles • Abnormal nuclear shape with crenelation of nuclear membrane •Margination of chromatin. <u>Early signs of necrosis</u> • Swollen, watery, electronlucent cytoplasm. • Disruption of cellular organelles with irregular nuclear profile of nuclear membrane. • Mitochondrion is swollen •Normal Rough endoplasmic reticulum	Normal • Normal, oval nuclear morphology • Normal cytoplasmic density • Normal neuropile. •Normal nuclear membrane •Nuclear pores visible •Normal RER, Golgi apparatus and mitochondria	• <u>Early signs of necrosis</u> •Swollen cytoplasm •Irregular nuclear profile of nuclear membrane. •Presence of abundant lysosomes. •Normal mitochondria and rough endoplasmic reticulum. •Cytoplasm is watery and electronlucent

HC, control hippocampus; HE, ethanol treated hippocampus; FC, control frontal cortex; FE, ethanol treated frontal cortex.

Chapter 3 (Oxidative stress and DNA repair) Summary and conclusions

	HE	FE
GSH	↑	↓
GSSG	↑	↓
Glutathione Peroxidase	↑ (GSH consumed)	↑ (GSH consumed) (FE>HE)
Glutathione-S-transferase	=	↑
Catalase	=	=

All modifications are compared to controls

ECN	EBN	ECA	EBA
↓	↓	↓	↓

All modifications are compared to controls

References

- Abraham WC, Hunter BE, Zornetzer SF, Walker DW. (1981) Augmentation of short-term plasticity in CA1 of rat hippocampus after chronic ethanol treatment. *Brain Res.* Sep 28; 221(2):271-87.
- Abraham WC, Rogers CJ, Hunter BE. (1984) Chronic ethanol-induced decreases in the response of dentate granule cells to perforant path input in the rat. *Exp Brain Res.* 54(3):406-14.
- Arendt T, Allen Y, Sinden J, Schugens MM, Marchbanks RM, Lantos PL, Gray JA. (1988a) Cholinergic-rich brain transplants reverse alcohol-induced memory deficits. *Nature.* Mar 31; 332(6163):448-50.
- Arendt T, Bigl V, Arendt A, Tennstedt A. (1983) Loss of neurons in the nucleus basalis of Meynert in Alzheimer's disease, paralysis agitans and Korsakoff's Disease. *Acta Neuropathol (Berl).* 61(2):101-8.
- Arendt T, Henning D, Gray JA, Marchbanks R. (1988b) Loss of neurons in the rat basal forebrain cholinergic projection system after prolonged intake of ethanol. *Brain Res Bull.* Oct; 21(4):563-9.
- Arendt T, Marchbanks R, Gray JA. (1987) Effects of prolonged ethanol consumption on cholinergic function in the basal forebrain and memory. *Biochem. Sci Trans.* 15, 499-500.
- Artal-Sanz M, Tavernarakis N. (2005) Proteolytic mechanisms in necrotic cell death and Neurodegeneration. *FEBS Letters* 579: 3287–96.
- Ayllon V, Martinez AC, Garcia A, Cayla X, Rebollo A. (2000) Protein phosphatase 1alpha is a Ras-activated Bad phosphatase that regulates interleukin-2 deprivation-induced apoptosis. *EMBO J.* May 15; 19(10):2237-46.
- Babu PP. (1997) Regional heterogeneity of plasma membrane proteins in rat brain. *Biochem Mol Biol Int.* 43, 1033-1039.

Bai L, Wang J, Yin XM, Dong Z (2003) Analysis of apoptosis, Basic principles and procedures In Essentials of apoptosis: A guide for basic and clinical research edited by Yin XM and Dong Z Humana press Inc., Totowa, NJ pp 239-251.

Baker K, Harding A, Halliday G, Kril JJ, Harper C (1999) Neuronal loss in functional zones of the cerebellum of chronic alcoholics with and without Wernicke's encephalopathy. *Neuroscience* 91:429-38.

Balduini W, Costa LG. (1989) Effects of ethanol on muscarinic receptor-stimulated phosphoinositide metabolism during brain development. *J Pharmacol Exp Ther.* 1989 Aug; 250(2):541-7.

Baskaran S, Lakshmi S, Prasad PR. (1999) Effect of cigarette smoke on lipid peroxidation and antioxidant enzymes in albino rat. *Indian J Exp Biol.* 1999 Dec; 37(12):1196-200.

Bellomo G, Vairetti M, Stivala L, Mirabelli F, Richelmi P, Orrenius S. (1992) Demonstration of nuclear compartmentalization of glutathione in hepatocytes. *Proc Natl Acad Sci U S A.* May 15; 89(10):4412-6.

Bengoechea O, Gonzalo LM. (1991) Effects of alcoholization on the rat hippocampus. *Neurosci Lett.* Feb 11; 123(1):112-4.

Benn SC, Woolf CJ (2004) Adult neuron survival strategies-slamming on the brakes. *Nat Rev Neurosci.* 5:686-700.

Ben-Sasson SA, Sherman Y, and Gavrieli Y. (1995) Identification of dying cells- In Situ staining In *Methods in cell biology*, Volume 46, Cell death edited by Schwartz LM and Osborne BA. Academic press, Inc California, pp 29-39.

Beracochea D, Lescaudron L, Tako A, Verna A, Jaffard R. (1987) Build-up and release from proactive interference during chronic ethanol consumption in mice: a behavioral and neuroanatomical study. *Behav Brain Res.* Jul; 25(1):63-74.

Bernstein C, Bernstein H. (2004) Aging and sex, DNA repair in, In *Encyclopedia of molecular cell biology and molecular medicine*, (Robert A. M. eds), Volume 1, pp 53-98. Wiley-Vch Verlag GmbH & Co. KGaA.

Berridge M, Lipp P, Bootman M. (1999) Calcium signalling. *Curr Biol.* Mar 11; 9(5):R157-9.

Bittigau P, Sifringer M, Genz K, Reith E, Pospischil D, Govindarajalu S, Dzierko M, Pesditschek S, Mai I, Dikranian K, Olney JW, Ikonomidou C. (2002) Antiepileptic drugs and apoptotic neurodegeneration in the developing brain, *Proc Natl Acad Sci U S A.* Nov 12;99 (23):15089-94.

Blomgren K, Zhu C, Wang X, Karlsson JO, Leverin AL, Bahr BA, Mallard C, Hagberg H. (2001) Synergistic activation of caspase-3 by m-calpain after neonatal hypoxia ischemia: a mechanism of pathological apoptosis? *J. Biol. Chem.* 276, 10191–8.

Bohr V (2005) DNA damage and repair In *Encyclopedia of Aging* eds Ekerdt DJ, volume 1, pp 369-375, Macmillan reference, Thomson gale, USA.

Bonthius DJ, West JR. (1990). Alcohol induced neuronal loss in developing rats: increased brain damage with binge exposure. *Alcohol. Clin. Exp. Res.* 14:107–18.

Bonthius DJ, Woodhouse J, Bonthius NE, Taggard DA, Lothman EW. (2001) Reduced seizure threshold and hippocampal cell loss in rats exposed to alcohol during the brain growth spurt. *Alcohol Clin. Exp Res.* 25:70–82

Cadete-Leite A, Tavares MA, Alves MC, Uylings HB, Paula-Barbosa MM (1989a) Metric analysis of hippocampal granule cell dendritic trees after alcohol withdrawal in rats. *Alcohol Clin Exp Res.* Dec; 13(6):837-40.

Cadete-Leite A, Tavares MA, Pacheco MM, Volk B, Paula-Barbosa MM (1989b) Hippocampal mossy fiber-CA3 synapses after chronic alcohol consumption and withdrawal. *Alcohol.* Jul-Aug; 6(4):303-10.

Cande C, Cohen I, Daugas E, Ravagnan L, Larochette N, Zamzami N, Kroemer G. (2002) Apoptosis-inducing factor (AIF): a novel caspase-independent death effector released from mitochondria. *Biochimie.* Feb-Mar; 84 (2-3):215-22.

Cardone MH, Roy N, Stennicke HR, Salvesen GS, Franke TF, Stanbridge E, Frisch S, Reed

JC. (1998) Regulation of cell death protease caspase-9 by phosphorylation. *Science*. Nov 13; 282(5392):1318-21.

Casciola-Rosen L, Nicholson DW, Chong T, Rowan KR, Thornberry NA, Miller DK, Rosen A. (1996) Apopain/ CPP32 cleaves proteins that are essential for cellular repair: a fundamental principle of apoptotic death. *J Exp Med*. May 1; 183(5):1957-64.

Cedric SR. (1989) Neurocellular anatomy, in *Basic Neurochemistry* (Eds George JS, Bernard WA, Wayne AR, Perry BM) Fourth edition, pp 3-33, Raven Press, New York.

Chance B, Maechly AC (1955). Assay of catalases and peroxidases. (Eds Colowick SP, Kaplan NO) *Methods in Enzymology* 2: 764-775.

Chang LW, Dyer RS (1995) Neurotoxicology of organotins and organoleads In *Handbook of neurotoxicology*, Marcel Dekker, New York, pp 143-169.

Charness ME, Diamond I. (1984) Alcohol and the nervous system In *Current Neurology*. (Ed Appel SH) New York: Wiley, pp. 383-421

Chen M, He H, Zhan S, Krajewski S, Reed JC, Gottlieb RA. (2001) Bid is cleaved by calpain to an active fragment in vitro and during myocardial ischemia/reperfusion. *J Biol Chem*. Aug 17; 276(33):30724-8.

Chen M, Won DJ, Krajewski S, Gottlieb RA. (2002) Calpain and mitochondria in ischemia/reperfusion injury. *J Biol Chem*. 2002 Aug 9; 277(32):29181-6.

Cheng EH, Wei MC, Weiler S, Flavell RA, Mak TW, Lindsten T, Korsmeyer SJ. (2001) BCL-2, BCL-X(L) sequester BH3 domain-only molecules preventing BAX- and BAK-mediated mitochondrial apoptosis. *Mol Cell*. 2001 Sep; 8(3):705-11

Chiang CW, Harris G, Ellig C, Masters SC, Subramanian R, Shenolikar S, Wadzinski BE, Yang E. Protein phosphatase 2A activates the proapoptotic function of BAD in interleukin-3-dependent lymphoid cells by a mechanism requiring 14-3-3 dissociation. *Blood*. 2001 Mar 1; 97(5):1289-97.

Clarren SK. (1986) Neuropathology in fetal alcohol syndrome In *Alcohol and brain*

development Ed: West JR, New York: Oxford University press, pp. 158–66.

Climent E, Pascual M, Renau-Piqueras J, Guerri C (2002) Ethanol exposure enhances cell death in the developing cerebral cortex: role of brain-derived neurotrophic factor and its signaling pathways. *J Neurosci Res* 68:213-225.

Committee for the purpose of control and supervision on experiments on animals (CPCSEA) (2003) Guidelines for laboratory animal facility. *Indian Journal of Pharmacology* 35, 257-274.

Crews FT, Collins MA, Dlugos C, Littleton J, Wilkins L, Neafsey EJ, Pentney R, Snell LD, Tabakoff B, Zou J, Noronha A. (2004) Alcohol-induced neurodegeneration: when, where and why? *Alcohol Clin Exp Res*. Feb; 28(2):350-64.

Crocker SJ, Smith PD, Jackson-Lewis V, Lamba WR, Hayley SP, Grimm E, Callaghan SM, Slack RS, Melloni E, Przedborski S, Robertson GS, Anisman H, Merali Z, Park DS. (2003) Inhibition of calpains prevents neuronal and behavioral deficits in an MPTP mouse model of Parkinson's disease. *J Neurosci*. May 15; 23(10):4081-91.

Czurko A, Nishino H. (1993) 'Collapsed' (argyrophilic, dark) neurons in rat model of transient focal cerebral ischemia. *Neurosci Lett*. Nov 12; 162(1-2):71-4.

Darzynkiewicz Z, Bedner E, Traganos F, Murakami T. (1998) Critical aspects in the analysis of apoptosis and necrosis. *Hum Cell*. Mar; 11(1):3-12.

Datta SR, Dudek H, Tao X, Masters S, Fu H, Gotoh Y, Greenberg ME. (1997) Akt phosphorylation of BAD couples survival signals to the cell-intrinsic death machinery. *Cell*. Oct 17; 91(2):231-41.

Datta SR, Katsov A, Hu L, Petros A, Fesik SW, Yaffe MB, Greenberg ME. (2000) 14-3-3 proteins and survival kinases cooperate to inactivate BAD by BH3 domain phosphorylation. *Mol Cell*. Jul; 6(1):41-51.

Daugas E, Susin SA, Zamzami N, Ferri KF, Irinopoulou T, Larochette N, Prevost MC, Leber B, Andrews D, Penninger J, Kroemer G. (2000) Mitochondrio-nuclear translocation of AIF in apoptosis and necrosis. *FASEB J.* 2000 Apr; 14 (5):729-39.

de Torres C, Munell F, Ferrer I, Reventos J, Macaya A.(1997) Identification of necrotic cell death by the TUNEL assay in the hypoxic-ischemic neonatal rat brain. *Neurosci Lett.* Jul 11; 230(1):1-4.

Dodd PR, Beckmann AM, Davidson MS, Wilce PA: Glutamate-mediated transmission, alcohol, and alcoholism. *Neurochem Int* 2000, 37:509-533.

Dodd PR, Beckmann AM, Davidson MS, Wilce PA: Glutamate-mediated transmission, alcohol, and alcoholism. *Neurochem Int.* 2000 Nov-Dec; 37 (5-6):509-33.

Douglas WE, Douglas RG. (2002) Assessing Cytochrome *c* release from mitochondria, in *Neuromethods, Apoptosis Techniques and Protocols*, (LeBlanc AC eds), Vol 37, pp 21-34, 2 nd Ed, Humana Press Inc, Totowa, NJ.

Duan H, Orth K, Chinnaiyan AM, Poirier GG, Froelich CJ, He WW, Dixit VM. (1996) ICE-LAP6, a novel member of the ICE/Ced-3 gene family, is activated by the cytotoxic T cell protease granzyme B. *J Biol Chem.* Jul 12;271(28):16720-4.

Dumont A, Hehner SP, Hofmann TG, Ueffing M, Droge W, Schmitz ML. (1999) Hydrogen peroxide-induced apoptosis is CD95-independent, requires the release of mitochondria-derived reactive oxygen species and the activation of NF-kappaB. *Oncogene.* Jan 21; 18(3):747-57.

Durand D, Carlen PL. (1984a) Decreased neuronal inhibition in vitro after long-term administration of ethanol. *Science.* Jun 22; 224(4655):1359-61.

Durand D, Carlen PL. (1984b) Impairment of long-term potentiation in rat hippocampus following chronic ethanol treatment. *Brain Res.* Aug 13; 308(2):325-32.

Durand D, Saint-Cyr JA, Gurevich N, Carlen PL. (1989) Ethanol-induced dendritic alterations in hippocampal granule cells. *Brain Res.* Jan 16; 477(1-2):373-7.

Duriez PJ, Shah GM. (1997) Cleavage of poly (ADP-ribose) polymerase: a sensitive parameter to study cell death. *Biochem Cell Biol*; 75(4):337-49.

Eckardt MJ, Martin PR. (1986) Clinical assessment of cognition in alcoholism. *Alcohol Clin Exp Res*. 1986 Mar-Apr; 10(2):123-7. javascript:PopupMenu2_Set(Menu3521368);

Eng LF. (1985) Glial fibrillary acidic protein (GFAP): the major protein of glial intermediate filaments in differentiated astrocytes. *J Neuroimmunol*. Jun; 8(4-6):203-14.

Eng LF. (1988) Regulation of glial intermediate filaments in astrogliosis. In: *Biochemical Pathology of astrocytes*, edited by Norenberg MD, Hertz L, Schousboe A. New York, AR Liss, pp79-90.

Fadda F, Rossetti ZL. (1998) Chronic ethanol consumption: from neuroadaptation to neurodegeneration. *Prog Neurobiol*. Nov; 56(4):385-431.

Farber NB, Olney JW. (2003) Drugs of abuse that cause developing neurons to commit suicide. *Brain Res Dev Brain Res*. Dec 30; 147(1-2):37-45.

Fernandes-Alnemri T, Armstrong RC, Krebs J, Srinivasula SM, Wang L, Bullrich F, Fritz LC, Trapani JA, Tomaselli KJ, Litwack G, Alnemri ES. (1996) In vitro activation of CPP32 and Mch3 by Mch4, a novel human apoptotic cysteine protease containing two FADD-like domains. *Proc Natl Acad Sci U S A*. Jul 23; 93(15):7464-9.

Ferreira VM, Frausto S, Browning MD, Savage DD, Morato GS, Valenzuela CF (2001) Ionotropic glutamate receptor subunit expression in the rat hippocampus: lack of an effect of a long-term ethanol exposure paradigm. *Alcohol Clin Exp Res*. Oct; 25(10):1536-41.

Ferrer I, Fabregues I, Rairiz J, Galofre E. (1986) Decreased numbers of dendritic spines on cortical pyramidal neurons in human chronic alcoholism. *Neurosci Lett*. Aug 15; 69(1):115-9.

Freund G. (1973) Chronic central nervous system toxicity of alcohol. *Annu Rev Pharmacol*. 13:217-27.

Gafni J, Ellerby LM (2002) Calpain activation in Huntingtons disease. *J Neurosci.* Jun 15; 22(12):4842-9.

Gallyas F, Zoltay G, Balas I. (1992) An immediate Light microscopic response of neuronal somata, dendrites and axons to contusing concussive head injury in the rat. *Acta Neuropathol (Berl)* ; 83(4):394-401.

Gavrieli Y, Sherman Y, Ben-Sasson SA. (1992) Identification of programmed cell death in situ via specific labeling of nuclear DNA fragmentation. *J Cell Biol.* 1992 Nov; 119(3):493-501

Gil-Parrado S, Fernandez-Montalvan A, Assfalg-Machleidt I, Popp O, Bestvater F, Holloschi A, Knoch TA, Auerswald EA, Welsh K, Reed JC, Fritz H, Fuentes-Prior , Spiess E, Salvesen GS, Machleidt W. (2002) Ionomycin-activated calpain triggers apoptosis. A probable role for Bcl-2 family members. *J Biol Chem.* Jul 26; 277(30):27217-26.

Goll DE, Thompson VF, Li H, Wei W, Cong J. (2003) The calpain system. *Physiol Rev.* Jul; 83(3):731-801.

Habig WH, Jakoby WB. (1981) Assays for differentiation of glutathione S transferases. *Methods enzymology* 77: 398-405.

Hagan JJ, Salamone JD, Simpson J, Iversen SD, Morris RG. (1988) Place navigation in rats is impaired by lesions of medial septum and diagonal band but not nucleus basalis magnocellularis. *Behav Brain Res.* Jan; 27(1):9-20.

Hajnoczky G, Buzas CJ, Pacher P, Hoek JB, Rubin E. (2005) Alcohol and Mitochondria in Cardiac Apoptosis: Mechanisms and Visualization. *Alcohol Clin Exp Res.* May; 29(5):693-701.

Halliwell B (2004) Free radicals in biochemistry and medicine In *Encyclopedia of Molecular cell biology and molecular medicine.* Edited by Meyers RA Second edition, Volume 4, Wiley. pp 633-649.

Harada H, Becknell B, Wilm M, Mann M, Huang LJ, Taylor SS, Scott JD, Korsmeyer SJ. (1999) Phosphorylation and inactivation of BAD by mitochondria-anchored protein kinase

A. Mol Cell. Apr; 3(4):413-22

Harding AJ, Halliday GM, Ng JLF, Harper CG, Kril JJ (1996) Loss of vasopressin-immunoreactive neurons in alcoholics is dose-related and time-dependent. *Neuroscience*. Jun; 72(3):699-708.

Harper C, Corbett D. (1990) Changes in the basal dendrites of cortical pyramidal cells from alcoholic patients--a quantitative Golgi study. *J Neurol Neurosurg Psychiatry*. Oct; 53(10):856-61.

Harper C, Kril J, Daly J. (1987) Are we drinking our neurones away? *Br Med J (Clin Res Ed)*. Feb 28; 294(6571):534-6.

Harper C, Matsumoto I. (2005) Ethanol and brain damage. *Curr Opin Pharmacol*. Feb; 5(1):73-8.

Harper CG, Kril JJ, Holloway RL.(1985) Brain shrinkage in chronic alcoholics: a pathological study. *Br Med J (Clin Res Ed)*. Feb 16; 290(6467):501-4.

Harris-Collazo MR, Kwok W, Mattson SN, Jernigan SN, Riley EP. (1998) Quantitative magnetic resonance imaging analysis of fetal alcohol syndrome. *J. Int. Neuropsychol.Soc*. 4:48

Harwood SM, Yaqoob MM, Allen DA. (2005) Caspase and calpain function in cell death: bridging the gap between apoptosis and necrosis. *Ann Clin Biochem*. 2005 Nov; 42(Pt 6):415-31.

Hatten ME, Liem RK, Shelanski ML, Mason CA.(1991) Astroglia in CNS injury. *Glia*.; 4(2):233-43.

Heaton MB, Moore DB, Paiva M, Gibbs T, Bernard O. (1999) Bcl-2 overexpression protects the neonatal cerebellum from ethanol neurotoxicity. *Brain Res*. Jan 30; 817(1-2):13-8.

Heaton MB, Moore DB, Paiva M, Madorsky I, Mayer J, Shaw G. (2003) The role of neurotrophic factors, apoptosis-related proteins, and endogenous antioxidants in the differential temporal vulnerability of neonatal cerebellum to ethanol. *Alcohol Clin Exp Res.* Apr; 27(4):657-69.

Hengartner MO. (2000) The biochemistry of apoptosis. *Nature.* Oct 12; 407(6805):770-6.

Herde KD, Mussche S, Roberg K (2003) Morphological changes in dying cells In *Cell proliferation and apoptosis* Eds. Hughes D, Mehmet H, BIOS scientific publishers Ltd, Oxford pp 201-231.

Herrera DG, Yague AG, Johnsen-Soriano S, Bosch-Morell F, Collado-Morente L, Muriach M, Romero FJ, Garcia-Verdugo JM. (2003) Selective impairment of hippocampal neurogenesis by chronic alcoholism: protective effects of an antioxidant. *Proc Natl Acad Sci U S A.* Jun 24; 100(13):7919-24.

Hissin PJ, Hilf R. (1976) A fluorometric method for determination of oxidized and reduced glutathione in tissues. *Anal Biochem.* Jul; 74(1):214-26.

Hosfield CM, Elce JS, Davies PL, Jia Z. (1999) Crystal structure of calpain reveals the structural basis for Ca (2+)- dependent protease activity and a novel mode of enzyme activation. *EMBO J.* Dec 15; 18(24):6880-9.

Hunt WA (1993) Role of free radical reactions in ethanol-induced brain damage: an introduction in *Alcohol induced brain damage*, Research monograph No.22, Edited by Hunt WA, Nixon SJ, NIH publication No. 93-3549, NIH, Rockville, MD, USA, pp 327-338.

Ikegami Y, Goodenough S, Inoue Y, Dodd PR, Wilce PA, Matsumoto I. (2003) Increased TUNEL positive cells in human alcoholic brains. *Neurosci Lett.* Oct 9; 349(3):201-5.

Ikonomidou C, Bittigau P, Ishimaru MJ, Wozniak DF, Koch C, Genz K, Price MT, Stefovskaja V, Horster F, Tenkova T, Dikranian K, Olney JW. (2000) Ethanol-induced apoptotic neurodegeneration and fetal alcohol syndrome. *Science.* Feb 11; 287(5455):1056-60.

Ishimaru MJ, Ikonomidou C, Tenkova TI, Der TC, Dikranian K, Sesma MA, Olney W. (1999) Distinguishing excitotoxic from apoptotic neurodegeneration in the developing rat brain. *J Comp Neurol.* Jun 14; 408 (4):461-76

Janicke RU, Sprengart ML, Wati MR, Porter AG. (1998) Caspase-3 is required for DNA fragmentation and morphological changes associated with apoptosis. *J Biol Chem.* Apr 17; 273(16):9357-60.

Jevtovic-Todorovic V, Hartman RE, Izumi Y, Benshoff ND, Dikranian K, Zorumski F, Olney JW, Wozniak DF. (2003) Early exposure to common anesthetic agents causes widespread neurodegeneration in the developing rat brain and persistent learning deficits. *J Neurosci.* Feb 1; 23(3):876-82.

Jiang X, Wang X. (2000) Cytochrome c promotes caspase-9 activation by inducing nucleotide binding to Apaf-1. *J Biol Chem.* Oct 6; 275(40):31199-203.

Jordan J, Galindo MF, Gonzalez-Garcia C, Cena V. (2003) Role and regulation of p53 in depolarization-induced neuronal death. *Neuroscience.* 122(3):707-15.

Jordan LB, Harrison DJ (2003) Apoptosis and Cell Senescence In *Molecular Biology in cellular Pathology*. Edited by Crocker J and Murray PG, John Wiley & Sons, Ltd. Pp 153-192.

Joza N, Susin SA, Daugas E, Stanford WL, Cho SK, Li CY, Sasaki T, Elia AJ, Cheng HY, Ravagnan L, Ferri KF, Zamzami N, Wakeham A, Hakem R, Yoshida H, Kong YY, Mak TW, Zuniga-Pflucker JC, Kroemer G, Penninger M. (2001) Essential role of the mitochondrial apoptosis-inducing factor in programmed cell death. *Nature.* Mar 29; 410(6828):549-54.

Kaminski M, Karbowski M, Miyazaki Y, Kedzior J, Spodnik JH, Gil A, Wozniak M, Wakabayashi T. (2002) Co-existence of apoptotic and necrotic features within one single cell as a result of menadione treatment. *Folia Morphol (Warsz).* 61(4):217-20.

Kaufmann SH, Desnoyers S, Ottaviano Y, Davidson NE, Poirier GG. (1993) Specific proteolytic cleavage of poly(ADP-ribose) polymerase: an early marker of chemotherapy-induced apoptosis. *Cancer Res.* Sep 1; 53(17):3976-85.

Kaufmann SH, Mesner Jr.PW, Martins M, Kottke TJ, Earnshaw WC (1999) Methods used to study protease activation during apoptosis, in *Apoptosis in Neurobiology*, (Yusuf A. H and Rose-Mary B. eds), pp 205-232, CRC Press LLC, Boca Raton, Florida, USA.

Keramaris E, Stefanis L, MacLaurin J, Harada N, Takaku K, Ishikawa T, Taketo MM, Robertson GS, Nicholson DW, Slack RS, Park DS. (2000) Involvement of caspase 3 in apoptotic death of cortical neurons evoked by DNA damage. *Mol Cell Neurosci. Apr*; 15(4):368-79.

Kerr JFR, Gobe GC, Winterford CM, Harmon BV.(1995) Anatomical methods in cell death in *Methods in cell biology Volume 46 Cell death* edited by Schwartz LM and Osborne BA, pp1-27 Academic press, Inc California, USA

Kiernan JA, Macpherson CM, Price A, Sun T (1998) A histochemical examination of the staining of kainite-induced neuronal degeneration by anionic dyes. *Biotech Histochem. Sep*; 73(5):244-54

Kim M, Roh JK, Yoon BW, Kang L, Kim YJ, Aronin N, DiFiglia M. (2003) Huntingtin is degraded to small fragments by calpain after ischemic injury. *Exp Neurol. 2003 Sep*; 183(1):109-15.

Kim YJ, Yi Y, Sapp E, Wang Y, Cuiffo B, Kegel KB, Qin ZH, Aronin N, DiFiglia M. (2001) Caspase 3-cleaved N-terminal fragments of wild-type and mutant huntingtin are present in normal and Huntington's disease brains, associate with membranes, and undergo calpain-dependent proteolysis. *Proc Natl Acad Sci U S A. Oct 23*; 98(22):12784-9.

Kril JJ, Harper CG. (1989) Neuronal counts from four cortical regions of alcoholic brains. *Acta Neuropathol (Berl). 79(2)*:200-4.

Kuida K, Zheng TS, Na S, Kuan C, Yang D, Karasuyama H, Rakic P, Flavell RA.(1996) Decreased apoptosis in the brain and premature lethality in CPP32-deficient mice. *Nature. Nov 28*; 384(6607):368-72

Lamarche F, Gonthier B, Signorini N, Eysseric H, Barret L (2003): Acute exposure of cultured neurones to ethanol results in reversible DNA single-strand breaks; whereas chronic exposure causes loss of cell viability. *Alcohol Alcohol*. Nov-Dec; 38(6):550-8.

Lazebnik YA, Kaufmann SH, Desnoyers S, Poirier GG, Earnshaw WC. (1994) Cleavage of poly (ADP-ribose) polymerase by a proteinase with properties like ICE. *Nature*. Sep 22; 371(6495):346-7

Lee MS, Kwon YT, Li M, Peng J, Friedlander RM, Tsai LH. (2000) Neurotoxicity induces cleavage of p35 to p25 by calpain. *Nature*. May 18; 405(6784):360-4.

Lescaudron L, Seguela P, Geffard M, Verna A.(1986) Effects of long-term ethanol consumption on GABAergic neurons in the mouse hippocampus: a quantitative immunocytochemical study. *Drug Alcohol Depend*. Dec; 18(4):377-84.

Lindahl T, Satoh MS, Poirier GG, Klungland A. (1995) Post-translational modification of poly (ADP-ribose) polymerase induced by DNA strand breaks. *Trends Biochem Sci*. Oct; 20(10):405-11.

Lindsay RM. (1986) Reactive gliosis In *Astrocytes: Cell Biology and Pathology of Astrocytes*, Vol.3, edited by Fedoroff S, Vernadakis A, Orlando, Academic Press, pp 231-262.

Liu X, Kim CN, Yang J, Jemmerson R, Wang X. (1996) Induction of apoptotic program in cell-free extracts: requirement for dATP and cytochrome c. *Cell*. Jul 12; 86(1):147-57

Lorenzo HK, Susin SA, Penninger J, Kroemer G. (1999) Apoptosis inducing factor (AIF): a phylogenetically old, caspase-independent effector of cell death. *Cell Death Differ*. Jun; 6(6):516-24.

Lowry OH, Rosebrough NJ, Farr AL, Randall RJ. (1951) Protein measurement with the Folin phenol reagent. *J Biol Chem*. Nov; 193(1):265-75.

Luetjens CM, Bui NT, Sengpiel B, Munstermann G, Poppe M, Krohn AJ, Bauerbach E, Kriegelstein J, Prehn JH. (2000) Delayed mitochondrial dysfunction in excitotoxic neuron

death: cytochrome c release and a secondary increase in superoxide production. *J Neurosci*. Aug 1; 20(15):5715-23

Macho A, Hirsch T, Marzo I, Marchetti P, Dallaporta B, Susin SA, Zamzami N, Kroemer G. (1997) Glutathione depletion is an early and calcium elevation is a late event of thymocyte apoptosis. *J Immunol*. May 15; 158(10):4612-9.

Mackey ME, Wu Y, Hu R, DeMaro JA, Jacquin MF, Kanellopoulos GK, Hsu CY, Kouchoukos NT. (1997) Cell death suggestive of apoptosis after spinal cord ischemia in rabbits. *Stroke*. Oct; 28(10):2012-7

Maier SE, Chen WA, Miller JA, West JR. (1997) Fetal alcohol exposure and temporal vulnerability: regional differences in alcohol-induced microencephaly as a function of the timing of binge-like alcohol exposure during rat brain development. *Alcohol Clin Exp Res*. Nov; 21(8):1418-28.

Marsden VS, O'Connor L, O'Reilly LA, Silke J, Metcalf D, Ekert PG, Huang DC, Cecconi F, Kuida K, Tomaselli KJ, Roy S, Nicholson DW, Vaux DL, Bouillet P, Adams JM, Strasser A. (2002) Apoptosis initiated by Bcl-2-regulated caspase activation independently of the cytochrome c/Apaf-1/caspase-9 apoptosome. *Nature*. Oct 10; 419(6907):634-7.

Martin LJ (2002) Neurodegenerative Disorders, in *Encyclopedia of the human brain*, (Ramachandran V. S. eds) Vol 3, pp. 441-463. Academic press, Elsevier Science, USA.

Mates JM. (2000) Effects of antioxidant enzymes in the molecular control of reactive oxygen species toxicology. *Toxicology*. Nov 16; 153 (1-3):83-104.

Matsumoto I, Burke L, Inoue Y, Wilce PA. (2001) Two models of ethanol withdrawal kindling. *Nihon Arukoru Yakubutsu Igakkai Zasshi*. Feb; 36(1):53-64.

Mattson SN, Riley EP. (1996) Brain anomalies in fetal alcohol syndrome in *Fetal Alcohol Syndrome: From Mechanism to Prevention*, ed. Abel EA, pp. 51– 68. CRC Press, Boca Raton, FL, USA.

McBain CJ, Mayer ML. (1994) N-methyl-D-aspartic acid receptor structure and function. *Physiol Rev*. Jul; 74(3):723-60.

McCarthy NJ, Evan GI. (1998) Methods for detecting and quantifying apoptosis. *Curr Top Dev Biol.*36:259-78

McConkey DJ (1996) Calcium flux measurement in cell death in *Techniques In apoptosis: A user's guide*. Cotter TG, Martin SJ, editors, London Portland Press: 133-48.

McEntee WJ, Mair RG. (1990) The Korsakoff syndrome: a neurochemical perspective. *Trends Neurosci.* Aug; 13(8):340-4.

McMullen PA, Saint-Cyr JA, Carlen PL. (1984) Morphological alterations in rat CA1 hippocampal pyramidal cell dendrites resulting from chronic ethanol consumption and withdrawal. *J Comp Neurol.* May 1; 225(1):111-8.

Mesulam MM, Mufson EJ, Wainer BH, Levey AI (1983) Central cholinergic pathways in the rat: an overview based on an alternative nomenclature (Ch1-Ch6). *Neuroscience.* Dec; 10(4):1185-201.

Miller MW, Potempa G. (1990) Numbers of neurons and glia in mature rat somatosensory cortex: effects of prenatal exposure to ethanol. *J Comp Neurol.* Mar 1; 293(1):92-102.

Miller MW. (1995) Generation of neurons in the rat dentate gyrus and hippocampus: effects of prenatal and postnatal treatment with ethanol. *Alcohol Clin Exp Res.* Dec; 19(6):1500-9.

Miller R, King MA, Heaton MB, Walker DW. (2002) The effects of chronic ethanol consumption on neurotrophins and their receptors in the rat hippocampus and basal forebrain. *Brain Res.* Sep 20; 950(1-2):137-47.

Miramar MD, Costantini P, Ravagnan L, Saraiva LM, Haouzi D, Brothers G, Penninger JM, Peleato ML, Kroemer G, Susin SA. (2001) NADH oxidase activity of mitochondrial apoptosis-inducing factor. *J Biol Chem.* May 11; 276(19):16391-8.

Montoliu C, Valles S, Renau-Piqueras J, Guerri C. (1994) Ethanol-induced oxygen radical formation and lipid peroxidation in rat brain: effect of chronic alcohol consumption. *J Neurochem.* Nov; 63(5):1855-62 .

Mooney SM, Miller MW. (2001) Effects of prenatal exposure to ethanol on the expression of bcl-2, bax and caspase 3 in the developing rat cerebral cortex and thalamus. *Brain Res.* Aug 17; 911(1):71-81.

Morel G, Cavalier A (2000) Tissue preparation, Chapter 2, In *In Situ Hybridization in Light Microscopy* (Eds Morel G, Cavalier A), CRC Press pp 61-88.

Nagy J. (2004) The NR2B subtype of NMDA receptor: a potential target for the treatment of alcohol dependence. *Curr Drug Targets CNS Neurol Disord.* Jun; 3(3):169-79.

Nakamura, W., Hosada, S. and Hayashi, K. (1974) Purification and properties of rat liver glutathione peroxidase. *Biochem. Biophys. Acta* 358, 251–261

Nicholson DW. (1999) Caspase structure, proteolytic substrates, and function during apoptotic cell death. *Cell Death Differ.* Nov; 6(11):1028-42.

Nicholson DW, Nicotera P, Melino G (2004) Caspases and cell death In *Encyclopedia of biological chemistry*, (Eds Lennarz WJ, Lane MD) Volume 1, Elsevier Inc pp 319-327.

Nordmann R., Ribiere C, Rouach H. (1990) Ethanol-induced lipid peroxidation and oxidative stress in extrahepatic tissues. *Alcohol Alcohol*; 25(2-3):231-7.

Nulman J, O'Hayon B, Gladstone J, Koren G (1998). The effects of alcohol on the fetal brain. The central nervous system tragedy In *Handbook of Developmental Neurotoxicology* (Eds Slikker W Jr, Chang LW), San Diego, CA: Academic, pp. 567–86.

Oberdoerster J, Rabin RA. (1999) Enhanced caspase activity during ethanol induced apoptosis in rat cerebellar granule cells. *Eur J Pharmacol.* Dec 3; 385(2-3):273-82.

Obernier JA, Bouldin TW, Crews FT. (2002) Binge ethanol exposure in adult rats causes necrotic cell death. *Alcohol Clin Exp Res.* Apr; 26(4):547-57.

O'Callaghan JP. (1988) Neurotypic and gliotypic proteins as biochemical markers of neurotoxicity. *Neurotoxicol Teratol.* Sep-Oct; 10(5):445-52.

O'Callaghan JP. (1991) Assessment of neurotoxicity: use of glial fibrillary acidic protein as

a biomarker. *Biomed Environ Sci.* Jun; 4(1-2):197-206.

O'Callaghan JP, Jensen KF. (1992) Enhanced expression of Glial fibrillary acidic protein and the cupric silver degeneration reaction can be used as sensitive and early indicators of Neurotoxicity. *Neurotoxicology.* Spring; 13(1):113-22.

Olney JW, Tenkova T, Dikranian K, Muglia LJ, Jermakowicz WJ, D'Sa C, Roth KA. (2002) Ethanol-induced caspase-3 activation in the in vivo developing mouse brain. *Neurobiol Dis.* Mar; 9(2):205-19.

Olney JW (2002) Alcohol damage to the brain, in *Encyclopedia of the human brain*, (Ramachandran V. S. eds) Vol 1, pp. 87-98. Academic press, Elsevier Science, USA.

Olton DS, Becker JT, Handelmann GE. (1979) Hippocampus, space and memory. *Behav. Brain Sci.* 2, 313-366.

Oscar-Berman M, Hutner N (1993) Frontal lobe changes after chronic alcohol ingestion In *Alcohol induced brain damage*, Research monograph No.22, Edited by Hunt WA, Nixon SJ, NIH publication No. 93-3549, NIH, Rockville, MD, USA, pp 121-156.

Oscar-Berman M, Marinkovic K (2003) Alcoholism and the brain: an overview. *Alcohol Res Health*; 27(2):125-33.

Pastorino JG, Shulga N, Hoek JB. (2003) TNF-alpha-induced cell death in ethanol-exposed cells depends on p38 MAPK signaling but is independent of Bid and caspase-8. *Am J Physiol Gastrointest Liver Physiol.* Sep; 285(3):G503-16.

Paul CA, Beltz B, Sweeney JB (1997) Field potential recording in the hippocampal slice In *Discovering Neurons*, Cold spring harbor laboratory press pp 183- 202

Paul CA, Beltz B, Sweeney JB (1997) Protocol 4 In *Discovering Neurons*, Cold spring harbor laboratory press pp 380-381.

Pauli J, Wilce P, Bedi KS. (1995) Acute exposure to alcohol during early postnatal life causes a deficit in the total number of cerebellar Purkinje cells in the rat. *J Comp Neurol.* Sep 25; 360(3):506-12.

Perez-Torrero E, Duran P, Granados L, Gutierrez-Ospina G, Cintra L, Diaz-Cintra S. (1997) Effects of acute prenatal ethanol exposure on Bergmann glia cells early postnatal development. *Brain Res.* Jan 23; 746(1-2):305-8.

Phanithi PB, Yoshida Y, Santana A, Su M, Kawamura S, Yasui N. (2000) Mild hypothermia mitigates post-ischemic neuronal death following focal cerebral ischemia in rat brain: Immunohistochemical study of Fas, caspase-3 and TUNEL. *Neuropathology.* Dec; 20(4):273-82.

Phillips DE. (1992) Effects of alcohol on the development of glial cells and myelin, In *Alcohol and Neurobiology. Brain Development and Hormone Regulation*, ed. Watson RR, pp. 83–108, CRC Press, Boca Raton, FL, USA

Piantadosi CA, Zhang J, Levin ED, Folz RJ, Schmechel DE. (1997) Apoptosis and delayed neuronal damage after carbon monoxide poisoning in the rat. *Exp Neurol.* Sep; 147(1):103-14.

Pieper AA, Verma A, Zhang J, Snyder SH. (1999) Poly (ADP-ribose) polymerase, nitric oxide and cell death. *Trends Pharmacol Sci.* Apr; 20(4):171-81.

Pinkus R, Weiner LM, Daniel V. (1996) Role of oxidants and antioxidants in the induction of AP-1, NF-kappaB, and glutathione S-transferase gene expression. *J Biol Chem.* Jun 7; 271(23):13422-9.

Plant N. (2003) Co-ordinated responses to toxicity, in *Molecular toxicology* edited by Plant N. pp45-62, Bios scientific publishers, Taylor & Francis, Oxon, UK.

Polster BM, Basanez G, Etxebarria A, Hardwick JM, Nicholls DG. (2004) Calpain I induces cleavage and release of apoptosis inducing factor from isolated mitochondria. *J Biol Chem.* Feb 25; 280(8):6447-54.

Rajgopal Y, Chetty CS, Vemuri MC. (2003) Differential modulation of apoptosis-associated proteins by ethanol in rat cerebral cortex and cerebellum. *Eur J Pharmacol.* Jun 6; 470(3):117-24.

Rajgopal Y, Vemuri MC. (2002) Calpain activation and alpha-spectrin cleavage in rat brain by ethanol. *Neurosci Lett*. Mar 22; 321(3):187-91.

Raji NS, Krishna TH, Rao KS. (2002) DNA-polymerase alpha, beta, delta and epsilon activities in isolated neuronal and astroglial cell fractions from developing and aging rat cerebral cortex. *Int J Dev Neurosci*. Oct; 20(6):491-6.

Rani BU, Singh NI, Ray A, Rao KS. (1983) Procedure for isolation of neuron- and astrocyte-enriched fractions from chick brain of different ages. *J Neurosci Res*. 10(1):101-5.

Rao KS. (1997) DNA-damage & DNA-repair in ageing brain. *Indian J Med Res*. 1997 Oct; 106:423-37.

Ravaglia S, Costa A, Ratti MT, Savoldi F, Bo P, Moglia A. (2002) Cognitive impairment and central motor conduction time in chronic alcoholics. *Funct Neurol*. Apr-Jun; 17(2):83-6.

Ray SK, Hogan EL, Banik NL. (2003) Calpain in the pathophysiology of spinal cord injury: neuroprotection with calpain inhibitors. *Brain Res Brain Res Rev*. May; 42(2):169-85.

Raymond AS, Susana CO (2003) Cell death, in *Encyclopedia of the Neurological Sciences*, (Michael JA, Robert BD. eds), Vol 1, pp. 542-545, Academic press, Elsevier science, USA.

Renis M, Calabrese V, Russo A, Calderone A, Barcellona ML, Rizza V. (1996) Nuclear DNA strand breaks during ethanol-induced oxidative stress in rat brain. *FEBS Lett*. Jul 22; 390(2):153-6.

Riley EP, Mattson SN, Sowell ER, Jernigan TL, Sobel DF, Jones KL. (1995) Abnormalities in the corpus callosum in children prenatally exposed to alcohol. *Alcohol Clin Exp Res*. Oct; 19(5):1198-202.

Riley JN, Walker DW.(1978) Morphological alterations in hippocampus after long-term alcohol consumption in mice. *Science*. Aug 18; 201(4356):646-8.

Robles E, Huttenlocher A, Gomez TM. (2003) Filopodial calcium transients regulate growth cone motility and guidance through local activation of calpain. *Neuron*. May 22; 38(4):597-609.

Rodriguez J, Lazebnik Y. (1999) Caspase-9 and APAF-1 form an active holoenzyme. *Genes Dev.* Dec 15; 13(24):3179-84.

Rogers CJ, Hunter BE (1992) Chronic ethanol treatment reduces inhibition in CA1 of the rat hippocampus. *Brain Res Bull.* Apr; 28(4):587-92.

Roth KA (2002) In situ detection of apoptotic neurons in *Neuromethods, Apoptosis Techniques and Protocols*, (LeBlanc AC eds), Vol 37, pp 205-224, 2 nd Ed, Humana Press Inc, Totowa, NJ.

Rothberg BS, Yasuda RP, Satkus SA, Wolfe BB, Hunter BE. (1993) Effects of chronic ethanol on cholinergic actions in rat hippocampus: electrophysiological studies and quantification of m1-m5 muscarinic receptor subtypes. *Brain Res.* Dec 24; 631(2):227-34.

Sallmann FR, Bourassa S, Saint-Cyr J, Poirier GG. (1997) Characterization of antibodies specific for the caspase cleavage site on poly(ADP-ribose) polymerase: specific detection of apoptotic fragments and mapping of the necrotic fragments of poly(ADP-ribose) polymerase. *Biochem Cell Biol*; 75(4):451-6.

Samson HH. 1986. Microencephaly and fetal alcohol syndrome: human and animal studies In *Alcohol and brain development* Ed: West JR, New York: Oxford university press pp. 167-83.

Saraste A, Pulkki K. (2000) Morphologic and biochemical hallmarks of apoptosis. *Cardiovasc Res.* Feb; 45(3):528-37.

Schindler CK, Shinoda S, Simon RP, Henshall DC (2004) Subcellular distribution of Bcl-2 family proteins and 14-3-3 within the hippocampus during seizure-induced neuronal death in the rat. *Neurosci Lett.* Feb 19; 356(3):163-6.

Schmechel DE (1999) Assessment of Ultrastructural changes associated with apoptosis, in *Apoptosis in Neurobiology*, (Eds: Hannun YA, Boustany RM), CRC Press LLC, Boca Raton, Florida, USA, pp153-181.

Segner H, Braunbeck T. (1998) Cellular Response Profile to Chemical Stress In *Ecotoxicology*, Edited by Schuurmann G, Markert B; John Wiley & Sons, Inc. and Spektrum

Akademischer Verlag Co-publication, pp 521-569.

Smith HA, Jones TC, Hunt RD. (1972) Introduction, the cell, death of cells and tissues In Veterinary pathology, Lea & Febiger, Philadelphia, USA, pp 1-33.

Spencer RL, Hutchison KE. (1999) Alcohol, Aging, and the Stress Response. Alcohol Res Health ; 23(4):272-83.

Spohr HL, Willms J, Steinhausen MC. (1993) Prenatal alcohol exposure and long term developmental consequences. Lancet. Apr 10; 341(8850):907-10.

Srinivasan A, Roth KA, Sayers RO, Shindler KS, Wong AM, Fritz LC, Tomaselli KJ.(1998) In situ immunodetection of activated caspase-3 in apoptotic neurons in the developing nervous system. Cell Death Differ. Dec; 5(12):1004-16.

Streissguth AP, Aase JM, Clarren SK, Randels SP, LaDue RA, Smith DF. (1991) Fetal alcohol syndrome in adolescents and adults. JAMA. Apr 17; 265(15):1961-7.

Streissguth AP, Landesman-Dwyer S, Martin JC, Smith DW. (1980) Teratogenic effects of alcohol in humans and laboratory animals. Science. Jul 18; 209(4454):353-61.

Stridh H, Kimland M, Jones DP, Orrenius S, Hampton MB. (1998) Cytochrome c release and caspase activation in hydrogen peroxide- and tributyltin-induced apoptosis. FEBS Lett. Jun 16; 429(3):351-5.

Strobl S, Fernandez-Catalan C, Braun M, Huber R, Masumoto H, Nakagawa K, Irie A, Sorimachi H, Bourenkow G, Bartunik H, Suzuki K, Bode W. (2000) The crystal structure of calcium-free human m-calpain suggests an electrostatic switch mechanism for activation by calcium. Proc Natl Acad Sci U S A. Jan 18; 97(2):588-92.

Sullivan EV (2003) Compromised pontocerebellar and cerebellothalamocortical systems: speculations on their contributions to cognitive and motor impairment in nonamnestic alcoholism. Alcohol Clin Exp Res. Sep; 27(9):1409-19.

Sultana R, Babu PP. (2003) Ethanol-induced alteration in N-methyl-D-aspartate receptor 2A C-terminus and protein kinase C activity in rat brain. Neurosci Lett. Sep 25; 349(1):45-8.

Susin SA, Lorenzo HK, Zamzami N, Marzo I, Snow BE, Brothers GM, Mangion J, Jacotot E, Costantini P, Loeffler M, Larochette N, Goodlett DR, Aebersold R, Siderovski DP, Penninger JM, Kroemer G. (1999) Molecular characterization of mitochondrial apoptosis-inducing factor. *Nature*. Feb 4; 397(6718):441-6.

Tan S, Wood M, Maher P. (1998) Oxidative Stress Induces a Form of Programmed Cell Death with Characteristics of Both Apoptosis and Necrosis in Neuronal Cells. *J Neurochem*. Jul; 71(1):95-105.

Towbin H, Staehelin T, Gordon J. (1979) Electrophoretic transfer of proteins from polyacrylamide gels to nitrocellulose sheets: procedure and some applications. *Proc Natl Acad Sci U S A*. Sep; 76(9):4350-4.

Troy CM, Salvesen GS. (2002) Caspases on the brain. *J Neurosci Res*. Jul 15; 69(2):145-50.

Trump BF, Berezsky IK, Chang SH, Phelps PC. (1997) The pathways of cell death: oncosis, apoptosis, and necrosis. *Toxicol Pathol*. Jan-Feb; 25(1):82-8.

Valles SL, Blanco AM, Pascual M, Guerri C. (2004) Chronic ethanol treatment enhances inflammatory mediators and cell death in the brain and in astrocytes. *Brain Pathol*. Oct; 14(4):365-71.

Velier JJ, Ellison JA, Kikly KK, Spera PA, Barone FC, Feuerstein GZ. (1999) Caspase-8 and caspase-3 are expressed by different populations of cortical neurons undergoing delayed cell death after focal stroke in the rat. *J Neurosci*. Jul 15; 19(14):5932-41.

Virdee K, Parone PA, Tolkovsky AM. (2000) Phosphorylation of the pro-apoptotic protein BAD on serine 155, a novel site, contributes to cell survival. *Curr Biol*. Sep 21; 10(18):1151-4.

Walker DW, Barnes DE, Riley JN, Hunter BE, Zornetzer SF (1980a) The neurotoxicity of chronic alcohol consumption, an animal model. In *Psychopharmacology of Ethanol*, pp.17-31. Ed.Sandler M, Raven Press, New York.

Walker DW, Barnes DE, Zornetzer SF, Hunter BE, Kubanis P. (1980b) Neuronal loss in hippocampus induced by prolonged ethanol consumption in rats. *Science*. Aug 8;

209(4457):711-3.

Walker DW, Freund G. (1971) Impairment of shuttle box avoidance learning following prolonged alcohol consumption in rats. *Physiol Behav.* Nov; 7(5):773-8.

Walker DW, Freund G. (1973) Impairment of timing behavior after prolonged alcohol consumption in rats. *Science.* Nov 9; 182(112):597-9.

Walker DW, Hunter BE. (1987) Neuronal adaptation in the hippocampus induced by long-term ethanol exposure. In *The Role of Neuroplasticity in the Response to Drugs*, pp. 108-131. Eds. Friedman DP, Clouet DH. NIDA Research Monograph 78. NIDA, Washington, DC.

Wang HG, Pathan N, Ethell IM, Krajewski S, Yamaguchi Y, Shibasaki F, McKeon F, Bobo T, Franke TF, Reed JC. (1999) Ca^{2+} -induced apoptosis through calcineurin dephosphorylation of BAD. *Science.* Apr 9; 284(5412):339-43.

WHO Global Status Report on Alcohol. (2004)
http://www.who.int/substance_abuse/publications/global_status_report_2004_overview.pdf

Whyte MK, Hardwick SJ, Meagher LC, Savill JS, Haslett C. (1993) Transient elevations of cytosolic free calcium retard subsequent apoptosis in neutrophils in vitro. *J Clin Invest.* Jul; 92(1):446-55.

Widmann C, Gibson S, Johnson GL. (1998) Caspase-dependent cleavage of signaling proteins during apoptosis. A turn-off mechanism for anti-apoptotic signals. *J Biol Chem.* Mar 20; 273(12):7141-7.

Will B, Hefti F.(1985) Behavioural and neurochemical effects of chronic intraventricular injections of nerve growth factor in adult rats with fimbria lesions. *Behav Brain Res.* Sep; 17(1):17-24.

Watkins S (1993) In situ hybridization and immunohistochemistry, chapter 14, In *Short protocols in molecular biology*, Vol. 2, edited by Ausubel FM, 5th edition, John Wiley, pp 14.0.1-14.6.13.

Young C, Klocke BJ, Tenkova T, Choi J, Labruyere J, Qin YQ, Holtzman DM, Roth KA, Olney JW. Ethanol-induced neuronal apoptosis in vivo requires BAX in the developing mouse brain. *Cell Death Differ.* 2003 Oct; 10(10):1148-55.

Zha J, Harada H, Yang E, Jockel J, Korsmeyer SJ. (1996) Serine phosphorylation of death agonist BAD in response to survival factor results in binding to 14-3-3 not BCL-X(L). *Cell.* Nov 15; 87(4):619-28

Zheng TS, Schlosser SF, Dao T, Hingorani R, Crispe IN, Boyer JL, Flavell RA. (1998) Caspase-3 controls both cytoplasmic and nuclear events associated with Fas-mediated apoptosis in vivo. *Proc Natl Acad Sci U S A.* Nov 10; 95(23):13618-23.

Zhou XM, Liu Y, Payne G, Lutz RJ, Chittenden T. (2000) Growth factors inactivate the cell death promoter BAD by phosphorylation of its BH3 domain on Ser155. *J Biol Chem.* Aug 11; 275(32):25046-51.

Zou H, Li Y, Liu X, Wang X. (1999) An APAF-1.cytochrome c multimeric complex is a functional apoptosome that activates procaspase-9. *J Biol Chem.* Apr 23; 274(17):11549-56.

Zou JY, Martinez DB, Neafsey EJ, Collins MA (1996) Binge ethanol-induced brain damage in rats: effect of inhibitors of nitric oxide synthase. *Alcohol Clin Exp Res.* Nov; 20(8):1406-11.